12-23-2004

Land Use Influence on the Characteristics of Groundwater Inputs to the Great Bay Estuary, New Hampshire

Thomas P. Ballestero
University of New Hampshire, tom.ballestero@unh.edu

Robert Roseen
University of New Hampshire, Durham

Gabriel F. Bacca-Cortes
University of New Hampshire, Durham

Land Use Influence on the Characteristics of Groundwater Inputs to the Great Bay Estuary, New Hampshire

A Final Report Submitted to
The NOAA/UNH Cooperative Institute for Coastal and Estuarine Environmental Technology (CICEET)

Submitted by

Dr. Thomas P. Ballestero
Dr. Robert M. Roseen
Gabriel F. Bacca-Cortes
Department of Civil Engineering
University of New Hampshire
Durham, NH

December 23, 2004

This project was funded by a grant from NOAA/UNH Cooperative Institute for Coastal and Estuarine Environmental Technology, NOAA Grant Number(s) NA17OR1401 and NA03NOS4190195

TABLE OF CONTENTS

LIST OF TABLES

LIST OF FIGURES

ABSTRACT

This research examines the sources and factors affecting nutrient-laden groundwater discharge to the Great Bay Estuary. To further understand this relationship, examination of groundwater residence time, a review of historic land uses, and nitrate source tracking strategies were used. Seven submarine groundwater discharge (SGD) sites were selected, and groundwater monitoring networks were installed to examine the relationship between land use and groundwater quality at the discharge zones. Field activities were performed in the summer and fall of 2003 and 2004. Estuarine water intrusion in groundwater discharge samples confounded the analyses for major ion chemistry and boron isotopes. CFC-derived and modeled groundwater ages in the study area averaged 23.2 years (±15.0 years). CFC analysis enabled correlation of nitrate concentrations at the SGD sites with the historic land use coverage for the years 1974 (for most of the sites) or 1962 (SGD 58.4). Two types of correlation were made: 1) between the agricultural and residential land use for all observed nitrate concentrations in the recharge areas, and 2) correlation with the nitrate concentrations between developed and undeveloped land uses. Both statistical correlations (Kendall's Tau and Spearman's Rho) indicated a connection between the increase of residential land use of the last three decades with the high nitrate-bearing groundwater discharging to the Great Bay (NH). The geochemical composition of the SGD water was also investigated by using simple mixing models that attempted to explain the water chemistry characteristics of the targeted SGD sites. Based on these models it was concluded that overburden groundwater comprises 75% to 95% of the groundwater discharging at the SGD sites. A significant correlation (Tau's, p=0.021) between nitrate-bearing groundwater and CFC-derived groundwater ages was detected supporting the hypothesis that high nitrate-bearing groundwater will be discharged to the Great Bay in the near future accounting for the increase of residential land use of 1990's. Continuous monitoring of SGD sites was suggested to be included as part of the periodic environmental quality monitoring activities of the Great Bay. Long-term step-wise sampling for groundwater dating is required to develop a stronger chronological evolution of groundwater nitrate inputs. Further research should concentrate on detailing the overburden water chemistry, flow paths, and nitrogen loading characteristics.

Keywords: Land Use, Groundwater Discharge, Residence Time, Nutrient Contamination, Environmental Tracers, Coastal Waters.

INTRODUCTION

OBJECTIVES

The objective of this study was to examine the relationship between nitrate concentrations in groundwater discharging to the Great Bay Estuary and land use upgradient of the discharge zones, with respect to groundwater residence time. Two main components were addressed to meet this objective: 1) to refine the characterization of groundwater discharge zones to the Great Bay Estuarine System from a residence time and water quality stand point; and 2) to define the source of groundwater discharge and to discern the origins of the nutrient loading and identify correlations between the measured nutrient loading and land use. The results of this study are intended to provide tools to local coastal managers for identifying present and future vulnerable areas of contamination and developing management strategies to reduce the effect on the environment of such sources of contamination.

The mean residence time of the groundwater in the area constitutes an important result of this study. It provides clues for resource managers in terms of the lag time between nutrient inputs in the watershed and the living-resource response, and to asses the effectiveness of nutrient reduction strategies. A secondary objective was to know the spatial origin of the groundwater discharging to the Great Bay Estuary from a regional to local scale (i.e. bedrock or overburden), coupled with the temporal component given by the residence time analysis. This result helped to determine if the nutrient loading source is local, or on a more regional scale.

This study was intended to evaluate and develop a relationship between groundwater nutrient loading to the Great Bay Estuary and land use practices within the groundwater recharge areas for the respective discharge zones. It enhances the capability of coastal resource managers and local regulators, planners, and decision-makers to prevent and mitigate anthropogenic contamination of coastal and estuarine ecosystems. The collected data and the analysis derived from this study also provided insight for the development of Total Maximum Daily Loads (TMDLs) for contaminants required from the states by 2015.

RESEARCH SUMMARY

This research was divided in two major components, which correspond to each of the two specific objectives: 1) to refine the characterization of groundwater discharge zones to the Great Bay Estuarine System from a residence time and water quality stand point; and 2) to define the source of groundwater discharge and to discern the origins of the nutrient loading and identify correlations between the measured nutrient loading and land use.

The first component of the study addressed the detailed characterization of the groundwater discharging to the Great Bay Estuary. This component was further subdivided into: 1) defining the experimental design and the monitoring network; 2) estimating the groundwater residence time; and 3) characterizing the groundwater chemistry. A preliminary selection of the monitoring network was made based on the examination of 1952's and 1974's aerial photographs for upgradient land use practices from the discharge zones that have a number of characteristics: no change and significant land use change over time, and sites with either the predominance of residential, agricultural, or undisturbed land uses. This preliminary selection coupled with other criteria such as: spatial location (inland, seaward), nitrate concentration, discharge intensity and size, and accessibility, allowed defining seven (7) submarine groundwater discharge (SGD) sites to be included in the study. The experimental design at each site was defined by the installation of one small diameter well (SDW) at the groundwater discharge zone (GWDZ), one SDW immediately upgradient from the GWDZ within the intertidal zone, and one SDW and one bedrock well both located in the upgradient land use from the GWDZ. The installation of the SDWs located within the intertidal zone was performed by boat during low tide conditions and the wells were manually driven into the gravelly formation with a slam bar until the best low salinity conditions were found. The SDW upgradient from the discharge zone, meant to intercept the shallow groundwater, was also driven manually. Privately-owned bedrock wells were also used for the study. A supportive response from the community allowed the access to private properties for the installation and sampling of the SDWs in the surrounding upgradient areas from the GWDZs and for the bedrock well sampling. The entire monitoring network was set in place during summer and fall of 2003. The monitoring network so installed was subjected to extensive sampling chiefly, for groundwater dating, stable isotopes, and general water chemistry.

The mean groundwater residence time was estimated using Chlorofluorocarbons (CFCs). Several environmental tracers were considered before choosing CFCs as a groundwater dating tool. The Tritium/Helium-3 ($^{3}H/^{3}He$) ratio technique was proven not suitable for the study area by previous USGS studies (Dr. Busenberg, personal communication). Kripton-85 (^{85}Kr) required too much of a sample volume (~100L) to be considered for the study. Sulfur-hexafluoride (SF_6) has a smaller groundwater dating coverage (25 years or younger) than the expected residence time of the study area. Enriched Tritium (^{3}H) concentrations were only considered for comparison with CFC residence times in three samples, but they were not able to precisely estimate the groundwater recharge year. CFCs as groundwater dating tools brings many advantages to the study: 1) provide three estimates of groundwater age from three different CFCs (CFC-11, CFC-12, and CFC-113) in a single analysis; and 2) able to date with groundwater ages of 50 years or younger, which is a time period where significant changes in land use were observed in the study area. A sampling method, recently developed by the USGS at Reston Virginia, was used for CFC sampling. Seventeen samples were collected for CFC analysis from overburden, bedrock, and SGD sites. Their analyses were performed at contracted laboratories.

Several analytes were considered for the general water chemistry analysis: Ca^{2+}, Mg^{2+}, Na^{+}, K^{+}, Fe^{2+}, Cl^{-}, SO_4^{2-}, HCO_3^{-}, NH_4^{-}, NO_3^{-}, DOC, SiO_2, Br^{-}, and B^{3+}. The Schooller and Piper trilinear diagram were used to enhance this analysis. The Schooller

diagram enables the comparison of the analytes concentration in different settings. The Piper diagram allowed observing the proportion of each analyte at a given site/sample with respect to the other analytes in the same and the other samples. These techniques helped identifying the main mechanisms that control the local groundwater chemistry and its evolution through the hydrological cycle from the time the atmospheric water precipitates, infiltrates, and reaches deeper zones in the aquifer system. An accurate identification of these controlling components and target analytes was needed to explain the groundwater characteristics by mixing of overburden and bedrock groundwater chemistries. This mixing determined the proportions of the two groundwater sources at the SGD sites. The mixing proportions constitute an important result from a spatial and temporal stand point since it indicates whether the groundwater discharging to the Great Bay Estuarine system is locally (overburden) or regionally (bedrock) recharged, transported, and nutrient-contaminated. This result was coupled and verified with the CFC residence time analysis for these water reservoirs. Both techniques suggested that mixing of the overburden and bedrock reservoirs occurs at the SGD sites and that the groundwater discharge is predominantly a local system with relatively short residence times and highly influenced by the surficial aquifer. These observations support the hypothesis that land use practices play an important role in affecting the chemical characteristics of shallow groundwater.

The second component entailed identifying the source of nitrate loading and establishing its relationship with historical land use practices in the study area. The past and present land use analyses for the study area revealed two main suspected nitrate sources: 1) the use of fertilizer related to past agricultural activities, and 2) septic tank effluent related to the recent (<30 years) residential development growth. The isotopic composition of Boron was used to identify the source of nitrate in groundwater samples. Finally, the results from residence time, groundwater chemical characteristics, and nitrate loading source were applied to find correlations between land use and nitrate concentration at the SGD sites.

GROUNDWATER RESIDENCE TIME

A detailed determination of the groundwater residence time was required to better understand the groundwater characteristics at the SGD sites, their relationship with the hydrogeological setting, and upgradient land use as a source of contamination. Chlorofluorocarbons (CFCs) were chosen as groundwater dating tools. CFCs are man-made organic compounds whose production began in the early 1940s, and were chiefly used as refrigerants and solvents. Their accumulations in the atmosphere started as soon as their production and were introduced in the hydrological cycle by precipitation that either made its way to surface water as runoff or as recharge to aquifers. This latter path makes them suitable for use as environmental tracers of past atmospheric CFC concentrations. Therefore, the residence time estimated with this technique comprises the elapsed time from the time of recharge (when the infiltrating water is isolated from the atmosphere) until the water is discharged to a river, well, spring, or sample. Because of their early releasing rates to the atmosphere, this technique allows dating groundwater 50 years old and younger.

Sampling for CFCs poses a challenge for the analyst since the sample cannot be exposed to the current CFC atmospheric levels. The sampling methodology for CFCs was recently improved (Spring 2003) by researchers at the Reston CFC Laboratory (USGS, Virginia). The previous methodology consisted in isolating the sample container with nitrogen gas and once the sample was taken, the borosilicate ampoule (container) was immediately flame sealed (in the field). The new method submerses the sample bottle in a larger glass container (beaker), isolating the sample from the atmosphere. The bottle is then sealed inside of the larger container with aluminum lined caps.

CFCs do not behave conservatively in certain environments. They can be distinctly modified by processes such as anaerobic degradation, contamination, and/or sorption, thereby altering the residence time estimates. In a groundwater system that has no alterations of this kind or where the effects of hydrodynamic dispersion and mixing at the borehole are not considered, the flow lines will define a piston type of flow. If these effects are present, the flow lines will have a non linear distribution of travel times. Exponential (EM) and a combination of exponential and piston flow (EPM) models were used to estimate (with the FLOWPC program) those different travel time distributions. In general, the modeled residence time derived from the piston flow model was the minimum; the exponential model was the maximum value. The ranges of residence time are very variable (20-30 years), however, only long term groundwater dating monitoring could provide better estimates by fitting a site specific model with the help of FLOWPC applications.

NITRATE LOADING SOURCE

Elemental boron and its isotopic composition were used as co-migrating solutes of nitrate contamination to identify its source. This isotopic technique was developed in the early nineties using either negative or positive thermal ionization mass spectrometry (NTIMS or PTIMS). Few laboratories in North America have the facilities and the expertise to perform this analysis. After an extensive search, the groundwater samples taken for Boron and its isotopic composition for this study were analyzed by the USGS Laboratory at Menlo Park (CA) with the cooperation of Dr. Thomas D. Bullen. This technique was very susceptible to increased concentrations of nitrate. This technique is based on the distinct Boron isotopic compositions in seawater, native groundwater, sewage-contaminated groundwater, and in groundwater affected by agricultural activities. Boron is present in septic tank effluents and in infiltrating waters from agricultural activities because of its use in detergents and fertilizers, respectively. It co-migrates with nitrate in the contaminating plume and fractionates differently depending upon its original source.

Particular attention must be taken in the experimental design when implementing this technique. Some samples need to be dedicated to describe the end member components of interest for the study, which in our case were: septic tank effluent, native groundwater, and groundwater affected by agricultural activities. These samples are meant to represent the extreme isotopic conditions (in the groundwater system) within which the groundwater samples of interest will plot accordingly to the degree of mixing with each end member water. It is always recommended to have at least a couple of samples for each end member; thereby a more representative range of its isotopic

composition is obtained. In the case of native groundwater, the selected wells should have a historical water quality data free of any chloride or nitrate source. When analyzing the data, the boron isotope technique provides a visual tool that coupled with other chemical and isotopic (^{2}H, ^{18}O, and $^{87}Sr/^{86}Sr$) data becomes a powerful analytical element that provides the analyst with insight on the nitrate sources and flow paths in a groundwater system.

CAPTURE ZONES DELINEATION AND LAND USE-NITRATE CORRELATIONS

To scale down the contamination source and land use analysis for the study, a time-related delineation of the groundwater flow path was required. Considering both the amount of hydrogeologic information available for each site and the quality of the capture zone delineation, the most up to date version of the EPA computer code WhAEM (Well-head Analytical Element Method) was selected among several other software (WHPA, ModPath, and ArcFlow). WhAEM provides a versatile graphical interface which constitutes a big step for the software of its generation (WHPA). MODPATH is widely used for groundwater modelers in the delineation of capture zones, however, the input parameters and the amount of information required to run the model were not available for each site. Attempts of using ArcFlow were made with its latest version (April 2004), however, problems with its ArcView interface prevent further analysis with this computer code which seems promising for this type of study. ArcFlow also uses the analytical element method theory having the advantage (against WhAEM) of counting on all the tools and graphical interfaces that ArcView (and GIS) provides.

The time-related capture zones were then superimposed over the land use mosaic that existed for the time estimated for groundwater recharge. Finally, non-parametric correlations were calculated between land uses and nitrate concentrations in groundwater. Other studies have found that agricultural activities are not only related to high nitrate concentrations but also to Ca^{2+} and Mg^{2+}. Correlations between land use and these chemical elements were not significant for the sites of analysis.

Consistent with similar studies, a statistically significant relationship was observed between the nitrate concentrations in groundwater and groundwater residence time. These results provide insight with regards to the future of the nitrate loading and its response in the groundwater system.

STUDY AREA

The study area (Figure 1) is the Great Bay Estuary watershed located in the New Hampshire seacoast. The area comprises portions of seven towns: Dover, Madbury, and Durham (in Strafford County), and Newmarket, Stratham, Greenland, and Newington (in Rockingham County). The largest cities in the watershed include Rochester, Dover, Portsmouth, and Exeter and have populations of 28,461, 26,884, 20,784, and 14,058, respectively (U.S. Census Bureau, 2002).

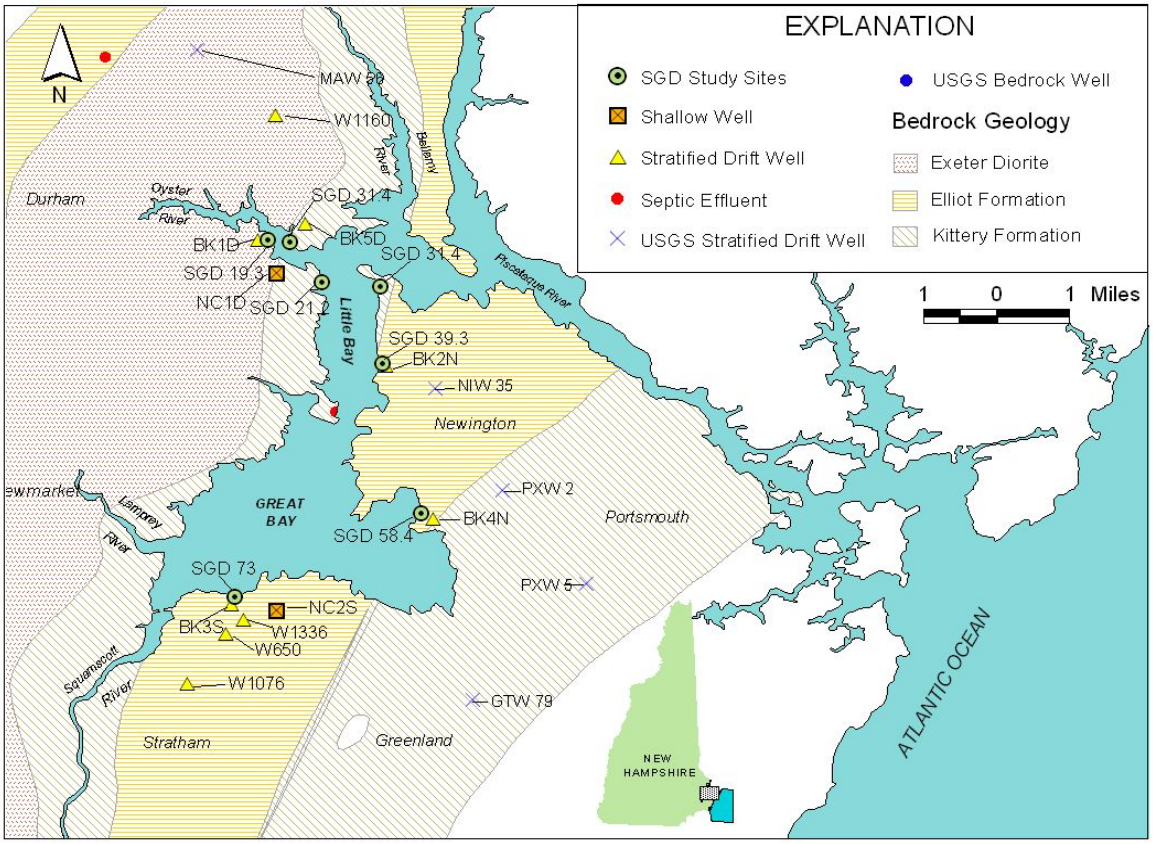

Figure 1: Location of the study area and distribution of the sites included in the project.

The entire estuary is composed of 7 contributing rivers (816 ft^3/s), approximately 144 miles of shoreline, with the tidal waters covering about 10,900 acres (Jones, 2000). In the Great Bay proper, there are 5 tributary rivers: the Oyster and Cocheco rivers (flowing into Little Bay) and the Lamprey, Squamscott, and Winnicut rivers (flowing directly into Great Bay). The daily tidal range is around 8 feet, which at low tide, and in the upper portions of the estuary, exposes significant fringing salt marsh and large mudflats and eelgrass beds (Roseen, 2002). Due, in part, to significant seawater-freshwater mixing, dissolved inorganic nitrogen (DIN) concentrations in both Little Bay and Great Bay are historically lower than those from the freshwater components upstream, averaging 0.31-0.50 mg N/L in the bays alone (Jones, 2000). Salmon Falls, Oyster, and Cocheco rivers average 0.67, 0.64, and 0.60 mg N/L, respectively, and have the highest DIN concentrations of the seven rivers. Groundwater DIN input concentrations were higher (0.81 mg N/L) than any other surface source (Roseen, 2002). With the exception of the Cocheco and Salmon Falls rivers, the nitrogen loading in the last 30 years for the rest of tributaries and estuarine waters is reported to be stable or lower than that which was observed in the 1970s (Jones, 2000).

Hydrogeologic Setting

The study area is characterized chiefly by three types of hydrogeologic units. The first unit is till, which covers most of the bedrock surface. Till is an unsorted mixture of clay, silt, sand, and gravel and depending on its level of compactness, is able to supply water to individual households using large diameter dug wells. In general, till is not considered to be a major source of ground water because of its low hydraulic conductivity (Moore, 1990; Stekl and Flanagan, 1991; Mack and Lawlor, 1992). The second unit is stratified drift, which consists primarily of sand and gravel deposits that were deposited in layers by meltwater streams flowing from the retreating glacial ice (Medalie and Moore, 1995). Often stratified drift can support municipal water supply wells, because of its high hydraulic conductivity ranging from 35 to 1000 ft/day. Although, stratified drift occurs spatially in very localized areas, its use accounts for 71.4 % of the total groundwater withdrawn for community water supplies in New Hampshire (Ayotte et al, 1999). Stratified drift aquifers occur in every town of the study area. Municipal supply wells are located in Newington, Portsmouth, Greenland, Stratham, Newmarket, Durham, Madbury, and Dover where multiple sets of wells supply water for these towns. The third hydrogeologic unit in the study area is bedrock. Bedrock is the main source of water supply to individual households. The study area is faulted and folded with a syncline extending from the northeast to the southwest (Novotony 1969). The Kittery and Elliot formations are metasedimentary bedrock units that overlay the majority of the study area (Figure 1). These formations were intensely metamorphosed and folded into the Great Bay Geosyncline during the Acadian Orogeny, which is the major fold of the Rockingham anticlinorium (Billings, 1956), and runs along the Little Bay until it meets the Piscataqua River. Based on Rb/Sr geochronologic analyses, both units were originally formed during the Silurian and metamorphism occurred during the late Devonian. The Kittery formation is composed primarily of silicate minerals including impure quartzite, with inclusions of slate, phyllite, and schist. Silicate minerals also dominate in the Elliot formation and the original argillaceous sediments have been metamorphosed to slate, phyllite, and poorly recrystalized quartzite (Novotny, 1969), that is part feldspathic, and part dolomitic (Lyons et al., 1997). Both metasedimentary formations compose part of the hydrogeologic unit, identified by Ayotte and others (1999) as dissolving significantly high arsenic concentrations in waters that are commonly designated for domestic use.

Also existing along the west side of the Great Bay, an extension of the Hillsboro Plutonic series (Exeter Diorite) overlays in a northwestern direction perpendicular to the direction of collision during the Acadian Orogeny. The igneous mass of the Exeter Pluton is the dominant feature of the Exeter Anticline. Dioritic in composition (Novotny, 1969), with main inclusions of plagioclase and microcline (Lyons et al., 1997), the Exeter Pluton has intruded into and displaced portions of the Kittery quartzite (Haug, 1976).

A remotely sensed lineament analysis and the correlation of the lineaments with bedrock fractures that store and transmit groundwater near the Great Bay was performed by Degnan and Clark (2002). A total of 287 fracture-orientation measurements from 49 outcrop stations were analyzed, finding the highest density of lineaments and fracture-correlated lineaments on the west side of the bay in the Exeter Diorite and Kittery

Formations, where the till overburden generally is thin (Degnan and Clark, 2002). These results led to the conclusion that the contribution of bedrock groundwater discharging at the submarine groundwater discharge (SGD) sites found in the Great Bay may be significant.

Discharging bedrock groundwater is thought to occur along the intertidal zone and below mean low water (MLW). The latter might be limited due to the clay-rich low permeability marine sediments deposited along the coastline forcing the groundwater to break above ground through less flow-resistant, highly-permeable, sand and gravel layers that are commonly found in the intertidal zone, resulting in occasional concentrated discharge zones. The discharge zones observed along the Great Bay shoreline were primarily concentrated discharge (rather than diffusive) reflecting the shallow depth to bedrock exerting control over flow patterns. Many diffuse discharge zones were also observed ubiquitously throughout the study area. However, areas with a diverse stratigraphy and/or bedrock influence can exhibit a combination of concentrated and diffuse discharge zones (Roseen, 2002).

During a tidal cycle, high salinity estuarine water is introduced into the aquifer at high tide that is flushed out at low tide by the greater aquifer piezometric head (Figure 2). A salt water wedge is formed when saline marine water displaces less dense groundwater from the aquifer. Since estuarine water salinity is far from being constant (14-32 ppt), the shape and position of the salt water wedge at particular locations within an aquifer is controlled primarily by the density of both seawater and groundwater and the rate and direction of regional groundwater flow (Freeze and Cherry, 1979).

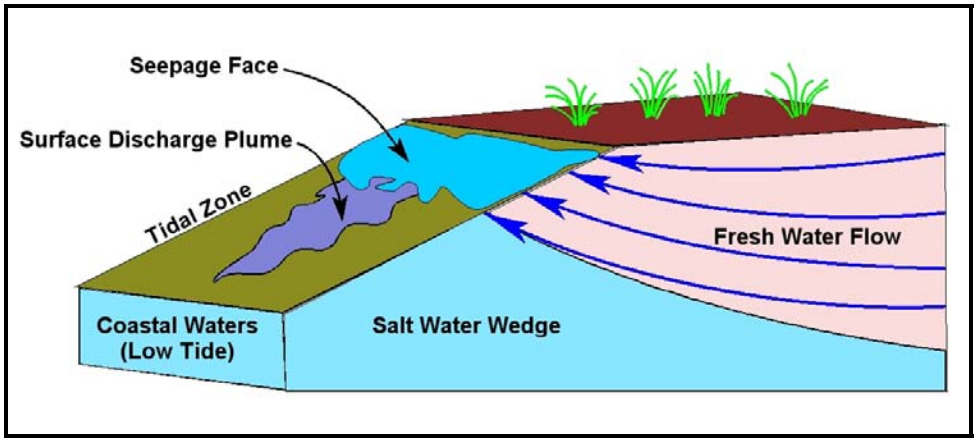

Figure 2: Schematic of mixed convection processes occurring at the groundwater discharge site (Roseen, 2002).

Land Use

The growth in population in southern New Hampshire over the past half century has had profound effects on the land-use and landscape of the region. With population growth comes new development for housing, commercial, industrial, and service land-uses. The additional population and demand for development has generated constant and

increasing pressure to convert open land, including existing agricultural and forestry lands in the region, into developed land (Rockingham Planning Commission, 2000). In 1940 the total population of the 27 communities in the Rockingham Planning Commission region was 42,769; 57 years later, in 1997, the population had nearly quadrupled to 169,960. Land use change data collected by this commission show dramatic declines in both agricultural (-62%) and forested land (-33%) losses between 1953 and 1982, and a corresponding rise in the developed land category. Using a recently released historic GIS-based land use coverage for the Strafford and Rockingham counties, interesting patterns are observed (Table 1) that verified previous analysis on this topic. Data in Table 1 was compiled for the towns of Dover, Madbury, Durham, Newmarket, Newfields, Stratham, Greenland, Newington and Portsmouth. The remarkable population growth observed from 1970 to 1990 throughout the watershed is reflected by the most recent land use distribution: residential, commercial, and industrial dominated the increases.

Table 1: Land use evolution (in percentage) based on historic GIS-based (1962, 1974, and 1998) coverage for Strafford and Rockingham Counties.

Land Use	Strafford County			Rockingham County		
	1962-1974	1974-1998	1962-1998	1962-1974	1974-1998	1962-1998
Residential	45.0	56.6	127.1	22.7	67.4	105.4
Industrial/commerical	67.6	53.6	157.5	84.2	99.0	266.6
Mixed Urban	0.5	17.0	17.6	0.3	-68.7	-68.6
Transportation/railrd	-9.4	22.9	11.3	-8.4	131.2	111.7
Agriculture	-28.9	-32.7	-52.2	-35.9	-39.4	-61.1
Forested	-2.7	-4.3	-6.9	6.9	-3.5	3.2
Water	0.8	5.8	6.7	0.9	0.5	1.4
Open Wetland	49.7	-10.4	34.2	3.9	7.9	12.1
Idle/other open	37.7	-23.0	6.0	23.2	-37.9	-23.5

As a general pattern for both counties, the extension of developed areas has increased over time with a concomitant loss of forested and agricultural lands. The New Hampshire Estuarine Project (NHEP) created different categories of sprawl indicators for the seacoast area of New Hampshire (NHEP, 2003). The category of land use and development included in that study revealed that eleven of the forty-two coastal towns included in the analysis had an increase in impervious area greater than the desired value of 10% (Figure 3); and also verified impervious surfaces and road miles as good predictors of sprawl. Associated with this increase in developed areas and population growth is the number of septic tanks for waste disposal and lawns that may result in increased non-point source impacts to ground and surface waters.

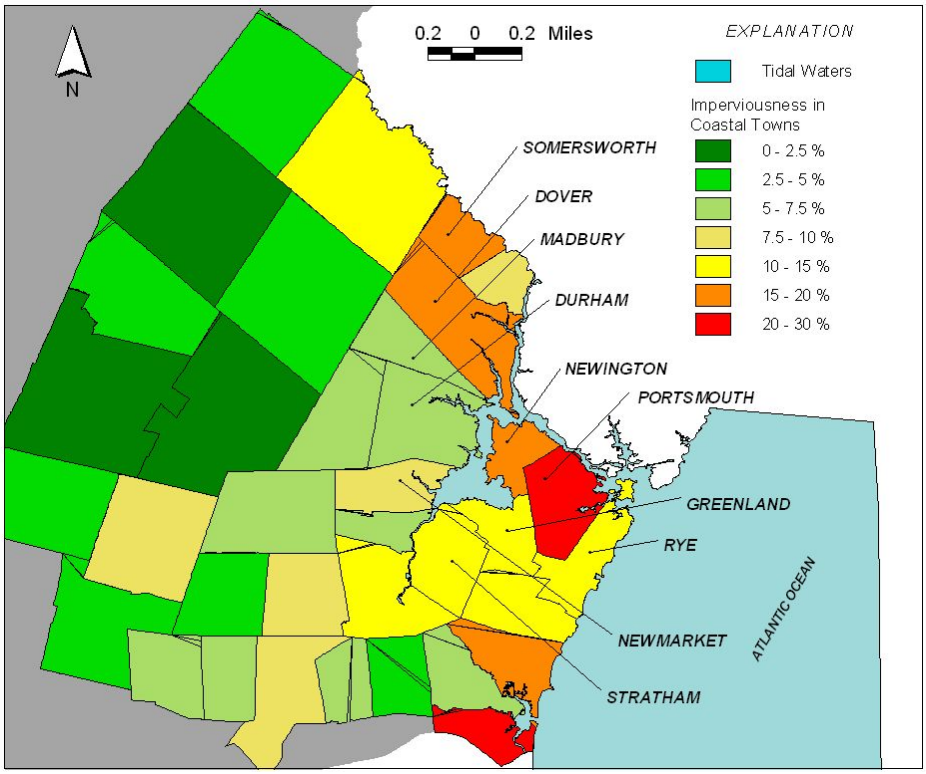

Figure 3: Spatial distribution of impervious surfaces (in percentage) in New Hampshire Coastal towns in 2000 (NHEP, 2003).

LAND USE-GROUNDWATER RELATIONSHIP STUDIES

The connection between the source of nitrate rich groundwater and contamination of coastal waters has recently been attracting the attention of local and nation-wide coastal managers (Frankic, 1999; Jones, 2000; Jones et al., 1996; Valiela and Bowen, 2002; Portnoy et al., 1998). This recent attention to coastal groundwater discharges is in part due to the difficult nature of quantifying groundwater discharge, and also in establishing a relationship between land use and the nutrient concentrations of the groundwater. The first difficulty has been addressed by previous research (Huntley, 1978; Banks et al, 1996; Portnoy et al., 1998; Roseen et al., 2002) in which thermal infrared (TIR) aerial photography was used to evaluate the inflow of groundwater to coastal systems. Unregulated sources of nutrient contamination are mostly non-point sources (NPS), including the atmosphere, groundwater, and runoff from roadways, agricultural lands, and residential lands. Nutrient pollution in estuarine environments is a well-known cause of eutrophication, contributing to increased algal and aquatic plant growth, and subsequently to oxygen-depleted waters. Non-point source contamination is a major cause of groundwater quality degradation and its relationship to land use has been well documented (Cain et al., 1989; Eckhardt and Stackelberg, 1995; Barringer et

al., 1990). This research addresses the relationship between nearshore land use and nitrate rich groundwater discharging into the Great Bay Estuary, NH.

There are several anthropogenic sources able to change the water chemistry of groundwater in surficial and deeper aquifers in the area of study such as: road salting; leaking from septic and fuel tanks; sewerlines; agricultural activities; and spills and leaks of chemicals near the land surface from other human activities (Robinson et al., 2004). Septic systems with inadequate design and those close to the end of their life spans are specific documented concerns as sources of contamination in coastal New Hampshire (Jones, 1998). About one-third of the rural and waterfront population (25 to 30 percent of the households) in the United States uses septic systems for wastewater disposal (U.S. Environmental Protection Agency, 2000). On-site sewage treatment is a common solution in most of the of the Great Bay watershed where few centralized water or sewer systems have been built. Jones and others (1996) assessed the movement of nitrogen, phosphate, and bacteria below septic systems at different sites in the Hampton Harbor area (coastal NH). They found that nitrogen species (DIN) migrate steadily and conservatively along the downgradient flow path from their respective effluent disposal areas. Closest to the leach field, nitrogen (as NH_4) dominated subsequently followed by NO_3-N that was diluted with regional groundwater flow but still exceeded the drinking water limit of 10 mg/L. Phosphate and bacteria, however, exhibited significant retardation with respect to the septic tank effluent. The retardation and their mixture with groundwater resulted with no-detectable levels in downgradient monitoring wells.

The effect of land use on underlying groundwater chemistry has also been investigated. Based on analyses of several compounds from 90 monitoring wells in a unconfined glacial aquifer intercepting five distinct land uses, Eckhardt and Stackelberg (1995) found that samples from the undeveloped areas have the lowest and smallest range in concentrations of several human-derived constituents (NO_3, B^{3+}, Cl^-); and, intermediate to high concentrations were found in suburban and agricultural land uses, with the widest variation. Concentrations of magnesium (Mg^{2+}), potassium (K^+), sulfate (SO_4^{2-}) and total dissolved solids were higher in sewered residential and commercial/industrial areas compared to other land uses, in a study at a sand-gravel surficial aquifer in Minnesota (Trojan et al., 2002). Trojan and others (2002) found a distinct fingerprint of high chloride (Cl^-), NO_3, boron (B^{3+}), and sodium (Na^+) for non-sewered residential areas; and, one of high B^{3+}, Ca^{+2}, Cl^-, NO_3^-, SO_4^{2-} and Na^+ for irrigated agricultural areas. Significantly greater arsenic concentrations were found in groundwater underlying agricultural land use than under developed areas along the New England coastal basins (Ayotte et al., 1999). The groundwater Arsenic concentrations were also significantly higher under one particular metasedimentary bedrock unit than under five other bedrock units in the study and it was in this particular unit where most of the agricultural land use occurred, which complicated the analysis of the arsenic source in drinking water bedrock wells. Ayotte and others (1999) statistically showed that these two high correlations with arsenic may exist simultaneously, by having a geologic arsenic source and an agricultural Arsenic source primarily present from the use of pesticides. Iron and manganese concentrations, in the same study, did not show any significant correlation with land use, and the differences observed were explained by a

lithogeochemical component. Nitrate concentrations measured in wells located in the metasedimentary bedrock unit (Ayotte et al., 1999) ranged from <0.05 mg/L to 9 mg/L with 65% of the sampled wells possessing a value lower than 0.05 mg/L, which can be considered as the native nitrate groundwater concentration.

The use of fertilizers in agricultural activities and their nitrogen input to groundwater has not been thoroughly quantified in the Great Bay watershed, as few farms are currently present compared with past land uses. The impact of the use of fertilizing and overwatering on nitrogen losses from home lawns, however, can also be important in large lot-size properties (Morton et al., 1988).

Recent research performed by Roseen (2002) identified and characterized submarine groundwater discharge (SGD) zones along the intertidal shore of the Great Bay Estuary with the use of thermal infrared (TIR) imagery and a GIS- based technique, verified with groundtruthing and piezometric monitoring. The TIR technique is based on the spatial variation of surface temperature taking advantage of the contrast between groundwater and estuarine water radiometric temperatures (Huntley, 1978; Banks et al., 1996). A total of 140-verified SGD sites were identified along the surveyed shoreline (Roseen, 2002). Groundtruthing characterization for some SGD sites involved the measurement of area, specific discharge, and temperature, and measurement of dissolved inorganic nitrogen (DIN). The level of nitrogen concentrations in the groundwater discharge to the bay averaged higher than those observed in all six tributary rivers to the Great Bay and Little Bay, accounting for 7.9% of the annual nitrogen loading; whereas the groundwater flow was only 3.3% of the freshwater flow. This relatively high nitrogen concentration at the SGD sites raised the questions about the spatial and temporal source of these discharging groundwaters.

METHODS

Using a multiple tracer approach, including major ion chemistry, chlorofluorocarbons (CFCs), boron, strontium, and oxygen and hydrogen isotopes, coupled with GIS-analysis and groundwater capture zone delineation, the question of whether or not land use practices affect the total contribution of nitrate-bearing groundwaters discharging to the Great Bay (NH) was investigated. Understanding the sources and timescales of nitrate contamination of groundwater contributions to the Great Bay is a tool that provides to coastal planners important information for the development of their management strategies to protect and eventually restore the water quality of discharging groundwaters.

SITE SELECTION

In complicated systems such as these, isolating the multitude of influential variables upon a system is unrealistic. Existing regimes included in the site selection were: seaward and landward sides of the bay, high and no nutrient contamination, areas with high and low volume discharge, and areas down gradient of developed and undeveloped lands. At least two sites for each of the specific hydrologic regimes within the Great Bay Estuarine system were considered. Seven SGD study sites were selected (Table 2). The intensity of flow and nitrate concentration, in Table 2, are based on the site characterization performed by Roseen (2002) classifying low, medium, and high specific discharges as those in the ranges of <22, 22-39, and 39< GPD/ft^2, respectively; and, low, and high nitrate concentrations those within the ranges: 0.01-0.10, and > 0.65 mg NO_3-N/L, respectively. Figure 1 shows the location of the monitoring network of SGD sites considered in the present study.

MULTITRACER APPROACH

Chlorofluorocarbons

CFCs as Environmental Tracers

Chlorofluorocarbons (CFCs; also called Freon or chlorofluoromethane) are manufactured volatile organic carbons used since the early 1930s as refrigerants, solvents, propellants, and cleaning agents. Their source is solely anthropogenic and they are also believed to catalyze the destruction of atmospheric ozone and are suspected to be a greenhouse gas (Rowland, 1991). CFC concentrations in the atmosphere have steadily increased ever since its early production. The most representative suite of CFCs used for refrigeration are CFC-12 (dichlorodifluoromethane, CF_2Cl_2), CFC-11 (trichlorofluoromethane, $CFCl_3$), and CFC-113 (trichlorotrifluoroethane, $C_2F_3Cl_3$), each

with relatively long estimated lifetimes of 45 ± 7, 87 ± 17, and 100 ± 32 years, respectively (Plummer and Busenberg, 1999, Fisher and Midgley, 1993).

Table 2. Land Use, hydrogeology, and water quality criteria for selection of SGD study sites.

Categories / Selected Sites	Spatial		Nitrate Concentration			Intensity of Discharge			Upgradient Land Use			
	Seaward	Landward	High NO_3	Low NO_3	Not Known	High	Medium	Low	Developed	Undeveloped	Agricultural	Recent LU Change
SGD 18.2.1	■			■			■			■		
SGD 19.3.1	■		■					■	■			
SGD 21.2.1	■		■				■				■	
SGD 31.4.1		■		■		■			■			
SGD 39.1.1.		■	■					■	■			
SGD 58.4.1		■			■			■				■
SGD 73.1.1		■		■			■		■			

The use of CFCs as environmental tracers of groundwater movement was first addressed by Thompson and Hayes (1979). Nowadays, several studies have proven the ability of CFCs to be used as a groundwater dating tool (Busenberg and Plummer, 1992; Dunkle et al., 1993; Ekwurzel et al, 1994) for young waters (<50 years of residence time).

Groundwater dating with chlorofluorocarbons in shallow aquifers assumes that CFC equilibrium existed between infiltrating water and the atmosphere, i.e. the groundwater age so-determined refers to the elapsed time since the infiltrating water was isolated from the unsaturated zone (recharging the aquifer at the water table interface) until it discharged to a well or spring where a sample is taken. This assumption only applies to areas with unsaturated thickness no deeper than 10 m (Cook and Solomon, 1995). For deeper water tables, due to the time lag between the ground surface and the water table, the CFC concentrations at the water table may be lower than the atmospheric concentrations, thereby assigning older recharge times than for the case of having a shallow saturated zone in which the lag time of transit through the unsaturated zone can be neglected.

The time history of atmospheric CFC concentrations and Henry's solubility law underlie groundwater dating with CFCs. Henry's law is:

$$p_i = \frac{C_i}{K_i} \qquad \text{(Eq. 1)}$$

where K_i is the Henry's law constant for the i^{th} CFC compound, p_i is the partial pressure of the i^{th} compound in a gas phase in equilibrium with water and C_i is the i^{th} concentration of the CFC compound. Solubility constants have been measured in water and seawater for CFC-12 and CFC-11 (Warner and Weiss, 1985) and for CFC-113 (Bu and Warner, 1995). A table summarizing the equation and fitting parameters for CFCs may be found in Plummer and Busenberg (1999) for the temperature-salinity relationship with K_i. Given the partial pressure (p_i) of the gas in air, from equation 1, and with the atmospheric (P) and water vapour (p_{H2O}) pressure conditions of a given location, the mixing ratios (pptv, i.e. parts per trillion in volume of dry air) for the i^{th} CFC, x_i, can be found by,

$$x_i = \frac{C_i}{K_i \cdot (P - p_{H_2O})} \qquad \text{(Eq. 2)}$$

To estimate K_i and the local water vapour pressure (p_{H2O}), the temperature and salinity of water at the time of recharge are required. For instance, solving the equations for K_i (0.0059 mol Kg^{-1} atm^{-1}) and $P_{corrected}$ or P- p_{H2O} (0.985 atm) (as in Plummer and Busenberg, 1999) given the local recharge temperature (see the Results chapter for more details on this temperature) and salinity of 8.4 ^oC and 0.0 ppt, respectively; a CFC-12 concentration in solution of 2.50 pmoles/Kg is obtained. Then, replacing these values in equation 2, yield the equivalent CFC-12 concentration in air from that in water, expressed in parts per trillion in volume (pptv).

The atmospheric source for CFCs (pptv) is relatively well known. The primary increasing trend (~1970-1990) is approximately linear. The CFC air growth curves (Figure 4) were developed by both actual air weekly measurements taken since 1976 (NOAA station at Niwot Ridge, CO) and reconstructing the series before 1976 from production data provided mostly by the Chemical Manufacturers Association (McCarthy et al., 1977; Fisher and Midgley, 1993).

When CFC concentrations are measured in water samples, and their equivalent in air are determined, they are compared with the respective growth curve (Figure 4) in air (or in water) to identify what is called the *apparent age*. Groundwater ages so determined do not account for transport processes that affect the CFC concentrations. Physical processes such as mixing and hydrodynamic dispersion; and chemical processes like sorption or degradation are not considered by this age. The apparent age assumes a piston-like flow moving through the aquifer from recharge to the sampling point.

In some areas where the infiltration is thought to occur rapidly, it is necessary to account for the amount of excess air introduced into the sample. Excess air is air that gets trapped in air bubbles during infiltration through the unsaturated zone and makes the concentration of dissolved gases in groundwater greater than the equilibrium solubility value. It is usually determined using the concentration of N_2 and Ar, which at the same time allows one to estimate the recharge temperature and altitude at which these gases were introduced into the water table. Excess air values are commonly as low as the analytical uncertainty of CFCs; henceforth they are often neglected. For example in the Mirror Lake study, Nitrogen and Argon bedrock groundwater samples plotted along the

line with atmospheric equilibrium (Busenberg and Plummer, 1996) and shallow wells showed little excess air (Goode et al., 1999). Recharge temperatures at Mirror Lake were estimated in 5 - 10 ^{o}C. This temperature is similar to the average annual ambient air temperature at that site.

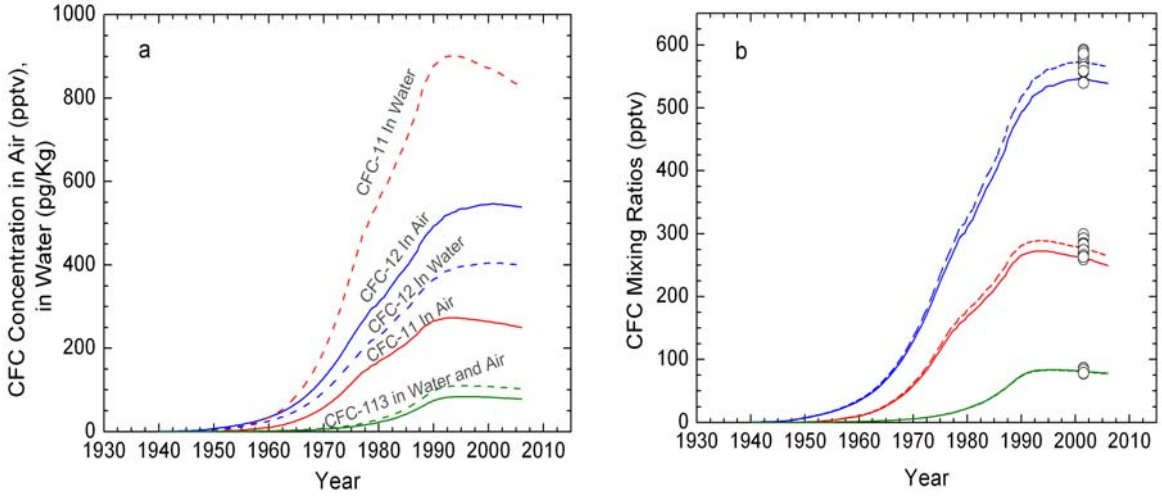

Figure 4. a) North American CFC-11 (red), CFC-12 (blue), and CFC-113 (green) growth curves in water (dashed lines) and air. Air concentrations were measured at NOAA station at Niwot Ridge, CO, and used by E. Busenberg (written communication April 13th, 2004); b) North American CFC growth curves in air (pptv) and local CFC-11, CFC-12, and CFC-113 concentrations in air samples (circles) taken at the University of New Hampshire campus on November 1st and December 5th of 2001 and analyzed by Climate Change Research Center (CCRC); dashed lines correspond to locally CFC-enriched growth curves (see Results chapter for further details)

CFC concentrations in water during their diffusive transit through the unsaturated and saturated zones may suffer alterations due to sorption in organic rich sediments, subsurface CFC sources (Thompson and Hayes, 1979), and degradation under anaerobic conditions (Goode et al., 1999). Sorption, which tends to mostly affect CFC-113 (Ciccioli et al., 1980; Bauer et al., 2001), may lead to an overestimation of the groundwater age. Degradation, which also depletes the CFC concentration under anaerobic conditions (<1.0 mg/L) was found to play an important role in formations that are overlain by glacial deposits in Mirror Lake, NH (Goode et al., 1999; Busenberg and Plummer, 1996). In the Mirror Lake study, CFC-11 and CFC-113 were absent and CFC-12 was reduced to one-third the concentration of modern air under anaerobic conditions. CFCs in uncontaminated sites were highly correlated with dissolved oxygen (DO). Methane was persistently detected in both anaerobic and aerobic samples; thereby indicating that at the saturated vadose zone interface, a mixing process existed. However, one quarter of the samples taken from piezometers at Mirror Lake were oversaturated with all three CFCs by several times the modern air concentrations. This high variability in CFC concentrations infers that a number of processes might be affecting the CFC advective transport in glacial drift environments.

Other non-atmospheric sources may also affect the concentrations of CFCs in surface and groundwaters (Schultz et al., 1976). It appears that sewage effluent is major contributor to CFCs in groundwater. Thompson and Hayes (1979) studied the source of a plume of CFC-11 in a residential area. CFC-11 and CFC-12 may be released to the ground from solvents, cleaning agents, and refrigerants. CFC-113 was used primarily by the electronics industry in the manufacture of semiconductor chips, for cleaning microelectronic components (Plummer and Busenberg, 1999). CFC-113-highly contaminated sites are often found at electronic component plants in the USA.

Models Used to Assess Groundwater Transit Times

As in other general studies, the SGD study sites of the present research can be classified as 'spring'-like discharge zones that assume completely different hydraulic conditions than artificially drilled wells. Meaning that what may be said about a sample taken from a well at a specific depth, most likely cannot be said about a sample from a spring. In terms of ground water age, the sample taken from a well might far better represent the age of the groundwater at a specific depth than a sample taken from a spring. At a spring, groundwater is confined in permeable sediments beneath impervious confining beds and is under sufficient hydrostatic pressure to rise to the surface in the overlying confining units (Rosenau et al., 1977). This forced convergence to the surface mixes the discharging groundwater with water at points far behind from the discharge zone thereby making the discharged water a mixture of ages. This justifies the use of several models to develop a more reliable value of mean transit time (or turnover time, mean residence time, age of water leaving a system, hydraulic age). The apparent age identified by the Piston-flow model is equivalent to the mean transit time since this model does not account for any alteration of the tracer in the groundwater system assuming that the travel time of the tracer is the same as the travel time of the groundwater; and because it is only dependant on the tracer atmospheric input function.

Lumped-parameter models (black-box models) have been used to describe groundwater discharge in tracer studies in order to identify water sources, interconnections of various systems, stratification, and mixing patterns (Maloszewski and Zuber, 1982). Several different models have been proposed to describe particular hydrogeologic settings, but all obey the convolution integral expressed as:

$$C_{out}(t) = \int_{-\infty}^{t} C_{in}(\tau) \cdot g(t-\tau) \cdot e^{-\lambda(t-\tau)} \cdot d\tau \qquad \text{(Eq. 3)}$$

or

$$C_{out}(t) = \int_{0}^{\infty} C_{in}(t-\tau) \cdot g(\tau) \cdot e^{-\lambda\tau} \cdot d\tau \qquad \text{(Eq. 4)}$$

where $C_{out}(t)$ and $C_{in}(t)$ are the output and input concentrations, respectively, and t is the calendar time or time of observation, τ is the time of entry, $g(t-\tau)$ (or $g(\tau)$) is the weighting function (also known as response function, transit time distribution, or residence time distribution (RTD)) defined as the transit time distribution function of a

tracer that entered the system at time τ. It is the function g(τ) that differentiates the various lumped-parameter models.
CFC–derived mean residence time can be determined using the following models (Figure 5):
i) Piston flow model (PFM), assumes steady state (recharge is equal to discharge) and the flow moves through the aquifer as an isolated plug until it discharges. Its response function is given by the Dirac delta function (∂):

$$g(\tau) = \partial(\tau - t_t) \qquad \text{(Eq. 5)}$$

In the case of a conservative tracer (no decay, sorption, or precipitation), $C_{out}(t)$ will match $C_{in}(t)$, the input function of the tracer.

ii) Exponential model (EM), which accounts for an exponential distribution of transit times, but no mixing of tracer occurs between the flow lines during transit. The EM model only accounts for mixing at the sampling site. EM creates short and unrealistic loops of flow lines close to the sample location without considering the part of the aquifer without the tracer, i.e. older CFC-free groundwaters (Maloszewski and Zuber, 1996). The EM response function is:

$$g(\tau) = \frac{1}{t_t} e^{\left(\frac{-\tau}{t_t}\right)} \qquad \text{(Eq. 6)}$$

iii) Combined exponential-piston flow model (EPM), was first introduced by Maloszewski and Zuber (1982) and resembles a well-mixed reservoir in series with a piston flow reservoir. Unlike the precedent models that have t_t as their only parameter, the EPM model also includes the parameter η, which is the ratio of the total volume to the exponentially distributed volume (with exponential transit times η). When η=1the EPM is the exponential model. For large values of η, the EPM model resembles the dispersion model (with low P_D value), which was not considered in this study.

$$g(\tau) = \frac{\eta}{t_t} \cdot e^{-(\eta\tau / t_t + \eta - 1)};\ for: \tau \geq t_t(1 - \eta^{-1}) \qquad \text{(Eq. 7)}$$
$$= 0;\ for: \tau < t_t(1 - \eta^{-1})$$

iv) Binary mixing model (BM), is not a lumped-parameter model but rather a simple binary mixture of groundwater from two end-member sources: a shallow reservoir recently recharged with young water and a deeper reservoir with water recharged with lower or tracer-free concentration (older than 50 years in the case of CFC's and tritium) concentration of the tracer (Busenberg and Plummer, 1999; Katz, 1999; Focazio et al., 1998).

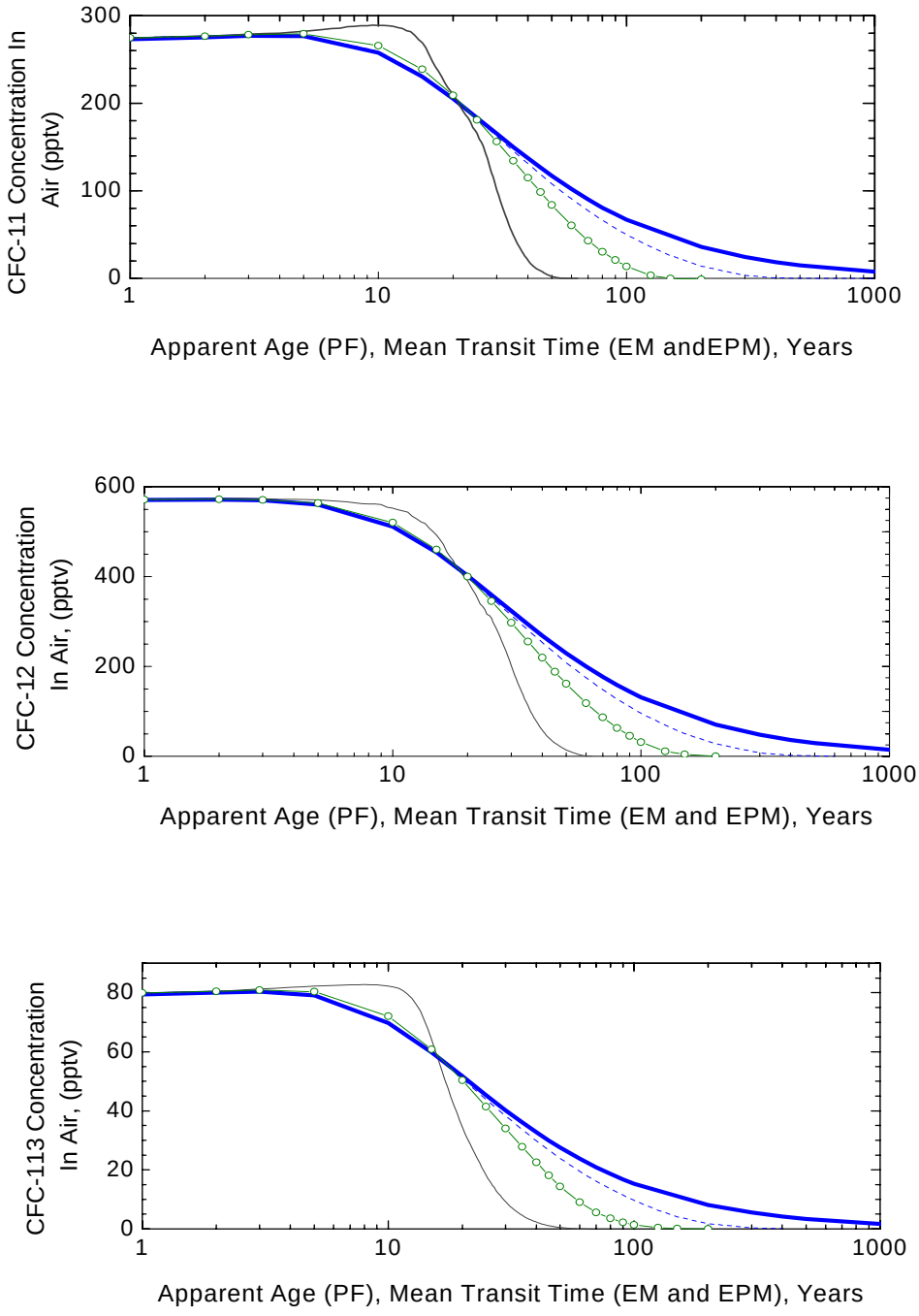

Figure 5. Distribution functions of apparent ages for Piston-Flow model (PFM in thin gray line) and mean transit time for Exponential Model (EM, in black thick line), and combined Exponential-Piston Model (EPM, in blue for $\eta = 1.1$ and green for $\eta = 1.35$).

The BM is expressed through the fraction of modern groundwater, f_{MG}, in the mixture:

$$f_{MG} = \frac{F_M - F_{OG}}{F_{MG} - F_{OG}} \quad \text{(Eq. 8)}$$

where F_M, F_{OG}, and F_{MG} are the CFC concentrations in the mixture (M), in the older groundwater (OG), and in the modern groundwater (MG), respectively.

In springs, the relation between apparent age and the actual groundwater residence time depends on the degree of mixing between two age-different waters.

Boron and Strontium Isotopes

Several studies have proven the ability of using boron isotopes as indicators of anthropogenic contamination from different sources (Vengosh et. al, 1994; Bassett et. al, 1995; Leenhouts et. al, 1998; Komor, 1997; Davidson and Bassett, 1993). Native groundwater has distinct differences in Boron isotope composition from these other sources: groundwater affected by sewage, agricultural activities, and sea brines or saltwater intrusion. Boron is a naturally occurring element in groundwater as a dissolved mineral from country rocks and from mixing with salty-meteoric waters. Boron moves conservatively along a sewage plume (LeBlanc, 1984) and hypothetical fertilizer source (Komor, 1997). Boron is mainly present in solution as undissociated boric acid $B(OH)_3$ and its conjugate base, tetrahedral borate, $B(OH)_4^-$ (Vengosh and Spivack, 1999). These Boron species regulate Boron fractionation; fractionation prefers ^{11}B (with 80.1% abundance) to dissolve boron in solution with trigonal coordination, thereby depleting ^{10}B (with 19.9% abundance) in solution but incorporating it on the solid phase with tetrahedral coordination, as most often found in clayey materials (Vengosh et al., 1994; Vengosh et al., 1999). Boron concentrations are not affected by oxidation/reduction, and evaporation but they are affected by mineral precipitation in extremely saline environments and by sorption on clay. The presence of boron in sewage-contaminated groundwater is due to its use in the form of sodium perborate as an oxidation-bleaching agent in domestic and industrial cleaning products (Vengosh et al. 1991) remaining unaffected, like other inorganic ions, during wastewater secondary treatment.

Vengosh and others (1994) showed that the boron isotopic compositions of sewage contaminated groundwater, native groundwater, and seawater ranged from 5.3 – 12.9 $^{o}/_{oo}$, ~30 $^{o}/_{oo}$, and 39 $^{o}/_{oo}$, respectively. In addition, Basset and others (1995) found that water affected by farm irrigation had a $\delta^{11}B > 40$ $^{o}/_{oo}$. The boron concentration and its isotopic composition together with strontium isotopes and other more conventional tracers (Cl^-, Br^-, NO_3, $\delta^{18}O$, $\delta^{2}H$) were incorporated into the current study to recognize the evidence of septic tank effluent and moderate agricultural activity as possible dominant sources of nitrate contamination of groundwater discharged to the Great Bay Estuary, NH and to quantify their fractions in groundwater samples. The mixing ratios of two or more waters with distinct isotopic ratios can be estimated using the mixing equation of end-member waters:

$$\delta^{11}B_{mixed} = \frac{\sum_i (\delta^{11}B_i)(B_i)(VF_i)}{\sum_i (B_i)(VF_i)} \quad \text{(Eq. 9)}$$

where *i* is the end-member component with the respective δ^{11}B, B (boron concentration) and VF (volume fraction) values. This equation assumes complete mixing without chemical reaction and that only the considered end-member components comprise the resulting sample.

Groundwater samples from overburden and bedrock wells, for these analytes, are expected to represent the surrounding targeted land uses (residential, residential mixed, agricultural, and undisturbed) in agreement with their respective local and regional scales. Consequently, to use the Boron isotopic technique together with common general chemistry to track the sources of nitrate that have affected native groundwater source, sampling of these potential end-member waters was performed. A well at Fabyan's Point (Newington, NH) used for the Bedrock Bioremediation Project (BBC, University of New Hampshire) as a native (undisturbed) groundwater source was included in this study (identified as BK4N). BK4N water samples exhibited no evidence of being affected by any anthropogenic activity based on a long-term water chemistry and microbiological database. Likewise, septic tank effluent from two different sites STE1 and STE2 and high nitrate-bearing groundwater wells W1076 (5.18 mg NO_3/L) and W 1160 (10.20 mg NO_3/L) were sampled to target either a distinct or overlapping boron isotopic fingerprint among these possible end-members.

Strontium isotopes have been used in groundwater studies, mainly to describe water-rock interaction when tracing the relative contribution of carbonate and silicate lithologies to water chemistry (dissolved ions, unlike water stable isotopes that trace the source and pathway of H_2O molecules) and mixing processes of different groundwaters (Lyons et al., 1995; Frost and Toner, 2004; Banner, 2004; Negrel et al., 2001; Vengosh et al., 1999; Pretti and Stewart, 2002). The Strontium isotope ratio, $^{87}Sr/^{86}Sr$, varies accordingly to both the original amount of Rubidium-87 (^{87}Rb) in a given rock or soil (at the time of its formation), which decays to Strontium-87 (^{87}Sr); and the fact that Strontium-86 (^{86}Sr) is one of the non-variant Sr isotopes. With time $^{87}Sr/^{86}Sr$ ratios of Rb-bearing minerals increase as ^{87}Rb decays to ^{87}Sr, leading to distinct $^{87}Sr/^{86}Sr$ ratios. The Strontium isotope ratio is not affected by fractionation or by mineral precipitation of the Sr in water and is only modified by dissolution of minerals and ion exchange reactions as a Sr-bearing mineral reacts along a groundwater flowpath (Bullen et al., 1996; McNutt, 2000). The distribution of Strontium in rocks is controlled by the extent to which Sr^{+2} can substitute for Ca^{+2} in calcium-bearing minerals (both ions have similar ionic radius, 1.13 and 0.99 Å, respectively), and the degree to which potassium feldspar, muscovite, and biotite substitute K for Rb (Faure and Powell, 1972). In general, low $^{87}Sr/^{86}Sr$ ratios are typical for groundwater flowing through a carbonate aquifer due to the ready enrichment of the Sr concentration in water. On the other hand, silicate groundwaters tend to have higher $^{87}Sr/^{86}Sr$ ratios and lower Sr concentrations (McNutt, 2000). Soil composition, in addition to the overall mineralogy of igneous and metamorphic rocks, marine carbonates, and evaporites, is also a controlling factor of the $^{87}Sr/^{86}Sr$ values.

Oxygen-18 and Deuterium

Oxygen-18 and deuterium have been widely used as environmental tracers in surface and groundwater hydrology (Clark and Fritz, 1997; Fritz and Fontes, 1980) in identifying groundwater sources and flow paths, freshwater-groundwater interaction, seasonality of recharging waters, and determination of groundwater velocities (Coplen and Kendall, 2000). While most oxygen and hydrogen atoms have a mass of 16 (8 protons and 8 neutrons) and 1 (1 proton and 1 neutron), respectively, a small number of oxygen and hydrogen atoms have a mass of 18 (8 protons and 10 neutrons) and 2 (1 proton and 2 neutrons). Water molecules in the ocean may contain either isotope for each element, in the species: $^{1}H_2{}^{16}O$, $H_2{}^{18}O$, and $^{1}H^{2}H^{16}O$. However, as water evaporates from the ocean surface a larger amount of $H_2{}^{16}O$ is evaporated compared to $H_2{}^{18}O$, this is because it is easier for lighter water molecules to evaporate needing less kinetic energy to go into gaseous state than the molecules composed of the heavier isotopes. Henceforth, as air masses move across continents and lose water through rainfall, they become depleted in the heavier isotopes that are hold more easily by the liquid phase (Kendall and Caldwell, 1998). Therefore, geographic and temporal variations are observed in the stable isotopic compositions of meteoric water. These variations are identified by: the continental effect, the elevation effect, the latitude effect, and the amount effect (Ingraham, 1998), where all are the result of temperature variations and air mass transport.

When plotting the stable hydrogen and oxygen isotopic concentrations in rainfall event from all over the world, the scattered data follows a linear relationship summarized by Rozanski and others (1993) that was called global meteoric water line (GMWL). However, when describing the isotopic composition of a specific region a local meteoric water line (LMWL) is required.

Water stable isotopes are effective and conservative tracers of mixing processes at the seawater-groundwater interface (IAEA, 2000). Oxygen and hydrogen isotopic compositions from two end member waters usually follow a mixing line, which makes them a powerful tool in studying paleowater-groundwater and seawater-groundwater interactions.

Chloride

Chloride is the most widely used environmental tracer and originates in precipitation and dry fallout and is transported into the subsurface with infiltrating water (Scanlon, 1991). The unsaturated zone prints the most distinctive geochemical characteristics on groundwater. The geochemical evolution in the saturated zone is less intense, but follows progressive changes in water quality towards areas of discharge (Herczeg and Edmunds, 2000). Chloride is an inert and highly soluble tracer that remains conservative in its passage to the unsaturated zone, unless halite soils are present. Chloride concentrates in the unsaturated zone due to evaporation and evapotranspiration. Chloride concentrations in unsaturated zone pore water are inversely related to recharge: high chloride concentrations indicate low recharge rates because chloride accumulates in the subsurface as a result of evapotranspiration whereas low chloride concentrations indicate high recharge rates because chloride is flushed through the subsurface (Scanlon, 1991; Scanlon, 2000). Chloride has been used in several studies to trace anthropologic

impacts and sources of contamination for its conservativeness and mobility in water very similar to the water molecules.

MONITORING NETWORK

Groundwater samples were collected from a monitoring network specifically installed for this study at seven submarine groundwater discharge zones (SGD) within the intertidal zone of the Great Bay Estuary, NH. These samples underwent chemical and isotopic analyses. Ideally, a SGD site was defined as having two small diameter wells (SDWs) set in the SGD, plus one SDW intercepting upgradient overburden groundwater and one upgradient bedrock well (Figure 6). A SDW is a 1-inch inside diameter stainless steel well with a 3-foot long screen. SDWs were driven in manually by using a slam bar, to a depth just below the water table or to a low-content salinity water layer. Upgradient SDWs were thought to target flow paths of specific land uses to quantify their water chemistry component on the discharging water to the Great Bay. Only two sites out of seven were completed this way.

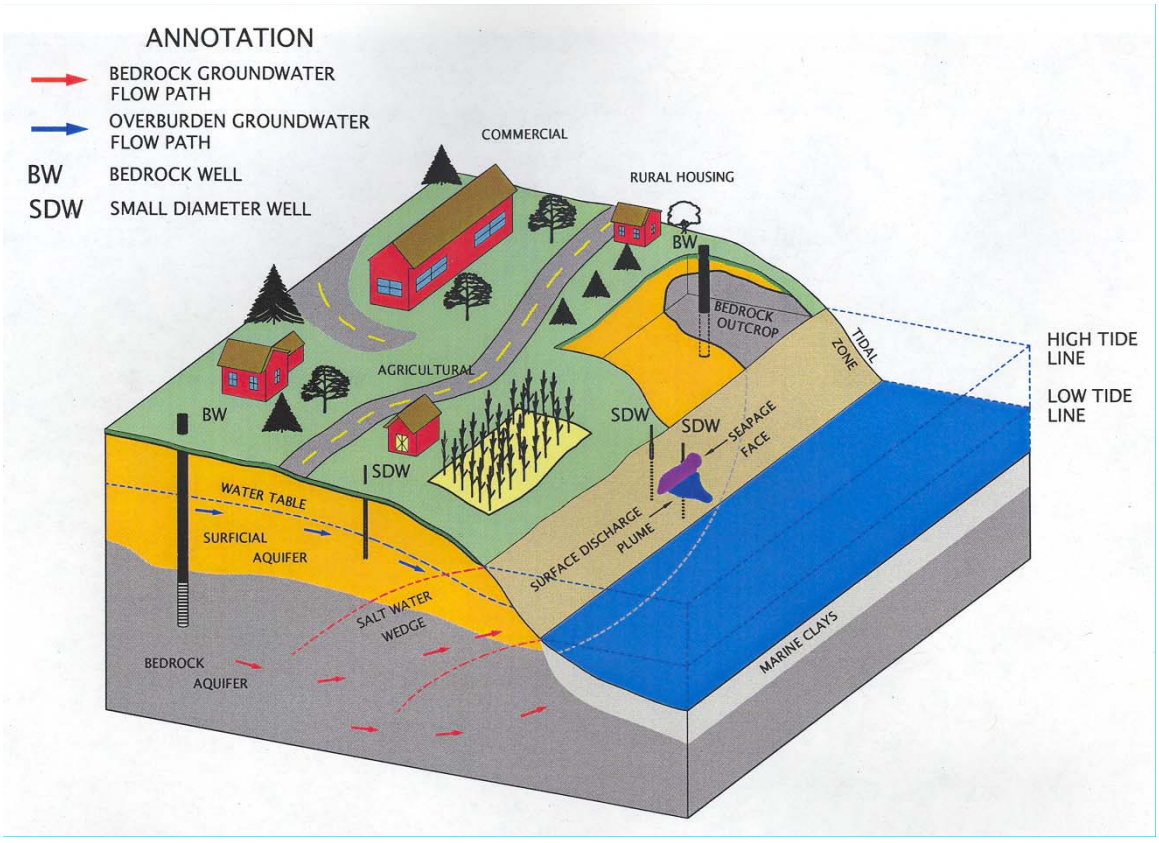

Figure 6: Block diagram representing the general experimental design for the project. Notice two SDWs in the intertidal zone, one SDW and one bedrock well (BW) upgradient from the discharge zone.

There were a variety of reasons for deviating from installing upgradient SDWs and most of the reasons were due to the spatial variability of each site with respect to the targeted groundwater discharge zone. In spite of having checked and revised the soil survey maps for selection of the area before going to the field, extended vertical layers of very stiff material made it difficult, and in some cases impossible, to manually install the SDWs deeper than 5-7 feet. In addition, the period of the year at which this activity was performed (Fall) had the water table at its greatest depth. In general, areas located at the south of SGD 21.2.1 (see Figure 1) did not have an overburden layer deeper than 2 feet. On the other hand, SDWs were installed into the ground as deep as 27 feet below the surface and no water table was found in the Newington area upgradient from site SGD 39.3.1. There were some ideal locations (proximity to targeted land uses and SGD sites) that were expected to obtain positive responses from the community, but this did not happen. This situation prevented monitoring specific land uses such as agricultural in sites SGD 31.4.1 and SGD 21.2.1.

WATER CHEMISTRY SAMPLING

Groundwater samples for CFC analyses at the GWDZs were taken during 8/28/2003 to 8/31/2003. At the time of sampling, low tide conditions were always sought in order to guarantee maximum freshwater upwelling. Freshwater upwelling was monitored by measuring conductivity/salinity, temperature, and in some cases pH. Samples were taken when these readings stabilized. Three or more well bore volumes were purged before sampling. Purging was accomplished by using a peristaltic pump with Viton tubing. This suite of sites was sampled by one of two methods of collection: a) using two 100-mL syringes and b) using two 100-mL glass bottle with foil-lined caps. Four samples for each sampling site were collected. This latter method had just recently been developed by the Dr. Busenberg's USGS CFC Laboratory at Reston, VA. Samples were promptly shipped and analyzed for CFCs after collection by the Tritium Laboratory at the University of Miami. The remaining set of CFC samples were taken during 11/16/2003 to 12/1/2003 for overburden SDWs and bedrock wells using the glass bottle with foil-lined cap method. Purging was consistant with the previous sampling events. Domestic bedrock wells were sampled using the existing pumps and taking the sample as close as possible to the wellhead before any treatment process. When sampling for CFCs out of the faucet, copper tubing was attached to the faucet using a commercial copper-made coupling. The Dissolved and Noble Gas Laboratory (University of Utah) analyzed these samples using a purge-and-trap gas chromatography procedure with an ECD detector following analytical procedures detailed by Busenberg and Plummer (1992). Nitrogen and Argon gas samples for determining the amount of excess air in groundwater were not taken for this study.

Samples for major ion chemistry (NO_3, NH_4, SO_4, Na, K, Mg, Ca, Br, Cl, F, Fe, SiO_2) and Boron and Strontium isotopes were filtered in the field through a pre-combusted GF/F 0.45 μm glass microfibre filters, collected in fresh manufacturer pre-cleaned HDPE 250-mL sample bottles and analyzed by ion chromatography (Hewlett Packard – Liquid Chromatograph with 712 WISP autosampler) at the Water Quality Analysis Laboratory (University of New Hampshire). No preservatives were used at the time of sampling. Due to the relatively high salinity content of a few samples, the ion

chromatography technique did not work well for a good number of ions; therefore a private laboratory (Resources Laboratory Inc.) with an inductively coupled plasma mass spectrometer (ICP-MS) facility was contracted to perform these analyses. Dissolved oxygen concentrations in samples were checked to be above 1.0 mg/L using a colorimetric technique (Chemets Kit). Groundwater samples for alkalinity were analyzed in the Environmental Research Group Laboratory using automatic titrators. Boron isotopes were measured by negative thermal ionization mass spectrometry (NTIMS) at the USGS Isotope Lab (Menlo Park, CA) using procedures described by Vengosh et al. (1989). Duplicate analyses were performed for each sample when determining the isotopic composition of both Boron and Strontium agreeing within 1 $^{o}/_{oo}$ and 0.00002, respectively. Isotopic ratios are reported as $\delta^{11}B$ and $^{87}Sr/^{86}Sr$, where $\delta^{11}B$ is:

$$\delta^{11}B(^{o}/_{oo}) = \left(\frac{(^{11}B/^{10}B)_{sample}}{(^{11}B/^{10}B)_{NBS951}} - 1 \right) \cdot 1000 \qquad \text{(Eq. 10)}$$

The stable isotopes of Oxygen ($^{18}O/^{16}O$) and Hydrogen ($^{2}H/H$) are used in this study to determine the origin of waters. Groundwater samples for $^{18}O/^{16}O$ and $^{2}H/H$ were collected in pre-cleaned 20mL vials without any preservative, stored, and analyzed by the Environmental Isotope Geochemistry Laboratory (University of Arizona) with an analytical precision of 0.08 and 0.9 $^{o}/_{oo}$, respectively. The ratios of stable isotopes are expressed using the delta (δ) notation in parts per thousand relative to Vienna Standard Mean Ocean Water reference and normalized on scales such that the Hydrogen (δD) and Oxygen ($\delta^{18}O$) isotopic composition of Standard Light Antarctic Precipitation (SLAP) reference water: –428 % and –55.5 %, respectively (Coplen, 1994; Coplen and Kendall, 2000).

DELINEATION OF CAPTURE ZONES

Groundwater capture zones (GCZ) for the SGD study sites were delineated using the computer program WhAEM2000 (version 3.1.1) released by the Environmental Protection Agency (USEPA). WhAEM was meant to be used to comply with the Wellhead Protection Programs (WHPP) and Source Water Assessment Planning (SWAP) for public water well supplies in the United States (Kraemer et al., 2004). The geohydrologic modeling approach of WhAEM2000 was used for delineating the capture zone areas in the present study. This modeling technique employs the analytical element method (AEM), which consists of the superposition of analytic functions to create an approximate, but analytic solution to the regional groundwater flow problem (Haitjema et al, 1995; Strack, 1989). Flow hydrogeologic features such as rivers, lakes, and no-flow boundary conditions are called *analytic elements* each of which is represented in the model by an *analytic function* (Haitjema, 1995). In the model, flow is considered to be essentially horizontal and follows the Dupuit-Forchheimer assumptions for the groundwater flow equation. By neglecting resistance to vertical flow, heads are constant in the vertical, conveniently eliminating one dimension in the differential equation (Kraemer, 2004),

$$\frac{\partial^2 \phi}{\partial x^2} + \frac{\partial^2 \phi}{\partial y^2} = -N \qquad \text{(Eq. 11)}$$

where Φ is the discharge potential which is $\Phi = kHh$, for confined flow, or $\Phi = (1/2)kh^2$, for unconfined flow.

The use of a model based on the AEM has the advantage of being more accurate because of the analytical solution and there is no need to discretize or grid (no finite difference grid or finite element mesh) the groundwater system (Haitjema et al., 2000). Hydrogeologic features are represented through analytic elements such as wells, line sinks, area sinks, horizontal barriers, and inhomogeneties. Inhomogeneties can be used to account for areas with different hydraulic conductivity, porosity, thickness, and recharge rate. Line sinks represent rivers or channels and their input parameters are the starting and ending heads that can be extrapolated from the DLG (digital line graphs) contour lines intercepting these features. The head values used to trace rivers in WhAEM2000 serve as topography constrains for the immediately surrounding and far-field areas away from the modeled site. Likewise, as in previous generations of wellhead protection models, the effect of several discharging wells (well interference) is also accounted for.

The graphical interface for WhAEM2000 is based on a BBM (binary base map), which is a compressed form of DLG (digital line graph) maps where hydrography, topography, and other line features are included. The graphical interface for the Great Bay area is shown in Figure 7.

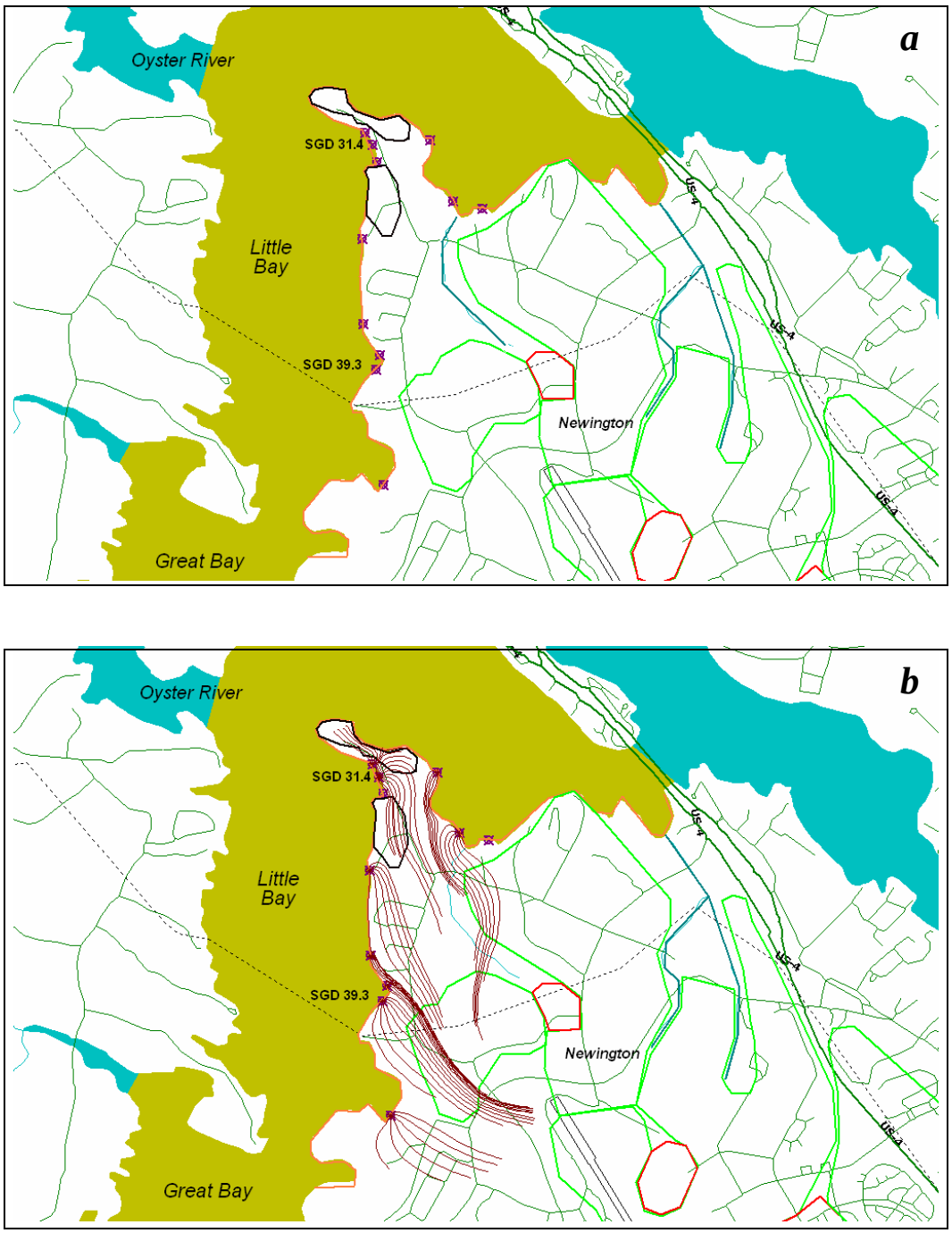

Figure 7. Example of WhAEM2000 graphical interface; a) hydrogeologic analytic elements for the sites SGD 31.4 and SGD 39.3 in the Great Bay area, inhomogenity areas in green represent semi-permeable soils (K < 40 ft/day), those in red represent sand-gravel pockets (100 ft/day); horizontal barrier along the shore in orange; line sinks in blue; and wells representing surrounding SGD sites; b) multiple particle tracing delineating capture zones for each SGD.

RESULTS

MULTITRACER APPROACH

Chlorofluorocarbons

An average annual air temperature of 8.4 ^{o}C (within the range 5 – 10^{o}C found at Mirror Lake by Goode et al., 1999, and Busenberg and Plummer, 1996) was used as the approximate temperature that occurred at the air-water interface during recharge (recharge temperature). This average temperature was based on the period of average annual values 1970-2002 recorded at the Durham (NH) NOAA station (ID: 272174) together with an altitude of recharge 24 m (80 ft, elevation at the Durham's NOAA station) to relate the concentrations of CFC in water (pg/kg) to the equivalent mixing ratios in air (pptv) by Henry's Law (Table 3). The Climate Change Research Center (CCRC) at the University of New Hampshire campus took nineteen air samples (Figure 4) during November and December of 2001 and analyzed for CFC-11, CFC-12, and CFC-113 concentrations. These samples revealed enrichment with respect to the North American growth curves (NOAA station at Niwot Ridge, Elkins et al. 1993) of 6% and 5% higher than the CFC-11 and CFC-12 growth curves. Johnston and others (1998) and Szabo and others (1996) also reported local enrichments of 10% and 4% in CFC-12 mixing ratios at Waterloo, Canada and in the Delmarva Peninsula air samples, respectively. Enrichments of CFC's in local air occur frequently at urban areas and adjacent vicinities. The one in the Great Bay area might be moderately influenced by being downwind of major metropolitan areas such as Boston, which is 60 miles away south. The identified local enrichment data was used to modify the CFC growth curves (Figure 4b).

Seventeen groundwater samples were analyzed for CFC-11, CFC-12, and CFC-113; data are shown in Table 3. Mixing ratios (pptv) and CFC-modeled recharge dates in Table 3 are based on enriched growth curves without considering the effect of excess air. CFC-modeled recharge years were expressed in terms of $\pm \sigma$ (standard deviation) based on the observed variability of three replicates in groundwater concentrations. CFC mixing ratios were highly variable ranging from 7.2 pptv to maximum values of 933.0, 2944.7, and 650.0 pptv for CFC-11, CFC12, and CFC-113, respectively. Modern water is defined as the water that recharged during the period in which the CFC mixing ratios in the atmosphere stopped increasing, reached a plateau, and started decreasing. This modern period started at different years for every CFC: 1994, 2001, and 1995, reaching concentrations at the plateau of 301.0, 583.0, and 86.1 pptv for CFC-11, CFC-12, and CFC-113 respectively.

Table 3. CFC-11, CFC-12, and CFC-113 concentrations in water, equivalent atmospheric partial pressure (for a recharge temperature and elevation of 8.4 °C and 24 m, respectively), and CFC-derived groundwater apparent age from bedrock wells (BK), shallow wells (NC) and wells at the submerged groundwater discharge (SGD) zones and Great Bay (GB) surface water. **[Contam.: concentration above maximum concentration in atmosphere: 311.6 pptv (CFC-11), 604.2 pptv (CFC-12) and 91.08 pptv (CFC-113); Mod or Modern: concentration in the decreasing limb of concentration in the atmosphere younger than 1994 (CFC-11), 2001 (CFC-12), and 1995 (CFC-113); Mod/Contam when two samples were Modern and one sample was Contam.; Contam/Mod when two samples were contaminated and one was Modern]**

Sample Name	Sampling Date	DO	CH4	Enriched Concentration in Solution in pg/kg			Calculated Atmospheric partial pressure in pptv			CFC-Piston Modeled Recharge Dates		
		mg/L	ug/L	CFC-11	CFC-12	CFC-113	CFC-11	CFC-12	CFC-113	CFC-11	CFC-12	CFC-113
BK1D	11/26/2003	>1.0	<10	707.1	325.6	17.2	226	459.8	13	1985.0 ± 0.3	1987.0 ± 0.6	1976.0 ± 0.6
BK2N	11/26/2003	>1.0	<10	852.2	2,085.30	76.3	272.3	2944.7	57.4	1988.5 ± 1.4	Contam.	1987.5 ± 0.3
BK3S	12/1/2003	>1.0	N/A	132.9	374.2	64.4	42.5	528.4	8	1967.5 ± 0.8	1990.5 ± 1.2	1972.0 ± 1.4
BK4N	11/26/2003	>1.0	<10	670.9	347.5	95.8	214.4	490.8	68.3	1984.0 ± 0.3	1988.0 ± 0.3	1989.0 ± 0.5
BK5D	11/25/2003	>1.0	<10	725.4	498.1	864.5	231.8	703.4	64.1	1985.5 ± 0.0	Contam.	1988.0 ± 0.3
NC1D	11/16/2003	>1.0	<10	538.1	430.1	10.6	171.9	607.3	48.4	1979.0 ± 0.5	Modern	1986.0 ± 0.5
NC2S	11/18/2003	>1.0	N/A	365.7	960.7	103	116.9	1356.6	72	1974.5 ± 0.8	Contam.	1989.5 ± 0.5
SGD 18.2U	8/31/2003	>1.0	N/A	789	349.3	90.8	252.1	493.2	53.5	1987.0 ± 0.0	1988.5 ± 0.8	1986.5 ± 19.5
SGD 19.3D	8/31/2003	>1.0	N/A	1,889.30	475.7	102	603.7	671.7	50.9	Contam.	Contam.	1986.5 ± 19.2
SGD 21.2	11/24/2003	>1.0	<10	998.1	420.4	85.2	318.9	593.7	76.7	Contam./Mod	Mod/Contam.	1990.5 ± 0.4
SGD 31.4U	8/29/2003	>1.0	<10	1,718.80	356.4	82.3	549.2	503.2	56	Contam.	1989.0 ± 0.5	1987.0 ± 0.3
SGD 39.3D	8/29/2003	>1.0	<10	1,113.60	1,436.00	74.5	355.8	2027.8	61.8	Mod/Contam	Contam.	1988.0 ± 0.0
SGD 58.4	8/31/2003	>1.0	20	216.5	192.5	71.2	69.2	271.8	7.6	1970.5 ± 1.3	1976.5 ± 0.9	1972.0 ± 0.8
SGD 73.1D	9/1/2003	>1.0	N/A	1,754.60	769.2	67.7	560.7	1086.3	492.7	Contam.	Contam.	Contam.
SGD 73.1D	11/30/2003	>1.0	N/A	2,919.70	905.8	10.1	933	1279.1	650	Contam.	Contam.	Contam.
SGD 73.1U	11/30/2003	>1.0	N/A	628.7	638	655.3	200.9	901	77.4	1982.5 ± 0.3	Contam.	1990.5 ± 1.8
GBW1	9/1/2003	>1.0	N/A	571.4	229.5	144.1	217.6	384.8	129.6	1984.0 ± 0.3	1983.0 ± 0.5	Contam.

Contaminated samples (i.e. Contam.) are those exceeding these latter, maximum values, indicating that their equivalent water concentrations are not in equilibrium with the atmosphere. These samples presumably found other, non-atmospheric sources of CFCs during their transit through the unsaturated and saturated zones. They cannot be interpreted with regard to groundwater residence times. Among the three CFCs, CFC-12 was the most frequently contaminated in the groundwater samples (47.1 % or 8 samples) followed by CFC-11 (29.4% or 5 samples), and lastly CFC-113 (17.6% or 3 samples). The CFC-12 apparent ages underestimates the apparent age, on average, by 6 years estimated from CFC-11 and CFC-113. CFC-11 and CFC-113 apparent ages differ on average by 3.3 years, being the group of CFCs with better consistency between each other.

The fact of finding such a large percentage of contaminated samples was surprising. CFC degradation was expected instead, as was found at Mirror Lake, NH. A threshold in dissolved oxygen (DO) of 0.5 mg/L was identified in the Mirror Lake studies (Goode et al. 1999) above which CFC concentrations are still detectable and useful for groundwater dating. The DO levels in all the sampled sites in the Great Bay were higher than 1.0 mg/L. Methane concentrations at these sites were either low (20 ug/L, SGD 58.4) or below the detection limit (for the rest of the samples), indicating that no significant anaerobic decomposition process occurred in the groundwater samples. Among the CFCs, CFC-11 is the most significantly depleted under scarce oxygen conditions because of its high solubility in water. CFC-11 was the second least contaminated of the CFCs, and given the observed DO and methane levels, CFC-11 was not expected to have been degraded in the aquifer systems.

With the exception of BK1D, CFC-11 gives the oldest apparent age for all sampled bedrock and shallow wells. This might suggest that some CFC reduction has taken place. Iron concentrations are low (< 0.1mg/L) in most of the samples except for SGD 31.4U (0.58 mg Fe/L) and the septic effluent at Jackson Laboratory (0.55 mg Fe/L). It is unlikely that an iron-reducing environment exists at SGD 31.4U site since DO > 1.0 mg/L, methane was below detection limit, a significant content of nitrate (no denitrification) and sulfate (no reduction to sulfide) were present in the sample (Lovley and Phillips, 1987) and in addition, the CFC-11 concentration was well above atmospheric equilibrium.

Sorption, that mostly affects CFC-113, is a process that is difficult to monitor either in the field or using other chemical parameters as indicators; only apparent age data reflect whether this phenomena has occurred with any significance. Bedrock and shallow wells showed detectable CFC-113 concentrations and no contamination was present in the shallow wells. In most of the studies (Ciccioli et al., 1980; Bauer et al., 2001) that looked at transport retardation of CFC-113 due to adsorption to the aquifer materials, it appears to systematically be the only CFC not contaminated, but depleted to a level yet able to date the groundwater. This was not the case with the data presented in Table 3. CFC-11's apparent ages are, in 8 samples, older than those of the other two CFCs, whereas CFC-113's apparent ages are older than the other CFCs in 7 samples. Except for BK1D, in all samples the CFC-113-derived apparent age either moderately agrees with other CFC-derived ages (BK2N, SGD 18.2U, SGD 31.4U, and SGD 58.4), underestimates the age with respect to another CFC (BK3S, BK4N, BK5D, NC1D,

NC2S, and SGD 73.1U) or remains as the only CFC able to date the groundwater (SGD 19.3D, SGD 21.2, and SGD 39.3D).

There might be a very site-specific combination of factors that has led to the discrepancies observed among the CFC-derived apparent ages for a given sample. Unfortunately, DO measurements were only noted as to whether the concentration was above or below 1 mg/L, thus a more accurate value would have given a better idea of how oxic or close to anoxic the environment was at the location of the groundwater sample. CFC-11 concentrations should be looked at from the perspective of an incomplete monitoring of possible reducing environments. CFC-12 has been reported in other studies to be affected by degradation to a lesser degree, but by having almost 50% of the samples contaminated with CFC-12 it is clear that degradation is not the prevailing factor. Lastly, quantifying sorption is a difficult task that implies the use of multilevel sampling to monitor changes in CFC-113 concentrations along the infiltrating flow path. Organic matter content is a good proxy in some environments, but it was not used in this study. However, the sources of the significant contamination of CFC-12 as well as for the other CFCs in some particular samples remains unknown.

Additional CFC data analysis is presented in Table 4. The CFC data shown in Table 4 are expressed in terms of the percentage of modern water present in the sample using the steady mixing ratios (in pptv calculated at equilibrium with the measured concentration in water at 8.4 ^{o}C) reached in 1994 by CFC-11, CFC-12, and CFC-113 when their accumulation in the atmosphere became stable before it started decreasing as a result of the ban on their production in the late 1980's. Also shown in Table 4 are modeled ages using different transit time distributions functions (Figure 5): piston (PFM), exponential (EM, E. Busenberg, written communication, 2004 and with the aid of the FLOWPC program (Maloszewski and Zuber, 1996)) and combined exponential-piston (EPM) for η=1.1 and η =1.35 (using FLOWPC program), and apparent ages using the ratio curves of two CFCs (Plummer et al., 1998). From the percentage of modern atmospheric (PMA) water values, in Table 4, it is easy to visualize that there are samples with a high degree of oversaturation (contamination) 3.2, 5.1, and 7.9 times the atmospheric equilibrium concentrations for CFC-11, CFC-12 and CFC-113, respectively. It is also clear that there are samples with very low percentage of modern water such as: BK3S (10%) and SGD 58.4 (9%). The overall percentage of modern water of uncontaminated samples of CFC-11 (63%) and CFC-113 (62%) in general is consistent for the study area. As expected, the CFC-12 value is biased towards the saturation level (72%). In Table 4, oversaturated and questionable CFCs are marked in italics. Contamination may also occur at lower saturation values (<100%) where one or more of the CFCs of a single sample are greater than the remaining one or two CFC but still not completely saturated. For example, BK3S shows some CFC-12 contamination (95%) without being saturated (<100%) with respect to modern atmospheric concentrations; which appears unrealistic for this 400-foot depth bedrock well.

Table 4. Equivalent atmospheric partial pressure of CFC water concentrations, percentage of modern partial pressures, apparent age (piston flow), age based on ratio of 2 CFCs (F, as Freons), exponential-modeled (EM) age, and exponential-piston modeled (EPM) age using η = 1.1 and η = 1.35 from bedrock wells (BK), overburden wells (NC) and wells at the submerged groundwater discharge (SGD) zones and Great Bay (GB) surface water.

Sample Name	Sampling Date	Percentage of Modern Atmospheric Water (PMA, %)			Best Estimate% of Modern Air -pptv	Modeled-Piston Flow Ages (years)			Ratio of 2 CFC Ages (years)		
		CFC-11	CFC-12	CFC-113		CFC-11	CFC-12	CFC-113	F11/F12	F113/F12	F113/F11
BK1D	11/26/2003	*78*[X]	*83*	16	16	18.9	16.9	*27.9*	*29.7*	NP	NP
BK2N	11/26/2003	*94*	*531*	70	70	15.4	Contam.	16.4	NP	NP	17
BK3S	12/1/2003	15	*95*	10	12	36.4	13.4	31.9	52.5	NP	18
BK4N	11/26/2003	74	89	83	82	19.9	15.9	14.9	34.5	14	NP
BK5D	11/25/2003	80	*127*	78	79	18.4	Contam.	15.9	NP	NP	13
NC1D	11/16/2003	59	*110*	59	59	24.9	<2.5	17.9	NP	NP	*11*
NC2S	11/18/2003	*40*	*245*	87	87	29.4	Contam.	14.4	NP	NP	NP
SGD 18.2-U	8/31/2003	*87*	*89*	65	65	12.7	11.2	13.2	*28.5*	*17*	*17*
SGD 19.3-D	8/31/2003	*209*	*121*	62	61	Contam.	Contam.	13.2	NP	NP	NP
SGD 21.2	11/24/2003	*110*	*107*	93	93	Contam.	<2.5	13.4	NP	NP	NP
SGD 31.4-U	8/29/2003	*190*	*91*	68	68	Contam.	10.7	12.7	NP	17	NP
SGD 39.3-D	8/29/2003	*123*	*366*	75	75	<9.0	Contam.	11.7	NP	NP	NP
SGD 58.4	8/31/2003	24	*49*	9	16	29.2	23.2	27.7	45	NP	39
SGD 73.1-D	9/1/2003	*194*	*196*	*598*	--	Contam.	Contam.	Contam.	NP	NP	NP
SGD 73.1-D	11/30/2003	*323*	*231*	*789*	--	Contam.	Contam.	Contam.	NP	NP	NP
SGD 73.1-U	11/30/2003	69	*162*	*94*	69	21.4	Contam.	13.4	NP	20	NP
GBW1	9/1/2003	75	69	*157*	72	15.7	16.7	Contam.	NP	NP	NP

([X]) Values in italics exceeding 100% are supersaturated. Values in italics below 100% are suspected to be influenced by oversaturation due to other external processes.

Table 4. (Continued) Equivalent atmospheric partial pressure of CFC water concentrations, percentage of modern partial pressures, apparent age (piston flow-based), age based on ratio of 2 CFC (F, as Freons), exponential-modeled (EM) age, and exponential-piston modeled (EPM) age using η = 1.1 and η = 1.35 from bedrock wells (BK), overburden wells (NC), and wells at the submerged groundwater discharge (SGD) zones and Great Bay (GB) surface water.

Sample Name	Sampling Date	Exponential Model (EM) Ages (years)			Exponential-Piston Model Ages (years) – η = 1.10			Exponential-Piston Model Ages (years) – η = 1.35			Expected Range of Residence Time (years)
		CFC-11	CFC-12	CFC-113	CFC-11	CFC-12	CFC-113	CFC-11	CFC-12	CFC-113	
BK1D	11/26/2003	15.5	14.5	90	14.5	15	70	17	15	50	28 – 50
BK2N	11/26/2003	6	NP	15	6	NP	15	6.5	NP	15.5	>17
BK3S	12/1/2003	160	8	160	110	8	105	70	9	60	34 – 60
BK4N	11/26/2003	18	12	9	18	12	10	19	13	11	17 – 34
BK5D	11/25/2003	15	NP	13	15	NP	13	15.5	NP	13	>17
NC1D	11/16/2003	28	NP	21	26	NP	20	26	NP	20	<11
NC2S	11/18/2003	50	NP	*8*	45	NP	7.5	7.5	NP	40	<8
SGD 18.2-U	8/31/2003	10	11.5	*17*	11	11.5	17	12	12	17	13 – 28
SGD 19.3-D	8/31/2003	NP	NP	20	NP	NP	20	NP	NP	*19*	13 – 19
SGD 21.2	11/24/2003	NP	NP	6	NP	NP	6.5	NP	NP	7	> 13
SGD 31.4-U	8/29/2003	NP	10	15.5	NP	11	15.5	NP	12	16.5	12 – 17
SGD 39.3-D	8/29/2003	NP	NP	14	NP	NP	14.5	NP	NP	14.5	12 – 15
SGD 58.4	8/31/2003	100	40	200	77	37	130	55	33	63	28 – 63
SGD 73.1-D	9/1/2003	NP	NP	NP	NP	NP	NP	NP	NP	NP	--
SGD 73.1-D	11/30/2003	NP	NP	NP	NP	NP	NP	NP	NP	NP	--
SGD 73.1-U	11/30/2003	21	NP	5	20	NP	5	21	NP	5	13 – 20
GBW1	9/1/2003	18	21	NP	18	21	NP	18	21	NP	16 – 21

(^{X}) Values in italics exceeding 100% are supersaturated. Values in italics below 100% are suspected to be influenced by oversaturation due to other external processes.

Percentages of modern atmospheric (PMA) equilibrated waters in some cases do not compare well with apparent ages because they are highly dependant on the accumulation rate of each CFC in the atmosphere, i.e. growth curve shape. A sample such as NC1D that implies degradation (oldest age given by CFC-11 and CFC-113) and also contamination of CFC-12 only and whose CFC-11 and CFC-113-derived apparent ages differ by 7 years, can actually have equal PMA values (59%), suggests that this sample may be composed of a given binary mixture (1994 water with CFC-free water) that might also explain the difference of the apparent ages due to the distinct solubility coefficients (CFC-11 is higher than CFC-113) of these CFCs in mixed waters.

Lumped-Parameter Modeled Groundwater Age

Considering all of the processes involved in changing CFC concentrations in a ground water sample and that can be misinterpreted (such as: having the status of the iron-reducing environment occurring at DO levels higher than 1.0 mg/L; not being able to properly identifying the level of contamination or adsorption of certain samples), CFC apparent ages are routinely thought to represent the minimum residence time of the groundwater in the aquifer system. From this observation, the percentage of modern atmospheric water that best quantifies the apparent age of the water sample is also shown in Table 4.

The derived ages of the lumped parameter models vary, but not significantly within the range of apparent ages (PFM) of 5 –17 years. The major variation in ages derived from lumped parameter models with respect to the PFM apparent ages is for residence times of 20 years and older. Both the PFM and exponential model (EM) constitute an envelope range of distribution functions of residence times: the EM-derived ages are the oldest that any lumped parameter model may estimate. Ages younger than the EM model are obtained from the combined exponential-piston model (EPM) for higher η-values (η is the ratio of the total volume to the volume with the exponential distribution of transit times, η = 1 (exponential)) i.e. with a reduced delay effect of flow lines before discharge. These models assume the use of additional evidence from hydrochemical composition analyses, hydrogeological setting, and/or paleo-groundwater dating measurements is available in the study area to explain the occurrence of larger residence times. In bedrock formations, as well as karstic aquifers, highly interconnected truncated vertical and horizontal flow paths make it difficult to depict a general "expected" residence time distribution pattern, however, the fact that the study area is located at the coast and that there is evidence (Degnan and Clark, 2002) of fracture lineaments connecting to the Great Bay lead to hypothesize that there might be a significant contribution of old (CFC-free) groundwater at the Great Bay intertidal discharge area. EPM models seem to be the most suitable for the hydrogeological setting of the study area. EPM models are more applicable in cases where groundwater has traveled a moderate distance from where recharge occurred and mixing can occur in long, open well bores (that connect various fractures) or at discharging springs. For this study, there is no additional information to quantify the fraction of the aquifer that behaves as either piston or exponential flow. To maximize the use of both the lumped parameter models and the FLOWPC program (Maloszewski and Zuber, 1996), it is necessary to

have a site-specific series of at least three tracer-based groundwater ages. This then allows fitting the parameters of the model (η, T (transit time)) to the measurements and creating a model for a given particular location. Due to the lack of this information, conservatively the EPM model was chosen to be the more representative to set the upper limit of the expected groundwater residence time for both the bedrock wells and the SGD sites. The NC sites were not included because of their high values suggesting long travel times that at the shallow depth these samples were taken (13 ft at NC1D and 8 ft at NC2S), it seems unrealistic.

Binary Mixing Models

Lastly, the simple binary mixing of old CFC-free water (>50 years) and young water can be expressed using two methodologies, assigning apparent ages with the growth curve of the ratio of two CFCs (CFC-11/CFC-12, CFC-113/CFC-12, and CFC-113/CFC-11, see Table 4), and setting the mixing line between two end members a water with a given CFC-derived groundwater age and a CFC-free water (Figure 8).

The use of CFC ratios for groundwater dating presupposes that no alteration of the air-water equilibrium concentrations by additional sources (contamination) or by microbial degradation or other geochemical processes has occurred. Apparent ages derived from the CFC ratios confirmed the ages of samples BK1D and BK2N (that were previously estimated by CFC-113) and the range of ages for a number of samples defined by the PFM and the EPM, in particular SGD 58.4; and defined a less questionable lower age limit for NC1D.

Samples that have not been altered by any of the previously mentioned CFC modifying processes will plot along the solid lines in Figure 8, which correspond to recharge of water in equilibrium with air (piston flow). Likewise as in Figure 5, the envelopes bounding the modeled CFC concentrations enclose the area where non-altered CFC concentrations should plot. Plots A and C show better agreement between the respective CFCs. In particular, according to these binary mixing models, bedrock well samples BK1D, BK3S, BK4N, and BK5D seem to have a significant young water component of 4, 18, 10 and 13 years old, respectively, in their composition with theoretically CFC-free water (> 50 years). Shallow well sample NC1S showed a younger component of 8 years and SGD 18.2 also had a young component of 8 years or less, being in between the 1995-mixing line and the piston flow line. Comparing BK1D, which is a 55-ft deep well with the bottom 10 ft into bedrock, with the nearby shallow site NC1D, it is possible to have recently recharged (4 years) water mixing with old water and in turn, that SGD18.2's water be the result of the mixture of BK1D and NC1D waters. Noticeably, with the exception of BK2N, all bedrock wells considered in the study have some modern (or younger) contribution. Infiltration through highly permeable pockets or fractures in nearby recharging areas can explain these observations. Due to the high frequency of contaminated samples from shallow wells, only SGD 18.2 and SGD 58.4 have fairly consistent apparent ages for all three CFCs; this latter plotting on the mixing line of a water with a young composition of 23 years old and CFC-free water.

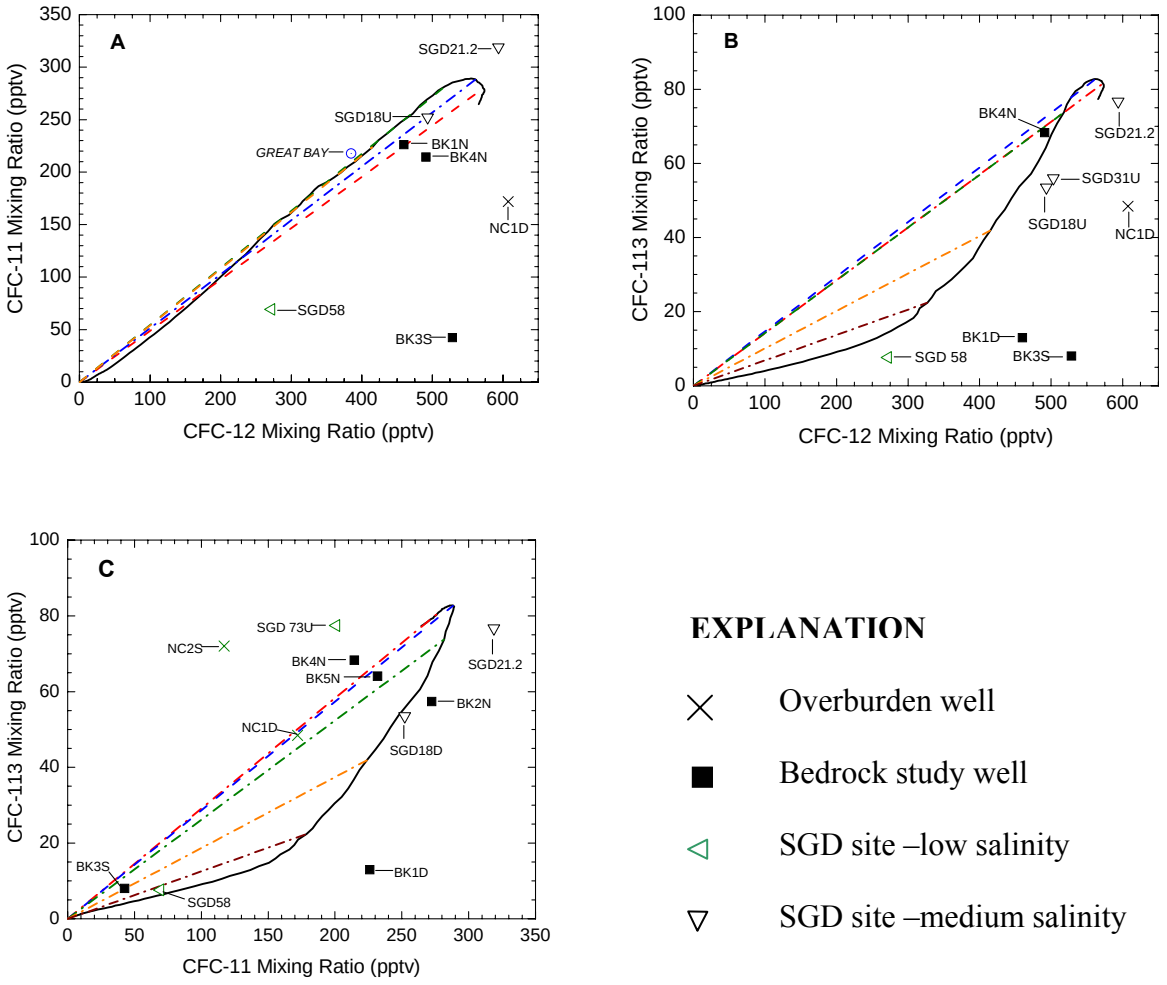

Figure 8. Equivalent atmospheric mixing ratios (pptv) of water sample CFC concentrations at 8.4 °C compared to each other with respect to predicted-equlibrium conditions (PF, solid line), and binary mixing models (dashed lines) of CFC-bearing water (air) with old CFC-free (>50 years) water for the years 2000 (red), 1995 (blue), 1990 (green), 1985 (orange), and 1980 (brown).

Silica as Proxy of Groundwater Age

Weathering of silicate materials from the Kittery and Elliot formations is known to dissolve silica (SiO2) in water. Most sampled groundwater was found to be supersaturated with respect to quartz (see Table 9). It has been observed that the longer the residence time (i.e. water-rock interaction) the larger the concentration of dissolved silica. This relationship is explored in Figure 9 for the collected data and the CFC-derived apparent ages.

There is a poor correlation of ages and silica (SiO_2) concentrations. CFC-12 and CFC-113-derived ages do not exhibit (for most of the samples) much variability with respect to SiO_2. An increasing trend (i.e. positive correlation) is not clear except for CFC-11-derived ages that show some clustering towards a positive correlation.

However, It is difficult to rely upon this relationship when the SiO_2 concentration for the overburden wells (6.7 – 7.5 mg/L) are within the concentration range observed in bedrock wells (5.8 – 7.0 mg SiO_2/L). This similarity in the SiO_2 concentrations does not agree with the hypothesis of SiO_2 enrichment for larger residence times. Therefore, SiO_2 must be affected by another process along its flow path towards deeper zones of the aquifer. SiO_2 did not constitute a good proxy for estimating residence time in the study area.

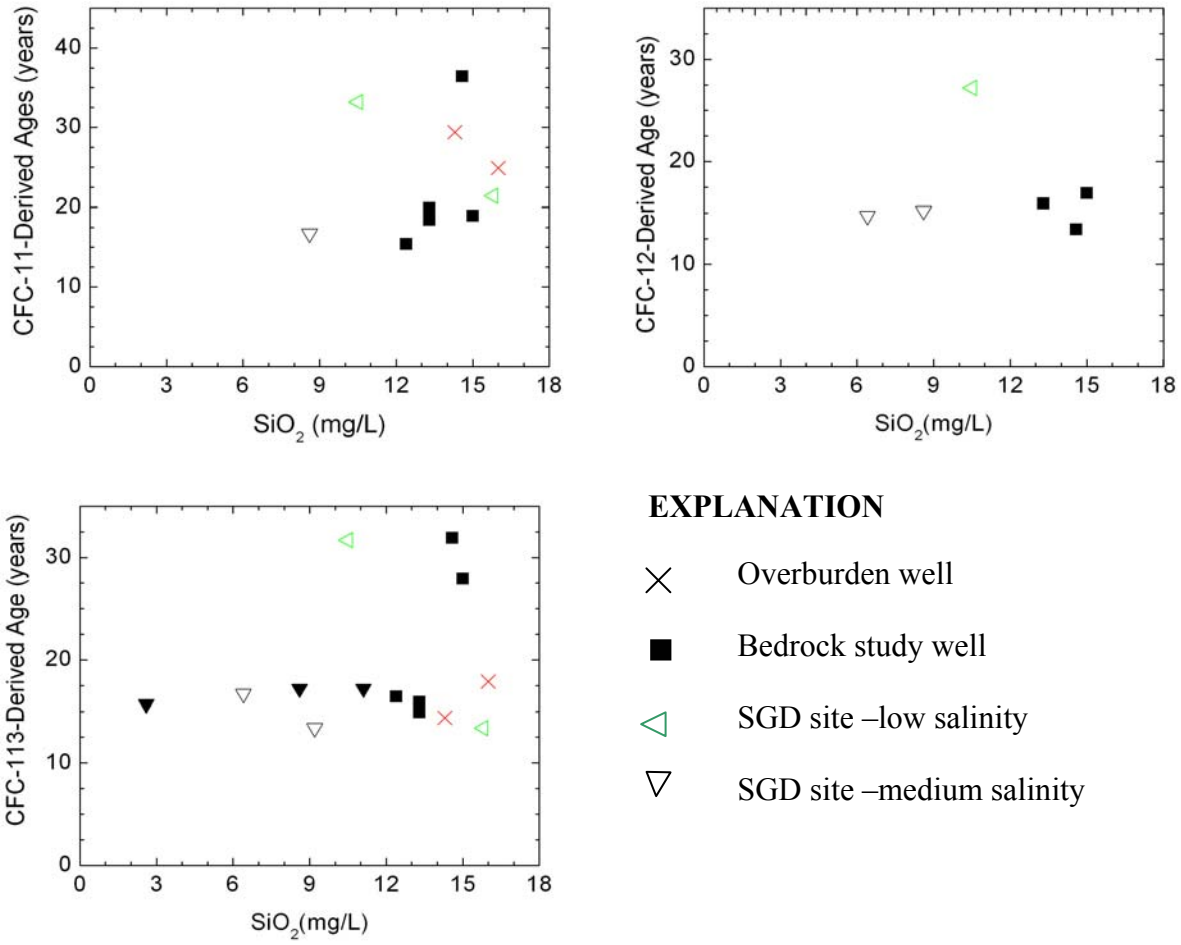

Figure 9. Silica and CFC-derived groundwater age relationship.

The last column in Table 4, the expected residence time for each site is summarized in a range of values in which the first term corresponds to the apparent age (PFM) and the second term is the age derived from either the two EPM models or the EM model. From these values, the regional residence time considering all the sampled sites was 25.7 ± 15.6 years; only considering the bedrock, overburden, and SGD groundwater samples the residence time was 37.2 ± 15.5 years, 9.5 ± 2.1 years, and 20.7 ± 13.3 years.

HYDROCHEMISTRY

Major ion chemical composition of shallow, stratified drift, and bedrock groundwaters and water at the SGD sites is presented in Table 5. Measurements of the major ion (Ca^{2+}, Mg^{2+}, K^{+}, Na^{+}, $NH4^{-}$, $NO3^{-}$, Cl^{-}, and SO_4^{2-}) chemical composition in precipitation samples collected for the past twenty years by the National Atmospheric Deposition Program (NADP) at the nearest NADP station to the study area: East, MA, was considered in the http://nadp.sws.uiuc.edu/sites/ siteinfo.asp?net=NTN&id=MA13). Hubbard Brook (NH) and East stations have great altitude differences with the East station, for most of the ions, displaying higher concentrations due to both the influence of the largely urbanized Boston area and the deposition of marine aerosols (given the elevated levels of Cl^{-}, Na^{-}, Mg^{+} and SO_4^{2-} concentration in rainwater enriched 4.1, 4.0, 2.7, and 1.2 times those measured at Hubbard Brook, respectively). Hubbard Brook, instead, is 20% enriched in NO_3^{-} and NH_4^{-}. Both stations have a multiannual pH mean value of 4.4.

Modeled And Measured Major Ion Concentrations

Assuming Cl^{-} as a conservative tracer recharging the surficial aquifer, the expected concentrations of Ca^{2+}, Mg^{2+}, K^{+}, Na^{+}, SO_4^{2-}, and Cl^{-} in groundwater from the surficial aquifer (overburden and stratified drift wells) were calculated weighting the ion concentration in rainwater with the chloride-based enrichment factor: $(Cl^{-})_{groundwater}/(Cl^{-})_{rainwater}$ (Table 6), using the rainwater chemical composition at East (MA, station ID:MA13) station. This station agrees more with the marine influence of the Great Bay as is shown by Mg^{2+}, Na^{+}, and Cl^{-} fractionation factors of rainwater relative to seawater that were calculated with the expression $(ion/Cl)_{rain}/(ion/Cl)_{sea}$ (Table 6). Estimates of background Cl^{-} concentration in uncontaminated wells ($Cl^{-} < 100$ mg/L) screened in the surficial aquifer were found to be approximately 15 mg/L and 81 mg/L in the stratified drift aquifer (from data collected by Moore, 1990; Stekl and Flanagan, 1992) and the shallow small diameter wells installed for the present study, respectively; and 16.1 mg/L in the bedrock aquifer.

Table 5. Chemical and isotopical analyses of selected samples. [All concentrations in mg/L unless specified]

Name	Date	pH	DO	Ca	Mg	K	Na	Alka. meq/L	Cl	SO_4	Br	Fe	Si
Bedrock wells Sampled for the Present Study													
BK1D	11/26/2003	6.9	>1.0	47	27	13	82	1.68	210	10	2.18	<0.05	15.0
BK2N	11/26/2003	6.6	>1.0	44	20	4.0	54	1.49	130	5.0	0.26	<0.05	12.4
BK3S	12/1/2003		>1.0	2.0	2.0	3.0	160	3.32	130	13	0.62	0.05	14.6
BK4N	11/26/2003		>1.0	29	7.0	1.0	14	1.64	7.0	5.0	0.00	--	13.3
BK5D	11/25/2003		>1.0	32	8.0	11	49	1.97	65	7.0	0.19		13.3
W1160													
W1076													
W650													
W1336													
Overburden Wells Sampled for the Present Study													
NC1D	11/16/2003	6.6	>1.0	46	7.0	7.0	39	1.58	77	5.0	0.27	--	16.0
NC2S	11/18/2003		>1.0	36	37	4.0	39	2.95	84	7.0	0.00	--	14.3
Septic Tank Effluent Samples													
STE1	11/25/2003		-	68	24	12	52	1.64	110	20	--	0.06	20.3
STE2	11/29/2003		-	57	13	13	150	-	370	13	2.22	0.55	19.7
Submerged Groundwater Discharge Sites Study Sites													
SGD 18.2-U	11/28/2003	6.6	>1.0	39	89	29	770	2.21	1700	71	5.91	0.05	11.1
SGD 18.2-D	11/28/2003		>1.0	120	300	110	2700	-	6200	900	18.44	0.22	5.1
SGD 19.3-U	11/28/2003		>1.0	200	520	190	4700	-	11000	1400	28.23	0.10	13.9
SGD 19.3-D	11/28/2003	6.7	>1.0	41	82	37	840	2.93	1800	71	5.84	0.06	2.6
SGD 21.2	11/24/2003		>1.0	100	200	70	1800	1.31	4000	580	10.20	<0.05	9.2
SGD 31.4-U	11/16/2003	6.9	>1.0	90	250	75	1700	1.10	4100	620	12.00	0.58	6.4
SGD 31.4-D	11/16/2003		>1.0	90	260	96	2500	-	4900	720	12.27	<0.05	8.1
SGD 39.3-U	11/16/2003		>1.0	200	610	220	5600	2.97	12000	1600	35.00	0.11	21.4
SGD 39.3-D	11/29/2003		>1.0	26	29	9.0	260	0.59	590	53	4.49	0.12	8.6
SGD 58.4	11/16/2003	7.2	>1.0	11	6.0	4.0	64	2.42	57	7.0	1.45	--	10.5
SGD 73.1-U	11/30/2003	7.4	>1.0	47	23	4.0	48	5.00	130	6.0	0.00	<0.05	15.8
SGD 73.1-D	11/30/2003	6.7	>1.0	50	26	5.0	73	2.94	200	8.0	0.81	<0.05	15.8
Seawater	(Hem,1985)		-	410	1350	390	10500	0.00	19000	2700	-	-	-
Bedrock Wells Sampled by USGS (Ayotte et al.,1999)													
ME-CW 2020	10/12/1999	8.3	1.0	12	2.0	1.2	11	0.95	9.0	3.0	0.01	0.37	19.0
ME-CW 2022	7/19/2000	6.6	5.3	27	5.0	3.5	19	0.70	9.0	7.6	0.02	0.01	16.0
ME-YW 852	10/14/1999	7.1	0.3	75	10	3.2	18	4.38	13	17	0.15	0.01	17.0
ME-YW 853	10/14/1999	9	0.3	9.7	2.0	3.1	30	1.20	5.0	16	0.03	0.01	10.0
ME-YW 854	10/12/1999	6.7	4.7	53	7.0	8.4	38	1.29	130	7.9	0.01	0.01	11.0
ME-YW 855	6/15/2000	7.2	0.3	12	4.0	2.8	4.4	0.70	5.0	15	0.08	1.50	19.0
ME-YW 856	6/14/2000	8.8	0.2	21	7.0	3.0	210	2.74	260	68	0.67	0.01	10.0
ME-YW 857	6/21/2000	8.8	3.5	13	7.0	2.9	39	2.16	11	22	0.04	0.01	9.0
NH-KFW 51	6/7/2000	7.9	0.2	49	27	1.3	11	3.67	23	54	0.07	0.33	13.0
NH-LIW 28	6/8/2000	6.8	5.9	48	11	1.0	18	2.48	42	18	0.01	0.01	8.7
NH-LMW 83	6/19/2000	6.4	5.9	38	2.0	1.6	7.9	1.72	11	20	0.01	0.01	10.0
NH-SAW 156	6/6/2000	7.6	0.2	56	5.0	2.2	9.8	2.13	47	19	0.06	0.19	21.0
Stratified Drift Wells Sampled by USGS (Moore, 1990)													
MAW 56	11/26/1985	6.5	-	6.3	2.0	2.1	4.2	0.23	3.0	16	-	0.01	20.0
SSW 10a	12/10/1985	6.7	-	21	6.0	2.3	10	1.15	7.0	14	-	0.03	17.0
SSW 10b	12/10/1985	6.8	-	33	7.0	3.6	20	0.82	62	16	-	0.05	12.0
Stratified Drift Wells Sampled by USGS (Stekl and Flanagan, 1992)													
GTW 79	9/3/1987	6.9	0.6	22	8.0	1.4	12	1.36	16	4.9	-	<0.01	16.0
NIW 35	8/17/1987	7.6	8.5	34	8.0	2.4	80	2.20	88	17	-	<0.01	14.0
PXW 2	9/3/1987	7.5	1.3	57	10	2.4	9.0	2.43	6.0	20	-	<0.01	14.0
PXW 5	8/17/1987	7.7	4.6	78	17	4.2	76	2.10	170	65	-	<0.01	13.0

Table 5. Chemical and isotopical analyses of selected samples. [All concentrations in mg/L unless specified] (*Continued*)

Name	Date	NH4	NO3	DOC	$\delta^{18}O$ ‰	$\delta^{2}H$ ‰	B ug/L	$\delta^{11}B$ ‰	Sr	$^{87}Sr/^{86}Sr$
Bedrock wells Sampled for the Present Study										
BK1D	11/26/2003	0.02	0.30	0.31	-8.6	-55.5	27	29.0	0.300	0.71146
BK2N	11/26/2003	0.01	2.49	0.29	-9.2	-59.8	20	13.2	0.290	0.71425
BK3S	12/1/2003	0.01	0.43	0.35	-8.8	-56.2	52	25.0	0.003	0.71160
BK4N	11/26/2003	0.00	0.28	0.33	-9.1	-57.4	15	16.7	0.135	0.71362
BK5D	11/25/2003	0.01	3.22	1.36	-8.8	-56.9	60	6.2	0.140	0.71376
W1160			10.20				18	20.7	0.113	0.71239
W1076			5.18				35	9.0	0.220	0.71275
W650			0.00				24	45.7	0.050	0.71168
W1336			0.01				5		5E-04	
Overburden Wells Sampled for the Present Study										
NC1D	11/16/2003	0.01	0.66	0.59	-8.4	-54.0	40	12.0	0.120	0.71647
NC2S	11/18/2003	0.01	1.43	0.59	-7.8	-50.2	46	27.2	0.307	0.71414
Septic Tank Effluent Samples										
STE1	11/25/2003	59.13	0.01	35.89	-9.3	-60.9	140	5.2	0.285	0.71470
STE2	11/29/2003	17.03	0.10	13.62	-	-	80	13.7	0.370	0.71285
Submerged Groundwater Discharge (SGD) Sites Study Sites										
SGD 18.2-U	11/28/2003	0.01	0.04	0.64	-8.9	-58.9	390	41.7	0.670	0.70984
SGD 18.2-D	11/28/2003	0.01	0.12	0.83	-5.6	-37.1	760	40.5	1.680	0.70923
SGD 19.3-U	11/28/2003	0.01	0.85	1.11	-3.7	-25.4	512	34.7	0.660	0.70939
SGD 19.3-D	11/28/2003	0.01	1.48	0.19	-7.2	-48.0	670	39.2	2.160	0.70915
SGD 21.2	11/24/2003	0.02	2.88	1.35	-6.6	-43.3	672	39.7	1.225	0.70961
SGD 31.4-U	11/16/2003	0.01	1.85	0.73	-6.0	-38.6	525	41.7	1.500	0.70942
SGD 31.4-D	11/16/2003	0.01	2.05	0.93	-6.0	-38.4	700	39.2	1.325	0.70930
SGD 39.3-U	11/16/2003	0.01	1.41	1.81	-2.7	-17.4	750	39.7	2.100	0.70916
SGD 39.3-D	11/29/2003	0.06	1.84	0.36	-8.1	-53.7	300	37.5	0.650	0.71025
SGD 58.4	11/16/2003	0.06	0.01	2.56	-7.2	-45.2	93	28.5	0.061	0.71239
SGD 73.1-U	11/30/2003	0.01	3.54	0.47	-8.5	-55.6	56	13.7	0.290	0.71171
SGD 73.1-D	11/30/2003	0.01	1.77	1.09	-8.4	-54.8	56	24.2	0.322	0.71235
Seawater	(Hem,1985)		0.76	-	-	-	4730	39.6	-	-
Bedrock Wells Sampled by USGS (Ayotte et al.,1999)										
ME-CW 2020	10/12/1999	< 0.02	<0.05	0.30	-9.96	-66.7	<16	-	0.076	-
ME-CW 2022	7/19/2000	< 0.02	0.49	0.30	-9.12	-56.9	<12	-	0.107	-
ME-YW 852	10/14/1999	0.03	2.40	1.60	-7.92	-50.9	E8.3	-	0.210	-
ME-YW 853	10/14/1999	< 0.02	<0.05	0.30	-8.97	-58.5	E12.8	-	0.043	-
ME-YW 854	10/12/1999	< 0.02	0.18	0.70	-9.03	-59.2	E10	-	0.300	-
ME-YW 855	6/15/2000	< 0.02	<0.05	0.30	-9.78	-64.0	<12	-	0.070	-
ME-YW 856	6/14/2000	0.08	<0.05	0.90	-9.66	-62.7	133.0	-	0.276	-
ME-YW 857	6/21/2000	< 0.02	<0.05	0.40	-8.83	-55.1	19.0	-	0.099	-
NH-KFW 51	6/7/2000	0.02	<0.05	0.70	-8.57	-54.4	<12	-	0.234	-
NH-LIW 28	6/8/2000	< 0.02	3.20	0.70	-8.65	-54.5	E7.4	-	0.179	-
NH-LMW 83	6/19/2000	< 0.02	0.84	0.70	-8.15	-51.8	26.6	-	0.100	-
NH-SAW 156	6/6/2000	< 0.02	<0.05	0.70	-8.28	-51.8	E8.2	-	0.144	-
Stratified Drift Wells Sampled by USGS (Moore, 1990)										
MAW 56	11/26/1985	0.01	-	1.2	-	-		-	0.035	-
SSW 10a	12/10/1985	<0.01	-	2.5	-	-	<10	-	0.110	-
SSW 10b	12/10/1985	0.01	-	1.5	-	-	<30	-	0.150	-
Stratified Drift Wells Sampled by USGS (Stekl and Flanagan, 1992)										
GTW 79	9/3/1987	<0.01	-	1.70	-	-	<20	-	0.170	-
NIW 35	8/17/1987	<0.01	-	8.30	-	-	<20	-	0.180	-
PXW 2	9/3/1987	<0.01	-	1.20	-	-	<20	-	0.230	-
PXW 5	8/17/1987	0.02	-	1.00	-	-	<20	-	0.350	-

Table 6. Rainwater fractionation factors relative to seawater chemical composition and modeled groundwater concentration with respect to Cl^- abundance in rainwater relative to groundwater as in the general expression: $[Cl^-]_{groundwater}/[Cl^-)]_{rainwater}$ x $[ion]_{rainwater}$.

Ion	Seawater (Hem, 1985)		Rainwater				Fractionation Factor		Conc. In groundwater from rainwater			
			Hubbard Brook (HB), NH		East (E), MA				Hubbard Brook (HB), NH		East, MA	
	[mg/L]	[mmol/L]	[mg/L]	[mol/L]	[mg/L]	[mol/L]	HB, NH	E, MA	[mg/L]	[mol/L]	[mg/L]	[mol/L]
Ca^{2+}	410	10.3	0.06	1.45	0.08	2.05	16.94	5.87	5.48	137	1.9	47
Mg^{2+}	1350	55.6	0.02	0.7	0.05	1.91	1.51	1.01	1.6	66	1.07	44
K^+	390	10	0.01	0.37	0.02	0.58	4.48	1.7	1.38	35	0.52	13
Na^+	10500	547	0.09	3.71	0.34	14.85	0.97	0.95	8.08	351	7.9	344
Cl^-	19000	535	0.17	4.83	0.65	18.28	1	1	15	423	15	423
SO_4^{2-}	2700	28	1.33	13.9	1.98	20.6	72.5	21.5	154.5	1609	45.8	477

Modeled major ion abundances for overburden, stratified drift, and bedrock groundwater systematically follow the trend exhibited by both the rainwater at East station (MA) as well as the observed concentrations in local groundwater. Only the modeled shallow groundwater concentrations closely match those ion concentrations measured in surficial (Moore, 1990; Stekl and Flanagan, 1989) and bedrock (Ayotte et al., 1999) aquifers and in waters at the discharge zone, with the exception of Ca^{2+} and Mg^{2+} which are enriched in the observed values and SO_4^{2-} which is depleted in the measured concentrations. The fact that only the modeled shallow groundwater concentrations match the observed values may be because of an uneven depositional distribution of chloride from the shallow and surficial and bedrock water, which can be, in general, explained by a combined effect of factors: i) The presence of a strong marine spray influence at shallow depths. This effect is verified by the fact that Na^+ and K^+ (to a lesser degree), are the ions in shallow groundwater, besides Cl^-, with lower fractionation factors (Table 7) relative to both seawater (0.9 and 3.3, respectively) and rainwater (0.9 and 2.0, respectively) whose effect is also present in the variability of the observed and measured major ion concentration plot (Figure 10). ii) Contamination of anthropogenic sources in the shallow groundwater from septic effluent, fertilizers, and road salt. iii) Halite mineral weathering. iv) The presence of a perched aquifer partially isolated by semi-to-impermeable clay-rich layers from deeper groundwater settings. This hypothetical distribution of high Cl^- in shallow groundwaters needs to be verified with a larger sample size to be collected mainly in the shallow aquifer.

The modeled chemical concentrations exhibited enrichment in the observed concentrations of Ca^{2+} and Mg^{2+} at shallow depths. Major ion enrichment at the depths intercepted by the small diameter wells (shallow groundwater in Figure 10) typically involves the combined effect of evapotranspiration and evapoconcentration on the surface and vadose zone, and ion exchange during transit through the surficial materials.

Table 7. Fractionation factors of shallow, surficial, and bedrock waters relative to meteoric and sea-water using Cl^- as a conservative tracer in the expression: $(ion/Cl)_{rainwater}/(ion/Cl)_{seawater}$.

Ion	Fractionation Factors (Shallow groundwater/Seawater)			Fractionation Factors (Shallow groundwater/Rainwater)			Fractionation Factors (Groundwater/Rainwater)	
	NC1D	NC2S	Average	NC1D	NC2S	Average	Surficial	Bedrock
Ca^{2+}	28	19.7	23.5	4.7	3.4	4	5.1	4
Mg^{+}	1.2	6.3	3.9	1.2	6.2	3.8	2.8	1.9
K^{+}	4.7	2.1	3.3	2.8	1.2	2	1.6	1.7
Na+	0.9	0.8	0.9	0.9	0.9	0.9	1.1	1.3
Cl^-	1	1	1	1	1	1	1	1
SO_4^{2-}	0.5	0.6	0.5	0.02	0.03	0.02	0.11	0.09

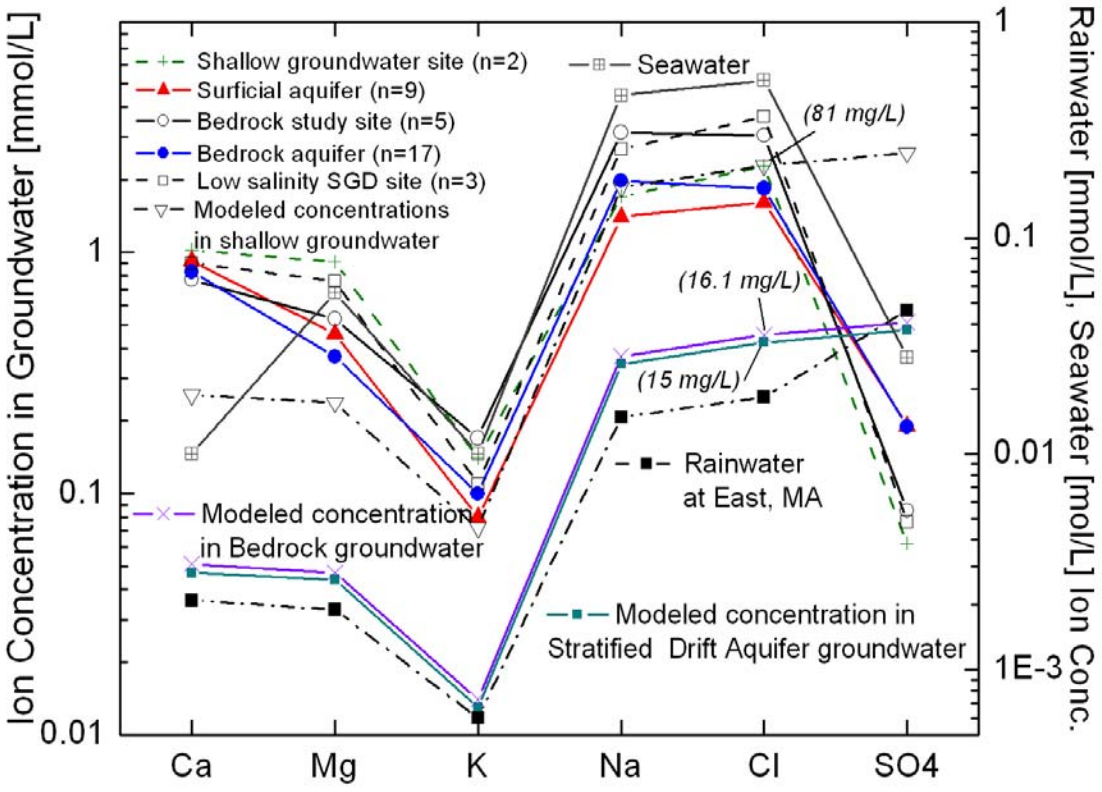

Figure 10. Schoeller diagram of measured concentrations and the modeled total deposition of major ions in shallow, stratified drift, and bedrock groundwater. Modeled ion concentrations calculated as in Table 5. Modern seawater concentrations after Hem (1985).

Fractionation factors between waters are shown in Table 6. From these fractionation factors, bedrock water exhibits the best relationship to rainwater than the chemical compositions of shallow and stratified drift waters. This observation verifies the fact that it is in the shallower deposits where most of the differentiation from the recharging rainwater takes place chiefly due to evapoconcentration and evapotranspiration processes. Along the continuing flow path to deeper waters with longer residence times, ion exchange may play a more important role in varying chemical composition.

Sulfate (SO_4^{2-}) behaves differently from the rest of the ions in that it exhibits depletion in the measured concentrations with respect to the modeled value. Sulfate (SO_4^{2-}) and NO_3^- in precipitation are largely responsible for the acidic pH values in rainwater (Kahl et al., 1991). Sulfate is enriched by atmospheric sources when comparing the SO_4/Cl ratio in rainwater (3.05) with that in seawater (0.14). This enrichment, found at Hubbard Brook and East stations, can be explained by the influence of numerous sulfur-based industrial sources in Maine (Kahl et al., 1991) and the urbanized Boston area, respectively, that most likely is not characteristic of the study area. The high SO_4^{2-} concentration in rainwater yielded the high modeled concentrations in groundwater, which may not be realistic for the study area. Soils in glaciated regions are characterized by having low pH and low SO_4^{2-} adsorption capacity (Fernandez and Structemeyer, 1985), characteristics that rule out any significant removal of SO_4^{2-}. .

Water quality data are not normally distributed because the data are bounded at zero and usually positively skewed thereby fitted better by distributions other than the normal (Helsel and Hirsch, 1992). Parametric statistic tests such as the t-test assume the data are normally distributed. Helsel and Hirsch (1992) suggest the use of non-parametric tests when dealing with water quality data. Normality was tested for our data using the Shapiro-Wilk test for each ion and each water (group). If even one of the groups considered in a given parametric test exhibits non-normality, the assumptions of a parametric analysis of variance are violated (Helsel and Hirsch, 1992). All of the ions, except Ca^{2+}, exhibited non-normality at a level of significance (α) of 0.05 at least in one of the groups; and the bedrock water group showed persistent non-normality for all the ions, except for Ca^{2+}. Calcium (Ca^{2+}) was normally distributed in all the water groups. This is primarily because the average Ca^{2+} concentration was substantially higher than zero and the standard deviation much less than the average.

Non-parametric tests for statistical significance were run (rank-sum test to compare a pair of variables (aquifers) and the Kruskal-Wallis test when comparing all aquifers) for the ions Ca^{2+}, Mg^{2+}, K^+, Na^+, and Cl^- in order to identify significant differences among the surficial and bedrock aquifer and water at the discharge zones. These tests can be employed on any type of data no matter how it is distributed: lognormal, normal, exponential, or any other distribution. They were used to test the null hypothesis (H_0) that the ion concentration means of each group were not significantly different from each other at a level of significance $\alpha = 0.05$ (two-sided). The rank-sum test, student-t test's equivalent non-parametric test, was used to compare ion concentrations in two groups (aquifers) having a sample size of 10 or smaller: low salinity SGD sites and wells intercepting immediately surrounding stratified drift groundwaters to the Great Bay (NH), listed in Table 5. For the two-sided test, reject H_0 if $W_{\text{rank's sum}} \leq x^*_{\alpha/2,\, n,m}$ or $W_{rs} \geq x^*_{\alpha/2,\, n,m}$, where *n* and *m* are the sample sizes. When

comparing ion concentrations in more than two groups (waters), the Kruskal-Wallis test was performed using the sequence of large-sample and rank transform approximations, this latter test being the ANOVA's equivalent non-parametric test (Helsel and Hirsch, 1992).

Results from these tests suggest that there is not enough evidence to reject the null hypothesis of equivalent means among the groups of water sampled in surficial and bedrock aquifer, and at the discharge zones with low salinity content. This result may be explained by the large variability in the ion concentration for all waters. The variability of these waters follows the order: $Mg^{2+} > Cl^{-} > Na^{+} > K^{+} > Ca^{2+}$ (Figure 10).

Trilinear Diagram Analysis

An overview of the chemical composition of the entire dataset was provided by use of the trilinear plotting technique (Piper, 1944); the trilinear diagram is shown in Figure 11. The five water types that were identified in the surficial and bedrock aquifers and in the water at the discharge zones and their abundance are listed in Table 8. The two most abundant water types in the surficial and bedrock aquifers are Ca-Na-HCO_3 and Na-Ca-HCO_3, which are characterized by the relative abundance of ions Ca^{2+}, Na^{+}, and HCO_3^{-}. Nearly 55 % of all available groundwater analyses from these aquifers are classified as either of these two water types. The next most common water types are Ca-Mg-HCO3-SO4, Ca-HCO3, and Na-Cl, which are characterized by a stronger presence of the cation Mg^{2+} and more of the anions HCO_3^{-}, Cl^{-}, and SO_4^{2-}. In general for all the water types, the most abundant ions are, in order, Ca^{2+}, HCO_3^{-}, Na^{+}, and Cl^{-}. Significant enrichment of Ca^{2+} occurs in the glacial till deposits that overlay most of the study area. Precipitation in the northeastern region of the United States is among the most acidic in the United States (Kahl et al., 1991). However, no evidence of calcium depletion is present in the collected data due to acidic deposition and intensive harvesting, as it was suggested by Federer and others (1989) for northeastern areas of the United States. Till deposits are commonly similar in chemical composition to the underlying rock. Kahl and others (1991) observed that soil weathering generally occurs at depths of 60 to 100 cm, which may justify Ca^{2+} enrichment in the overburden.

The trilinear diagram allows comparison of the ion proportions in milliequivalents (meq%) for the samples from different sources, and hence, different concentrations. Cations and anions are plotted in separate trilinear diagrams; and the Piper diamond plots summarize the projections from both these trilinear diagrams. The following analysis is based on both ways of plotting, the Piper trilinear and the Piper diamond diagrams.

As in the Schoeller diagram, the great variability of Ca^{2+}, Na^{+}, HCO_3^{-}, and Cl^{-} contributions to the individual and overall water chemistry is also observed in the trilinear diagram. The acidic character acidic of rainwater is clearly identified in Figure 11 with no HCO_3^{-} present and high SO_4^{2-} proportion. After atmospheric deposition and infiltration the water exhibits weathering and is enriched in Ca^{2+}, Mg^{2+}, and HCO_3^{-}.

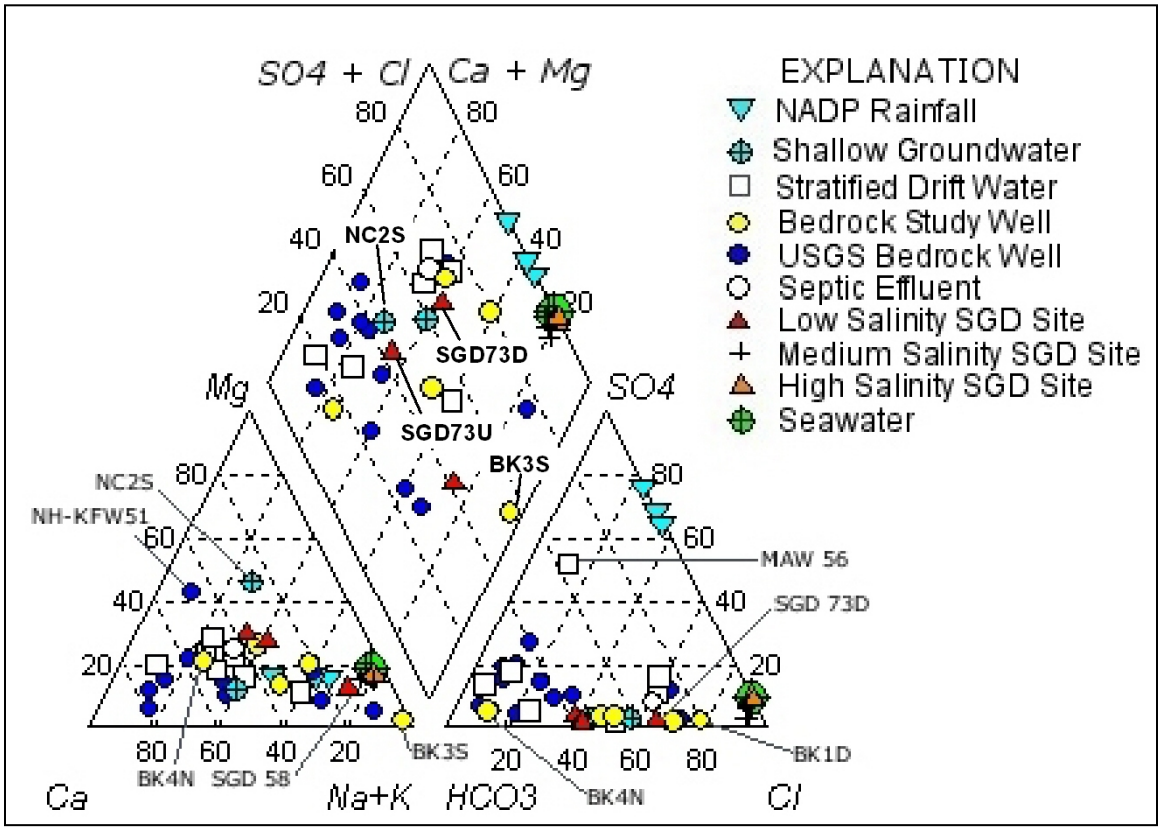

Figure 11. Chemical trilinear diagrams for shallow (present study), stratified drift (USGS, Moore, 1990; Stekl and Flanagan, 1992), and bedrock (present study and Ayotte et al., 2001) groundwaters and waters at the discharge zone.

Table 8. Major water types, their specific cation and anion compositions, and their abundance in the SGD sites and surficial and bedrock aquifers.

Water Type	Cation types	Anion types	Number (percentage) of samples, by aquifer			
			SGD Sites (Salinity)		Surficial	Bedrock
			Low	Med-High		
Ca-Na-HCO_3	Ca-Na, Ca-Na-Mg	Cl-HCO_3, HCO_3 SO4, HCO3-Cl	SGD 73U (33%)	-	4 (44%)	4 (24%)
Na-Ca-HCO_3	Na-Ca, Na-Ca-Mg	HCO_3, Cl-HCO3, HCO3-Cl, Cl	SGD 73D (33%)	-	1 (11%)	5 (29%)
Ca-Mg-HCO_3-SO4	Ca-Mg, Ca-Mg-Na	HCO_3-SO4, HCO3-Cl	-	-	2 (22%)	3 (18%)
Ca-HCO_3	Ca, Ca-Mg, Mg-Ca-Na	HCO_3, HCO3-Cl	-	-	2 (22%)	3 (18%)
Na-Cl	Na-Cl, *Na*	HCO3, *HCO_3-Cl*, Cl-HCO3	SGD 58 (33%)	10 (100%)	-	2 (12%)

Atmospheric deposition through rainfall may constitute the main source of SO_4^{2-} in groundwaters given the lack of sulfide-bearing rocks (i.e. pyrite, present in 0.5-1.5% in some rock analysis (Novotny, 1969) in the area. Modeled SO_4^{2-} concentrations in groundwater were all above observed values. In Figure 13c, the actual mixing line between rainwater and seawater should be displaced towards a lower SO_4^{2-} value in rainwater. This modified line would not make appear the local samples so depleted in SO_4^{2-}. The SO_4/Cl molar ratio in stratified drift and bedrock waters varied from 0.16 to 0.10, respectively, possibly indicating that recharge to bedrock also occurs from other non-consolidated materials (with SO_4/Cl ratio of 0.03) such as glacial till, other than isolated overlying stratified drift aquifer from where most of the recharge to bedrock is expected to occur.

Most groundwaters and SGD sites with low salinity are either Ca-HCO_3 or Na-Cl type waters (Figure 11). Two important processes describe the distribution of the results in Figure 11, direct salinization and a sequence of cation exchange followed by salinization. This latter process is identified with what would closely be an end-member of this mineralizing path, BK3S (Na-Cl-HCO_3, 95, 50, and 45 % meq, respectively). This bedrock well is located ~400 ft away from the Bay and intercepting bedrock at ~400 ft below ground. Its water chemistry has most likely evolved from being Ca-HCO_3 to Na-HCO_3 and lastly to Na-Cl. The first step of this evolution consists of exchanging Ca^{2+}, and to a lesser degree Mg^{2+}, for Na^{+}; followed by the second step, which is an early stage of salinization (Figure 12). The final result is a stronger proportion of sodium than that in seawater plotting below the seawater point, which indicates the cation exchange contribution.

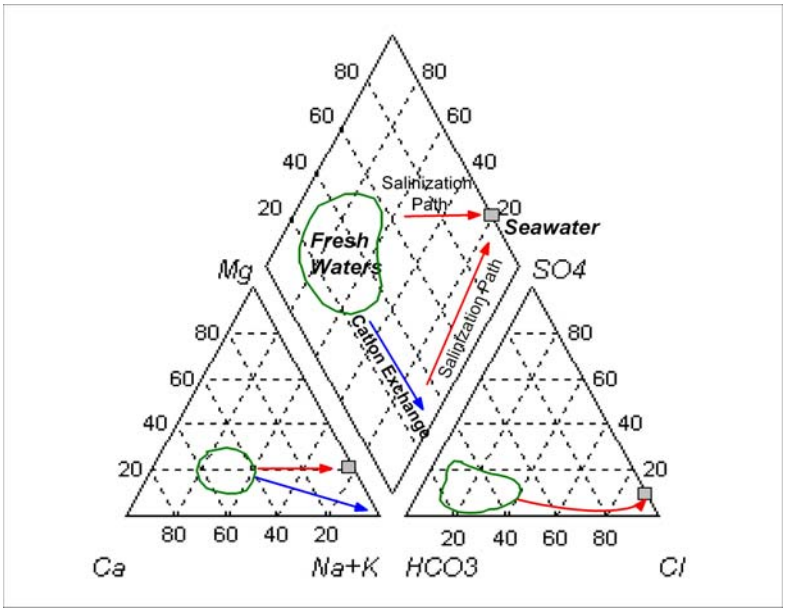

Figure 12. Geochemical evolution of groundwater experiencing different degrees of salinization. Blue arrows indicate cation exchange reactions and red arrows indicate salinization paths (Adapted after Allen, 2004).

Bedrock wells, ME-CW 2020, ME-YW 857, and ME-CW 853 with Ca-Na-HCO_3, Na-Ca-HCO_3, and Na-Ca-HCO_3 water types, respectively, confirm the cation exchange part of the sequence without having yet experienced any salinization based on their low chloride contributions to their water chemistry. BK3S has already gotten Cl^- exchange contributions from seawater mixing, which does not strictly make it an end-member of this hypothetical mixing path. On the other hand, bedrock well ME-YW-856 has followed the salinization path, after cation exchange, displaying chloride concentration to 64% meq.

Direct salinization is more likely to occur in younger waters or in areas of overexploitation of the resource where recharge is not able to satisfy all the demand. This is the case for bedrock well BK1D (Na-Ca-Mg-Cl, with 58, 22, 20, and 78% meq, respectively) which is characterized as not being as enriched in Na^+ as BK3S but still exhibiting important contributions from other cations; and for being more enriched in Cl^- than BK3S and ME-YW-856. Sites SGD 73D (Na-Ca-Cl-HCO3, with 41, 31, 64, and 34 % meq, respectively) and BK2N (39, 35, 70, 28 % meq, respectively) plot close to this path line thereby confirming the fingerprint of this salinization mechanism.

Several studies have reported that sodium enrichment in groundwater without an associated increase in chloride (i.e. Na/Cl ratios higher than in seawater, Figure 13a) can be caused by the dissolution of Na-bearing minerals and/or cation exchange reactions of Ca^{2+} and Mg^{2+} ions for Na+. Shallow (NC1D, NC2S), stratified drift (PXW5), bedrock (BK2N) and SGD (SGD 73U, 73D) waters plot right on the seawater-diluted line of Na-Cl (Figure 13a), probably indicating the marine and sea spray influence of the recharging waters. Most of the data, however, plot above the seawater-diluted line reflecting the presence of another Na^{2+} source. The Na/Cl molar ratio remains almost unchanged in shallow groundwater (0.75) relative to rainfall of 0.83 (Na/Cl in seawater is 0.85), but a substantial increase is observed in stratified drift waters (1.51) and in bedrock waters (2.10 considering USGS wells (N=12) and 1.47 in study wells only (N=5)). Sulfate/Chloride and Na/Cl ratios in different stages of the aquifer system indicate that the source of recharge to the bedrock aquifer is probably from the local overlying surficial aquifer system.

Figure 13 examines the relationship of Cl^- with some ions; including B^{3+} and NO_3^- presenting some additional evidence to what was already observed from Figure 11. Unlike with Na^{2+}, a non-linear relationship of chloride with Ca^{2+}, SO_4^{2-}, and DOC is exhibited. BK3S plots on opposite sides of the seawater-dilution line in Figure 13a and 11b manifesting the cation exchange path (Ca^{2+} for Na^+) described in Figure 11. Enrichment in Ca^{2+} is observed in shallow groundwater (Figure 13b) for most of the sites except for BK3S, ME-YW856, and SGD 58, which are the same

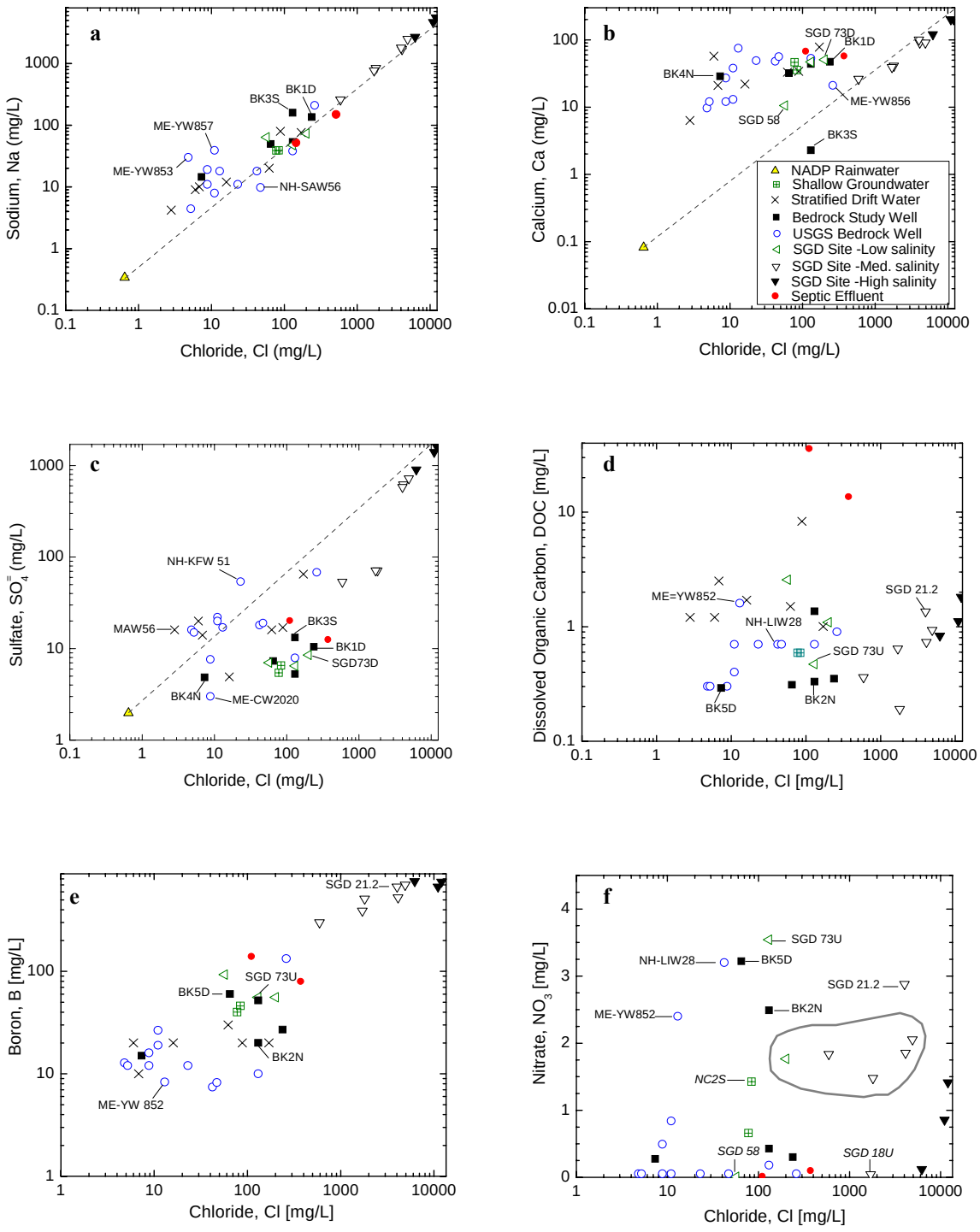

Figure 13. Relationship of Na^{+} (a), Ca^{2+} (b), SO_4^{2-} (c), DOC (d), B^{3+} (e), and NO_3^{-} (f) with Cl^{-}; in different waters. When pertinent, the seawater dilution line (dashed line) is also drawn the rainwater composition as its end-member. All concentrations are in milligrams per liter. In the DOC vs. Cl^{-} plot, high NO^{3-} concentration sites are labeled.

in the concentration of most of ions, except for Mg^{2+} and NO_3^-, in which NC2S is notoriously enriched. This small diameter well is located in a densely populated area where the intercepted water could have been affected by fertilizers. Septic systems effluent alone cannot explain (Mg^{2+} in STE1 was 23 mg/L) the high Mg^{2+} (37 mg/L) levels measured at NC2S.

DOC and B^{3+} were plotted against Cl^- (Figure 13d, 13e) to test their ability to distinguish contaminated waters with high NO_3^- concentrations from different groundwater sources. There is almost a linear trend between the boron and chloride concentrations: a number of other studies have found B^{3+} to be as conservative as Cl^- to trace aquifer contamination (Leenhouts et al., 1998). Some uncontaminated sites, however, also have relatively high boron and chloride concentrations without necessarily having significant levels of nitrate. In general, nitrate concentrations do not correlate well with DOC (Figure 13d), only for those samples with excessively high nitrogen content such as those from septic tank effluents (red dots). Chloride, boron and dissolved organic carbon do not provide additional information regarding the source and interaction of nitrate-bearing waters. This is the reason that boron isotopes were used: to attempt a differentiation between possible sources of nitrate in local groundwaters.

Water Chemistry of SGD sites

Most of the SGD samples were in the range of 1.0-2.0 mg NO_3/L. Unfortunately, no nitrate concentration data were available in surrounding stratified drift aquifers and only two concentrations were obtained from the small diameter wells installed for the project.

High salinity concentrations (>2 ppt) in some SGD sites prevented further hydrochemical analysis when comparing to the water chemistry of surficial and bedrock groundwaters, which are thought to be their source. Waters affected by this level of salinity completely changed their hydrochemistry to a Na-Cl water type. Groundwater diluted with seawater will significantly increase its TDS concentration, and especially the ions, Cl^-, Na^+, SO_4^{2-}, Mg^{2+}, K^+, and Ca^{2+} so that any fingerprint from upgradient flow paths becomes indistinguishable since every sample composition will depend on the degree of mixing at that particular site and on the tidal cycle when the sample was taken. Therefore, only the samples from SGD 58, 73U, and 73D were considered in this analysis.

After having discovered that bedrock fracture lineaments intercept the Great Bay's shores, waters at the discharge zones observed in the intertidal zone were thought to be composed of contributions from both surficial and bedrock aquifers. Overburden water in both stratified drift and glacial till deposits in major and minor degree recharge the bedrock. Given the topographic characteristics of the areas immediately upgradient from the SGD sites and their surrounding hydrogeologic setting, it was deduced that most of the SGD flow was of surficial origin and, in general, with short enough residence times that significant bedrock formation recharge was not in these flow paths. From the previous analyses it was noted, with a few number of samples though, that the shallow groundwater in glacial till has very consistent characteristics (NC1D, NC2S). Stratified drift and bedrock groundwaters, however, have more variability in their water chemistry compositions.

Using the AquaChem software package (Waterloo Hydrogeologic Inc.) allowed identifying the contribution of two water members (surficial and bedrock water samples) by linearly mixing (minimum Euclidean distance to targeted concentrations) their major ion chemistry compositions in a proportion that better describes the water chemistry at the SGD sites. The ions considered in the linear mixing scenarios were Na^+, Ca^{2+}, Mg^{2+}, Cl^-, and SO_4^{2-}. Particular attention was given to closely predict the concentrations of Cl^- and Na^+ in the targeted SGD water samples; primarily by considering Cl^- as a conservative ion in most aquifer systems and secondly for their importance in the local aquifer system.

The presumed sources of water yielding the water chemistry at SGD 58 were the immediately upgradient bedrock well (BK4N) and a well intercepting the stratified drift aquifer over the Pease International Airport (NIW-35). To recreate the chemistry of SGD 58, 35% of bedrock water (BK4N) and 65% overburden water were required. When mixing BK4N with NC1D, a shallow well with low concentrations of nitrate that was expected to better explain the chemistry at SGD 58 than the farther NIW-35 site, 25% bedrock contribution was found without accounting for the Na-enrichment of the SGD 58 site discussed in Figure 11 and Figure 13a and 13b.

At SGD 73U and 73D, BK3S and NC2S are the water members that best explain their water chemistries however in different proportions. The chloride ion was not well explained given its high concentrations in both these SGD sites, therefore, mixing was considered with and without Cl^-. Eighteen percent and 6% bedrock contributions were found with and without considering Cl^- in the set of explanatory ions for SGD 73U; and, 50% and 24% with and without including Cl^- for SGD 73D. Using the CFC analysis, the calculated bedrock contributions for SGD 58, 73U, and 73D sites are in agreement with the ionic mixing estimates. BK4N and BK3S exhibited 16% and 12% modern water, respectively, when using CFC's. This mixing was previously suggested by the bedrock piezometric map delineated around the bay (Roseen, 2003).

Hydrogen and Oxygen Isotopes

The δD and $\delta^{18}O$ values of groundwaters from the surficial and bedrock aquifers and waters at the discharge zones are presented in Table 5 with an analytical precision of 0.9 $^o/_{oo}$ and 0.08 $^o/_{oo}$, respectively; and their relationships are shown in Figure 14, plotted together with the global meteoric water line (GMWL). The GMWL (Rozanski et al., 1993) is $\delta^2H = 8.2\,\delta^{18}O + 11.3$; and the $\delta D - \delta^{18}O$ relationship at Truro (Nova Scotia) was chosen as the local meteoric water line (LMWL), $\delta^2H = 7.28\,\delta^{18}O + 4.27$, $r^2 = 0.94$, http://www1.ncdc.noaa.gov/pub/data /paleo/ precip_isotopes/). Truro's meteoric water line is similar to the one observed at Hattreras, NC ($\delta^2H = 6.12\,\delta^{18}O + 4.33$ $r^2 = 0.82$), which is the nearest available long-term record along the Atlantic Coast of the United States. The deuterium intercept in these meteoric water lines differs slightly. The slope corresponds to the ratio of the fractionation factors during evaporation. However, Hattera's LMWL seems to have a major kinetic fractionation effect during evaporation (Clark and Fritz, 1997) than Truro's LMWL given its lower slope. The δD and $\delta^{18}O$ values are enriched at Hatteras station with ranges of -0.7 $^o/_{oo}$ to -40.3 $^o/_{oo}$ and -0.2 $^o/_{oo}$ to -7.0 $^o/_{oo}$, respectively. This enrichment can be explained considering the fact that

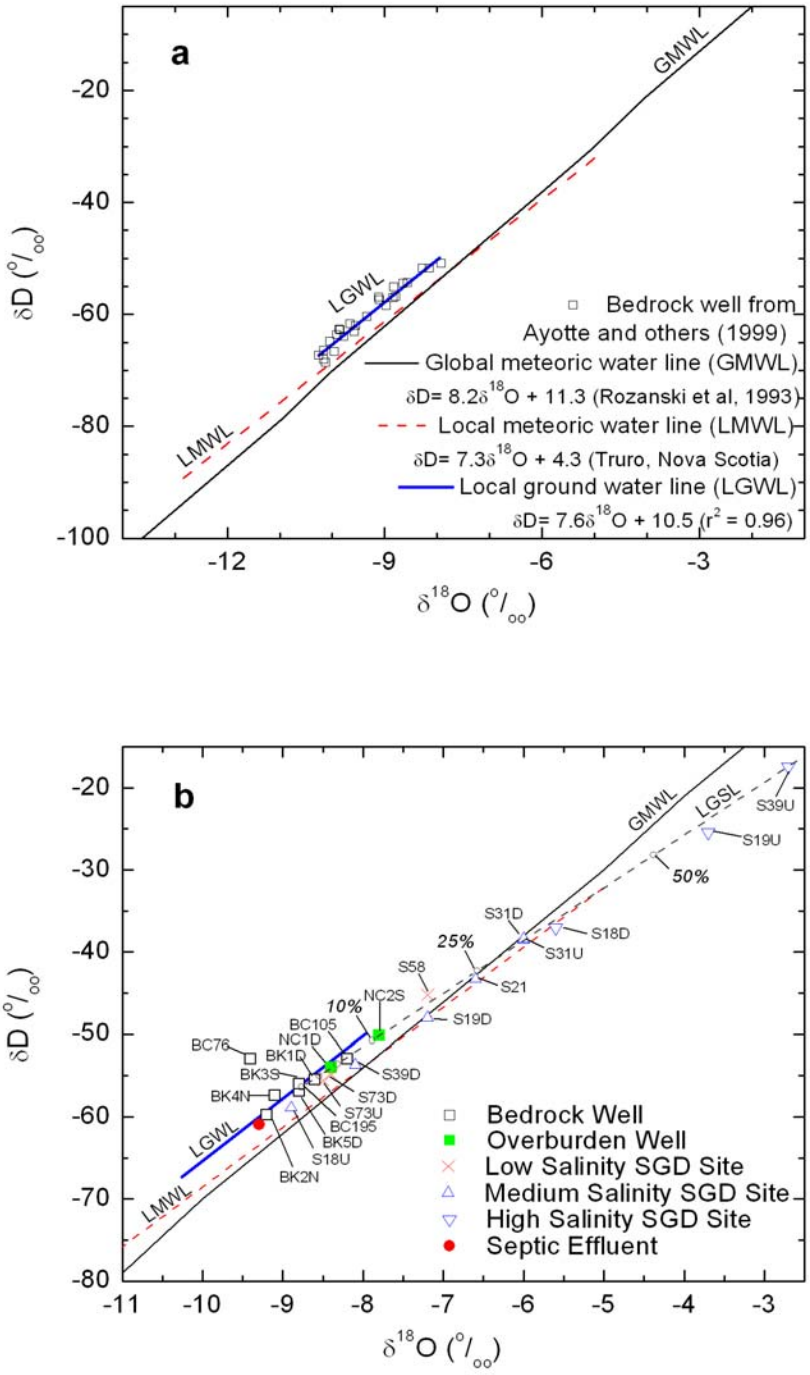

Figure 14. a) Global (GMWL), and local meteoric (LMWL), and groundwater (LGWL) lines identified for this study; b) Deuterium and Oxygen-18 content of samples from overburden and bedrock groundwater and of water at SGD sites with different salinities compared to GMWL (Rozanski et al., 1993), LMWL (Truro, Nova Scotia), and LGWL. Also plotted is the local groundwater-seawater mixing line (LGWL) for the area of study.

isotopic fractionation is highly temperature and latitude dependant: the closer the waters are to the equator the more enriched are the heavy isotopes relative to polar waters.

Considering the isotopic composition of water from bedrock wells used by the USGS (Ayotte et al., 1999) for determining the lithogeochemical character in the New England Coastal Basins, with ranges from -7.9 to -10.3 $^{o}/_{oo}$ and -50.9 to -68.6 $^{o}/_{oo}$, for $\delta^{18}O$ and δD respectively, confirmed the observed trend (Figure 14a) in other studies along the mid-Atlantic Coastal aquifers of United States (Dunkle et al., 1993; Plummer et al., 2001); by plotting parallel to the LMWL with an overall deuterium excess of 14 $^{o}/_{oo}$. This clustered data in Figure 14a defines the local groundwater line, LGWL ($\delta^{2}H = 7.57\ \delta^{18}O + 10.5$ $r^2 = 0.96$). There is no evidence of evaporation affecting these waters.

The δD and $\delta^{18}O$ values of groundwater from the surficial aquifers and bedrock aquifers, and low salinity water at the discharge zones plotted along the previously described LGWL with a deuterium excess *d* ($d = \delta D - 8\delta^{18}O$) ranging from +4.5 $^{o}/_{oo}$ to +15.1 $^{o}/_{oo}$ and averaging +12.6, +13.9, +12.6 $^{o}/_{oo}$, respectively, which are characteristic of spring recharge. Hydrogen and oxygen isotopic values of overburden wells overlap those of SGD sites but both are slightly enriched relative to bedrock sites, which do not show any particular relationship with their host geological formation. The source of the water from these bedrock sites is apparently local given their short residence time (<50 years) and no indications of an old water component with distinct isotopic composition was found.

SGD 73U and 73D sites, in particular, have δD and $\delta^{18}O$ values that are between the overburden and bedrock water samples. The location and surface materials at the recharge area may explain the isotopic composition enrichment of water from the surficial aquifer with respect to that from the bedrock. Bedrock aquifers usually obey a more regional recharge pattern in the area of study, when neither sink-holes nor karst systems are present. Highly permeable materials facilitate recharge to deeper zones of the aquifer. Stratified drift aquifers around the area of study might constitute an important source of recharge to bedrock given the significantly greater depth and hydraulic conductivity of these surficial materials compared to glacial till material that dominate elsewhere. In the stratified drift aquifers, rapid percolation of water results in a lower air-water interaction at the surface and the unsaturated zone. In other surficial deposits, surficial perched aquifers are usually formed allowing for continuing isotopic fractionation and leading to an enrichment in the heavier isotopes, hence developing a higher isotopic composition while no evidence of evaporation is observed. SGD 58 and NC2S are the sites with higher water stable isotopic composition, the former being distinctly located at one end of the LGWL curve whereas its upgradient bedrock site (BK4N) plots near the other end of the LGWL line. This observation suggests that had SGD 58's water been a mixture of bedrock and overburden waters, the overburden might be the major source of such water. Surficial aquifer sites, NC1D and NC2S, have distinct δD and $\delta^{18}O$ values compared to precipitation (Figure 14b) and surface water (not shown), even though their water samples were taken at 13 ft and 9 ft below ground. They seem to have a larger isotopic variability than bedrock waters, although the reduced number of samples in the surficial aquifer does not allow for a strong statistical inference on this observation. NC2S, the most isotopically enriched site of the two, is, according to the CFC analysis in the present study, composed of 87% modern water that may have recharged the aquifer anytime after 1994. Given both the depth at which this small

diameter well was installed and seasonality of δD and $\delta^{18}O$ implies that recently recharged water contributes flow to this site, as identified by the CFC analysis.

The SGD sites of medium and high salinity are significantly enriched with respect to both isotopes and systematically indicate the level of influence of estuarine water in their water samples. Having the combined-average isotopic composition of bedrock, overburden, and low-salinity SGD sites as the fresh-meteoric water end-member component and the isotopic composition of modern oceanic water ($0\ ^{o}/_{oo\ (VSMOW)}$ for both δD and $\delta^{18}O$) as the other end-member, the local groundwater-seawater mixing line (LGSL) can be defined (Figure 14b). The LGSL indicates the relative proportion of seawater or leakage that has mixed with meteoric water (recharge water) in the area of study. Considering simple volumetric mixing, SGD sites seem to be well fitted along this mixing line, such as SGD 21 and BK1D whose water samples seem to be composed of 25% and 2.5% of seawater (2.5 to 5% using boron isotopes analysis), respectively. Likewise, using the recognized correlation of $\delta^{18}O$ with ocean salinity and geochronology studies, from a relationship between chloride concentration and $\delta^{18}O$ values it is possible to obtain a clearer mixing line (Figure 15 and the insert for a broader view) using the same end-member waters as for LGSL (local groundwater-seawater line).

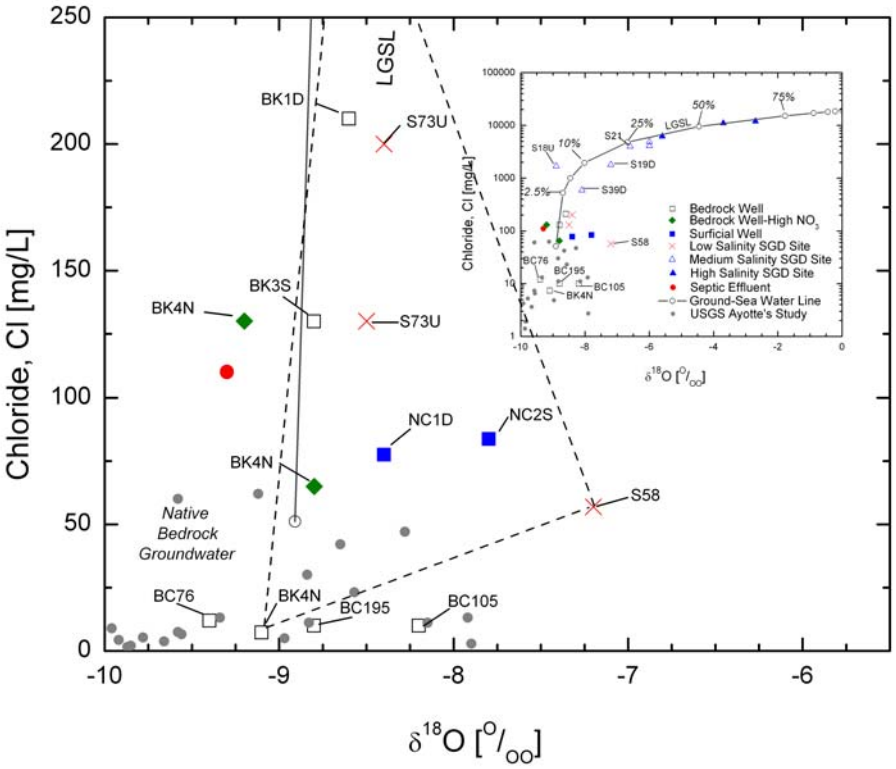

Figure 15. Plot of Cl- and Oxygen –18 concentrations for shallow and bedrock groundwater and at SGD sites. Also plotted is the groundwater-seawater mixing line.

In δD-$\delta^{18}O$ and Cl-$\delta^{18}O$ relationships, SGD 39D, 19D, and 18U remain systematically depleted relative to the LGSL mixing line. In particular, SGD 18U's Cl-$\delta^{18}O$ relationship indicates that a simple mixing between these two end members cannot explain its distinctive isotopic composition. Looking closely at the δD-$\delta^{18}O$ relationship, however, the groundwater at these sites might seem to be influenced by recently recharged water from precipitation that in the case of SGD 18U may have occurred through a gravel pit just immediately upgradient from the discharge zone. Nevertheless, there is no apparent explanation in observing this phenomenon in sites SGD 19D and 39D, which leads them to be considered as part of the intrinsic variability of these parameters that is also present in the precipitation data.

SGD sites with medium and high seawater mixing ratios reflect the complex dynamics of the saltwater wedge at the discharge zones where a large volumetric retention of high tide waters (with mixing ratios of approaching 100%) occurs on a daily basis with outflow during the low tide cycle. SGD 58 and 73U are not affected by any trace of seawater, the former, however, is the most enriched site of the study (Figure 14b) and has a distinctive Cl-$\delta^{18}O$ composition when compared to its upgradient bedrock sites BK4N, BC105, BC195, BC76 and BK2N.

Boron Isotopes

Boron isotopic ratios clearly identify a septic nitrogen-bearing source. The boron isotopic ratio of septic tank effluent ranges from 5.2 to 13.7 $^{o}/_{oo}$ (Figure 16, Table 5) for the study area. This range overlaps those of nitrate-bearing overburden and bedrock waters and is similar to the isotopic ratios measured in Israel 5.3 – 11.2 $^{o}/_{oo}$ (Vengosh et al., 1994) and overlaps those of natural Na-borates 0 $^{o}/_{oo}$ to 10 $^{o}/_{oo}$, which are used in the industry as bleaching agents. Septic effluent STE1 clearly stands in Figure 16 as a main end-member component given both its distinct boron isotopic composition and its boron concentration. STE2 lacks this clear fingerprint probably because of its origin. The STE2 sample was taken from the Jackson Estuarine Laboratory (JEL) wastewater system, which is a separate black water system and therefore may not have as much sodium perborate compounds as in the cleaning wastes of a household source. Also, the JEL samples differ from normal household wastewater due to the use of estuarine water (higher Cl^-, $\delta^{11}B$) for some activities at the facility.

Background bedrock groundwater in the data is clearly represented by BK4N when looking at Figure 16 and Figure 17 and is verified by its low chloride (7.0 mg/L), DOC (0.33 mg/L), and nitrate (0.28 mg/L) concentrations. BK1D shares similar chemical characteristics (0.31 mg DOC /L and 0.30 mg NO_3/L) except in its chloride content (210 mg/L). This private well (with 5-10 ft in Bedrock and 50 ft below ground), during the last two years (based on private well water quality testing data), has exhibited considerably increased chloride and sodium concentrations

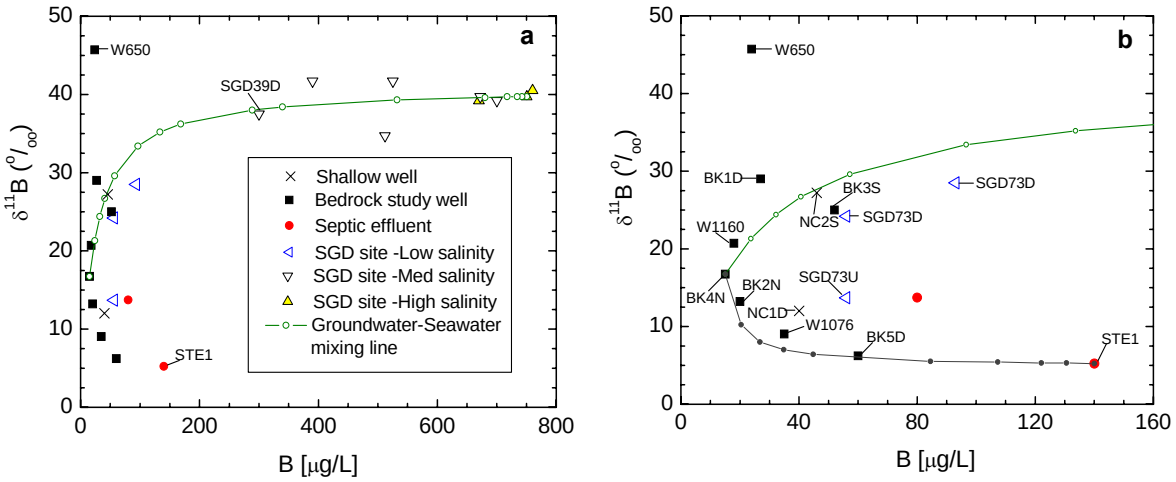

Figure 16. Relationship of boron and boron isotopic composition ($\delta^{11}B$) for groundwater and at SGD sites.

indicating an interception, within its radius of influence, of new water with different characteristics or/and with seawater. This latter description is in agreement with both the isotopic (29 $^{o}/_{oo}$) and elemental (27 mg/L) boron composition of its groundwater sample. Both bedrock wells define a $\delta^{11}B$ range for native groundwater between 16.7 – 29 $^{o}/_{oo}$, which is the expected range (a similar range was reported by Vengosh and Spivack, 2000) for coastal zones where the marine end member tends to dominate due sometimes to the presence of marine aerosols with high $\delta^{11}B$. BK1D may constitute a bedrock background groundwater well for mixed groundwater with marine influences. Both sample locations: overburden well samples and samples from SGD sites with low salinity content, overlap this range. Samples from these locations also plot in the lower range of $\delta^{11}B$ values where sites with high nitrogen content plot closely (BK2N, 2.49 mg NO3/L; W1076, 5.18 mg NO_3/L; WH, 3.22 mg NO_3/L) along a hypothetical mixing line connecting the latter native groundwater site sample with the septic tank effluent sample. The rest of samples (SGD 58.4, NC2S, and SGD 73D) plotted with boron isotopic composition similar (24.2 – 28.5 $^{o}/_{oo}$) to that of BK1D but enriched in their elemental boron concentration (46 – 93 mg B/L).

NC1D sample plots closely along a hypothetical mixing line between the BK1D and septic tank effluent samples (Figure 17). This indicates a mixing ratio of 5% septic tank effluent with background groundwater. The SGD 73U site can be considered completely absent of any marine influence given its chloride (130 mg/L equal to BK2N), sodium (48 mg/l), boron (56 ng/L), and $\delta^{11}B$ (13.7 $^{o}/_{oo}$) contents. Elemental boron and boron isotopic enrichments are frequent indicators of marine influence. In spite of having a relatively low salinity concentration at the time of sampling, sites SGD 58.4 (0.4 ppt) and SGD 73D (0.3 ppt) seem to have an important marine component given by both their high boron isotopic compositions and chloride concentrations, demonstrating the sensitivity of this analytical technique in detecting marine influences in groundwater systems.

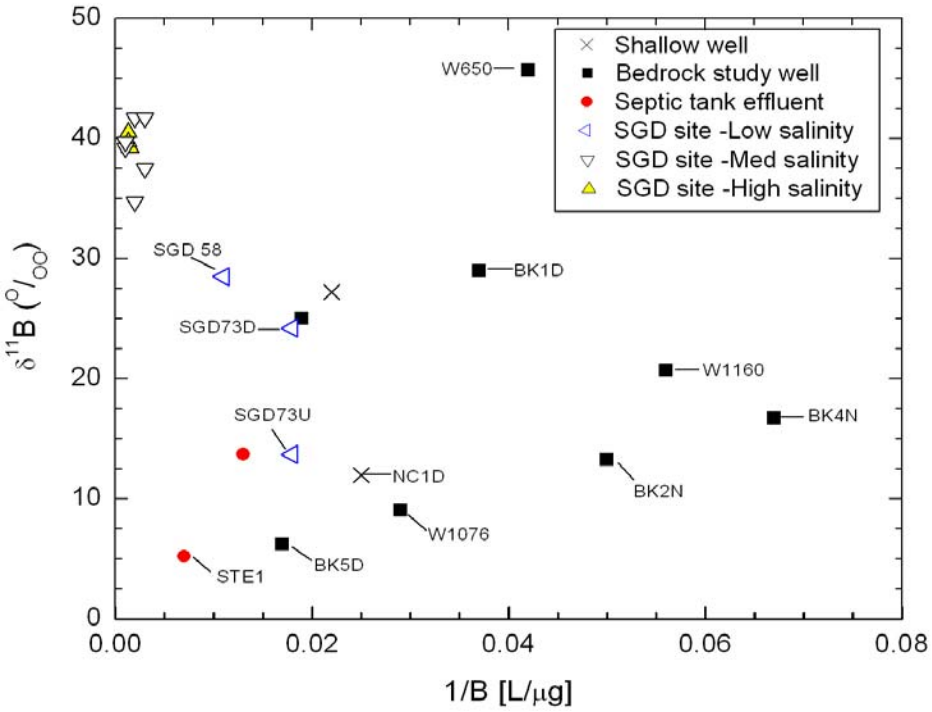

Figure 17. Plot of $\delta^{11}B$ and 1/B for groundwater and at SGD sites.

Noticeably, SGD 73U and SGD 73D sites have the same boron concentration but different isotopic composition. Marine influence at the downgradient site alone, cannot explain their different $\delta^{11}B$ values since the marine influence is frequently accompanied by a significant increase of boron concentration, as is the case for SGD 58.4 when compared with its background isotopic composition dictated by BK4N located in the immediately upgradient vicinity. Likewise as for SGD 73D, NC2S's $\delta^{11}B$ value (27.2 $^{o}/_{oo}$) is not in agreement either with a septic effluent influence or with its nitrate concentration (1.43 mg/L). NC1D ($\delta^{11}B$ = 12.0 $^{o}/_{oo}$) is surrounded by a low-use agricultural field on which fertilizer has been applied on a yearly basis and no septic system is found within a 500 ft perimeter, which may lead to characterize it as a distinct fertilizer-affected groundwater. There is no further evidence to support this distinct contaminant source besides the relatively high Mg^{2+} concentration in the sample. The boron isotope technique, however, is only able to trace nitrate sources from agricultural activities where boron-based fertilizer has been applied in the study area (Dr. Thomas Bullen, personal communication) which does not correspond to the majority of the fertilizers as other studies have suggested (Komor, 1997).

The distinct boron isotopic compositions can be used to trace groundwater flow paths by considering the location where the samples in the systems were taken. Having bedrock wells (BK4N, W1076, BK5N, and BK2N) lined-up along the septic affected groundwater mixing line indicates: i) there are similarities in the recharge conditions among these sites; and, ii) they may be representative samples of regional groundwater

for the area. Upgradient from all these sites there is a very well identified stratified drift recharge zone with transmissivities that range from < 500 – 2000 ft^2/day (Moore, 1990). Water in overburden may pass through high clay content zones in both the vadose and saturated zones. Therefore, boron adsorption, which is reflected in $\delta^{11}B$ enrichment, is likely to occur in these conditions. Had it occurred, the boron source isotopic fingerprint still remains identifiable. However, at least for bedrock wells, this process does not seem to have significantly affected their regional isotopic composition. On the other hand, adsorption may explain NC1D and SGD 73D boron isotopic signatures. The surficial materials at these sites consist of rich-deposits of glacial till and peat, typical of marsh environments, respectively. In the case of SGD 73D, for which no boron depletion is observed when compared with its immediately upgradient pair SGD 73U, a cycle of boron enrichment-adsorption and consecutive $\delta^{11}B$ enrichment when interacting with recently infiltrated high tidewater would explain the similar boron concentrations.

Considering the previous analysis from Figure 16, a $\delta^{11}B$ range of 6.2-13.7 $^{o}/_{oo}$ indicates groundwater affected by septic effluent. For unknown reasons, the boron isotopic composition of sites W1160, SGD 73D and NC2S deviate from the expected values (when considering their nitrate concentrations).

Strontium Isotopes

The total Sr^{2+} concentrations and the $^{87}Sr/^{86}Sr$ ratio measured at selected samples are presented in Table 5. The relationship between $^{87}Sr/^{86}Sr$ and Sr^{2+} distributions obtained from the groundwater samples are shown in Figure 18 (Sr^{2+} is expressed in the form Cl/Sr). The use of a conservative tracer in the numerator accounts for any dilution effects. The ratios of $^{87}Sr/^{86}Sr$ for water collected from the shallow and bedrock wells, however, overlapped in their ranges of 0.71414 to 0.71647 and 0.71146 to 0.71425, respectively. $^{87}Sr/^{86}Sr$ values for overburden wells tend to be more radiogenic (higher $^{87}Sr/^{86}Sr$) and variable (considering the number of samples) than water from the bedrock aquifer, decreasing from a high value of 0.71647 at 10 ft below surface (NC1D) to 0.71146 at 10 ft under bedrock (BK1D) both in areas with similar soil composition. The Sr^{2+} concentrations do not significantly differ with depth when comparing samples taken from both the shallow and the stratified-drift aquifer wells with those from the bedrock. In the study area, distinct Sr^{2+} ranges for freshwater (0.05 mg/L to 0.37 mg/L) and brackish water (0.65 mg/L to 2.16 mg/L) can be identified.

The $^{87}Sr/^{86}Sr$ ratio tends to be less radiogenic for samples with higher salinity content decreasing asymptotically towards the average isotopic seawater composition (0.7092). Figure 18 shows another line of evidence of seawater intrusion at BK1D and in less degree at the low salinity SGD sites. Two groups of samples can be identified from Figure 18: I) those sites with low Cl/Sr ratio (<4) and more radiogenic; and ii) those sites with Cl/Sr greater than 6 and less radiogenic.

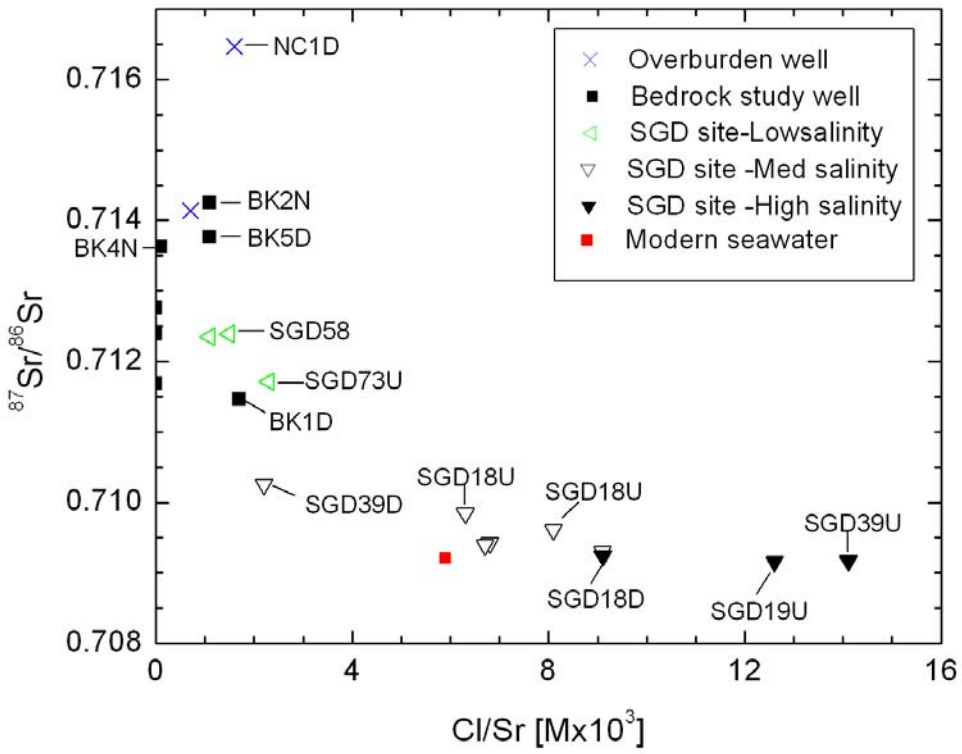

Figure 18. $^{87}Sr/^{86}Sr$ and Cl/Sr ratios measured in overburden and bedrock groundwater, and Great Bay intertidal discharging water.

The Cl/Sr ratio of the seawater end member separates these two groups with the second group having higher Cl/Sr ratio than seawater. The high Cl/Sr ratio of the second group is indicative of lowering Sr^{2+} concentrations due to a cation exchange mechanism that has affected their water composition before mixing with seawater.

Strontium (Sr^{2+}) concentrations correlate positively with Ca^{2+} and K^{+} concentrations. Calcium (Ca^{2+}) correlates better in the upper aquifer ($r = 0.79$) than in the bedrock aquifer ($r = 0.65$); in contrast, K^{+} correlates better in bedrock ($r = 0.45$). Ca/Sr ratio, however, does not depict a clear relationship between the two aquifers and the water at the discharge zones. $^{87}Sr/^{86}Sr$ ratios exhibited low correlation with Sr^{2+} concentrations in the bedrock aquifer.

Flow Path Analysis

SGD sites were thought to be the discharging location of an upgradient flow path that extends over both the overburden and bedrock aquifers. The upgradient overburden and bedrock wells from each SGD site were thought to be representatives of their respective aquifers. This hypothesis needs to be examined to evaluate the conclusions drawn from it.

Groundwater discharge usually occurs at very spatially located gravel sediments along the tidal flats. This coarser material allows less resistance to flow than other overlying confining layers mainly composed by marine sediments. The surrounding hydrogeological settings at the groundwater discharge zones are varied and complex. Some are located in areas dominated by a salt marsh environment, where *spartina alterniflora* and *spartina patens* commonly grow; others are close to bedrock outcrops and inland vegetation.

The monitoring well at the discharge zone at SGD 18.2 and SGD 31.4 had higher salinity content than the small diameter well (SDW) located immediately upgradient from it that was thought to intercept the same discharging groundwater to the bay. However, at other SGD sites (SGD 19.3 and SGD 39.3), the monitoring well at the discharge zone had lower salinity content. High salinity contents prevented any comparison between these monitoring wells at a given SGD site.

Nevertheless, being silica (SiO_2) completely absent from seawater chemical composition, it allowed tracking a time-related groundwater fingerprint in some seawater-contaminated samples based on its accumulation with time through mineral dissolution of host rock. For instance, SGD 39.3U (Upgradient) with a salinity of 18.8 ppt had the highest SiO_2 concentration (10 mg/L and probably higher due to dilution with seawater) of all the monitoring wells used for this study, but the downgradient site (SGD 39.3D) showed a depleted value (4 mg SiO_2/L). This observation implies two possible explanations. i) Mixing of SGD 39.3U water with other groundwater with lower SiO_2 content; or ii) they have different flow paths. From the sampled sites, neither overburden nor bedrock well has lower salinity than 4 mg SiO_2/L, but probably this concentration has also been diluted by seawater at the time of sampling. A similar ambiguity on the hypothetical flow path is observed at SGD 19.3.

Silica concentrations are a good proxy to identify SGD 73.1 (both upgradient and downgradient = 7.3 mg SiO_2/L) with a consistent flow path that intercepts the upgradient and downgradient SDWs at the discharge zone. As $^{87}Sr/^{86}Sr$ and $\delta^{11}B$ analyses have previously shown SGD 73.1 (as well as SGD 58.4) exhibits a very slight seawater intrusion. The contribution from seawater for this site is readily subjected to comparison using the molar concentration ratios at SGD 73.1 summarized in Table 9 in which their evolution along the hypothetical flow path is presented. This comparison assures the use of SGD sites with low salinity content for further analysis, since seawater did not distinctively affect their water chemistry composition.

In Table 9 the evolution of the hypothetical flow path is expressed in terms of molar concentration ratios. Potassium and SO_4^{2-} remained unchanged along the flow path. Calcium, Mg^{2+}, and Sr^{2+} (high Ca/Sr ratio) are significantly depleted at BK3S due to the cation exchange mechanism observed in Figure 11 in which Na^+ is enriched (Table 9). Ca/Cl and Mg/Cl ratios suggest mixing of BK3S and NC2S at SGD 73.1 but Na/Cl do not, indicating that cation exchange at the level observed in BK3S is a result of long water-rock interaction. Likewise as for SiO_2, SGD 73.1U and SGD 73.1D molar ratios are very similar, verifying the flow path hypothesis in the intertidal zone. However, there is not such correspondence of these sites with either NC2S or BK3S when looking at Na/Cl, Ca/Mg, and Ca/Sr ratios, which are composed by the ions associated with the described cation exchange process resulting in the depletion of Ca^{2+}, Mg^{2+}, and Sr^{2+} concentrations in water and the Na^+ enrichment in water.

The Piper diagram (Figure 11) can also be used for tracing the chemical evolution of waters along a specific flow path. The cation trilinear diagram and the diamond diagram suggest that mixing between NC2S and BK3S (or the water they represent) is possible. Because of the high Cl^- concentration at SGD 73D, this relationship is not kept at the anion triangulation.

Table 9. Evolution of molar concentration ratios along hypothetical flow path at SGD 73.1 site and saturation ratios (SR) with respect to different minerals.

Ratios	Units	Bedrock Well (BK3S)	Overbuden (NC2S-SDW)	Upgradient SGD 73.1	Downgradient SGD 73.1	Seawater
Ca/Cl	[M]	0.01	0.38	0.32	0.22	0.02
Na/Cl	[M]	1.9	0.72	0.57	0.56	0.85
Mg/Cl	[M]	0.02	0.64	0.26	0.19	0.1
K/Cl	[M]	0.02	0.04	0.03	0.02	0.02
B/Cl	[M] * 10^(-3)	1.31	1.8	1.41	0.92	0.05
Br/Cl	[M] * 10^(-3)	2.12	0	0	1.79	-
SO4/Cl	[M]	0.04	0.03	0.02	0.02	0.05
Ca/Mg	[M]	0.61	0.59	1.22	1.16	0.2
Ca/Sr	[M]	1457	256	353	342	112
Minerals	Ions	SR	SR	SR	SR	-
DOLOMITE	Ca, Mg, CO_3	0.11	0.84	1.25	0.6	-
MAGNESITE	Mg, CO_3	0.06	0.28	0.31	0.18	-
QUARTZ	SiO_2	1.68	1.66	1.83	1.83	-
CHALCEDONY	SiO_2	1.22	1.21	1.33	1.33	-

Since it is not possible to assert that without cation exchange there will be more concordance in describing the water chemistry at the SGD sites, an either positive or negative answer for the hypothesis of overburden and bedrock aquifer convergence at the discharge location remains veiled.

DELINEATION OF CAPTURE ZONES

Parameters To Include Into WhAEM

Analytic elements for the project were included into the analysis from previous studies on the geohydrology of the area primarily from Moore (1990), Stekl and Flanagan (1992), and Mack (2003). Thickness (b) varies in the unconsolidated materials from 20 ft – 100 ft; and a value of 0.2, for porosity (n) in glacial till deposits, was found to be representative. There are, however, several reported values for recharge rates (r) to the surficial aquifer. Recharge rates reported by some authors are, for instance, ⅓ of annual precipitation (Hill, 1979); or ½ of annual precipitation specifically for stratified drift

aquifers (MacNish and Randall, 1982); or 16% (0.5 $ft^3/s/mi^2$) of annual precipitation found in Maine for recharge over till-covered bedrock areas (Morrisey, 1983), which correspond to 0.0033, 0.0049, and 0.0015 ft/day, respectively for an annual precipitation rate of 3.58 ft (43 in).

Figure 19 displays modeling results when employing the ranges of input parameters within the published ranges and by using a simple reservoir model. These serve as controlling parameters of the WhAEM2000 model. These residence times (T) are based on the application of a simple reservoir model (Focazio et al., 1998), i.e. assuming the system acts as completely isolated with no losses or additional inputs considered other than discharge and recharge, respectively (T= bn/r).

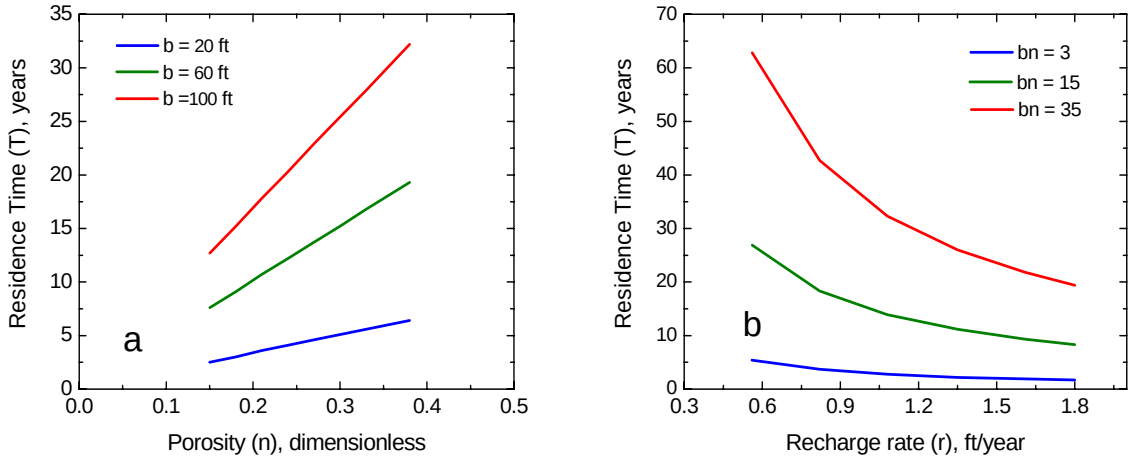

Figure 19. Residence time estimated using a range of published values for porosity (n), aquifer thickness (b) and recharge rate (r), assuming a simple reservoir model expressed in terms of a) iso-thickness lines; and b) varying recharge rates and thickness with n = 0.2.

Increased residence times occur, according to the reservoir model depicted in Figure 19, in waters whose flow path is characterized by having a high porosity and large aquifer thickness; also by low recharge rates. Comparing the piston groundwater age, determined for SGD sites with the use of CFC analysis, with the ranges in residence times in each one of the curves of Figure 19a and 19b the aquifer thickness (60 ft), porosity (0.2), and recharge rate (1.08 ft/year or 0.0033 ft/day) are reasonable values to incorporate in the WhAEM2000 model. This comparison can be also extended over the CFC-derived mean apparent age for the overburden aquifer (9.5 ± 2.1 years), when getting the residence time (~10 years) from Figure 19a for the aquifer thickness (60 ft) and porosity (0.2) values of 60 ft and 0.20, respectively.

Hydraulic conductivity (K) is another important input parameter for WhAEM2000. In stratified drift aquifers, K-values for the area of study have been reported on the order of 50 to 500 ft/day. For a superfund site at the Pease International Tradeport (Newington, NH), on the other hand, a mean K-value of 10 ft/day was reported for the underlying bedrock aquifer (Pulido and Ballestero, 2003). Hydraulic

conductivity values ranging 15 – 40 ft/day were assigned to till-covered areas located in the proximities of the discharge zones (Figure 18a).

The SGD study sites were modeled for low tide conditions, i.e. no-flow boundary condition was established for estuarine water by locating a "horizontal barrier" element along the shore of the Great Bay. Multiple surrounding SGD sites that were not included in the study were considered as discharging wells using the flow characterization made by Roseen and others (2002). In so doing, and for simplifying the model size, one single well represents the sum of discharges of multiple clustered SGD sites, except for the SGD site of interest. No other inflow or flow loss was considered for the surficial groundwater flow analysis.

The WhAEM2000 model requires that a travel time for particle tracing be designated to run the model. For this purpose, results from groundwater dating with CFCs were used in the model. Most of SGD sites have an expected range of residence time (Table 4) from 12 to 20 years, except for SGD 18.2 and SGD 58.4 for which longer residence times are estimated. Therefore, the mean expected residence time between the upper and lower limits of this range for each SGD site was the travel time input parameter included in WhAEM2000.

Land Use Mosaics within GCZ and Nitrate-Bearing Groundwater

WhAEM2000 has the capability of exporting the delineated capture zones in shape file facilitating their analysis in an ArcView environment (Figure 20). Digital land use coverage in the Strafford and Rockingham Counties were made available by GRANIT (2004) for the years 1962, 1974, and 1998. The residence time-derived capture zones were then matched accordingly to the nearest land use coverage year. With the exception of SGD 18.2 and SGD 58.4, the 1974 land use coverage was the nearest available land use coverage for the mean expected residence time of most of the SGD sites; even though, their values fall in the mid- and early 1980's. Unfortunately, no digital land use coverage was available during the 1980's, which would certainly have shown the first stages of increasing population growth in the area. In Table 8 summarizes the percentage of the most important land use categories in the coverage of the years 1962, 1974, and 1998 identified within the capture zone of each SGD study site.

The average linear flow velocities (bulk velocities) calculated using the distance traveled (from flow path delineation) of a particle within the capture zone divided by the CFC-groundwater age of water in days, a reasonable range (0.2 – 1.0 ft/day) for the local overburden materials was obtained. This result confirms both the CFC-derived groundwater ages and the K -values used in WhAEM.

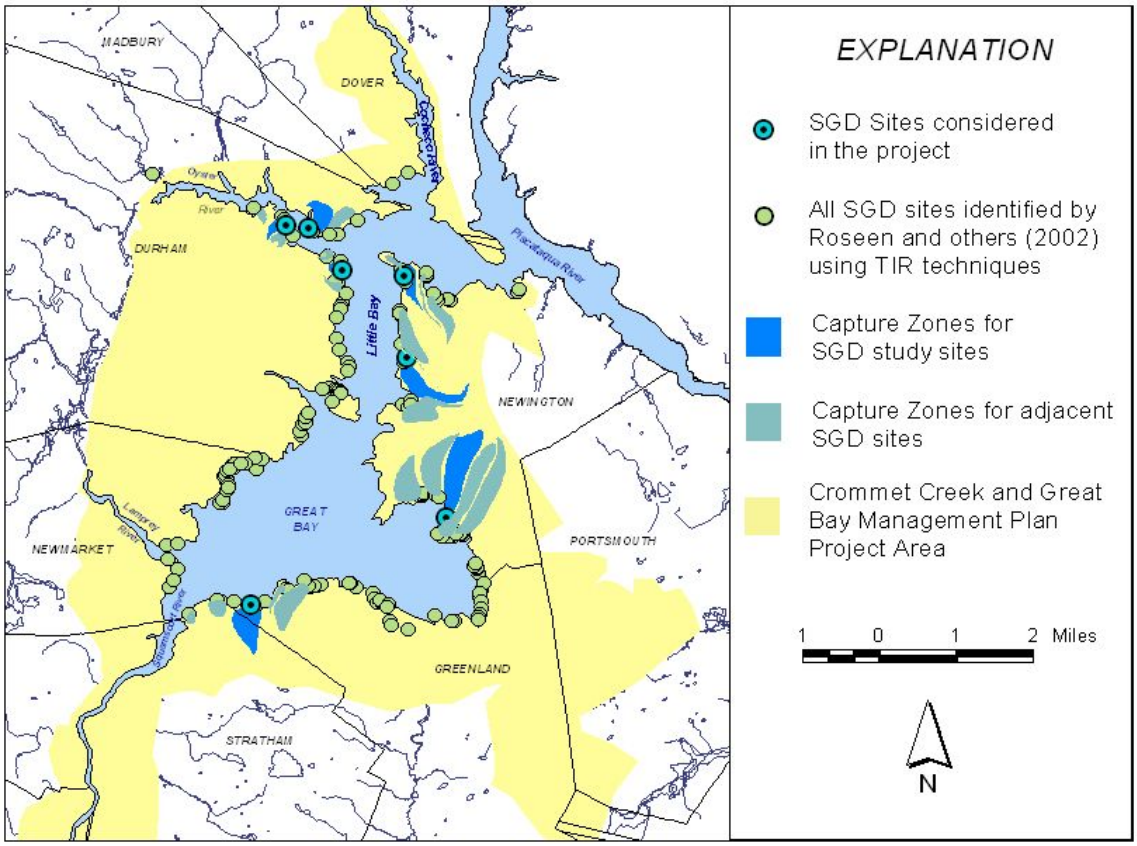

Figure 20. Delineated capture zones for SGD study sites using WhAEM2000 and recreated in ArcView for further analysis.

The ratios of percentage of residential and agricultural land use when normalized by the percentage of forested use helped identifying the dominant land use at a given site (Table 8). From Table 9, the agricultural land use adjacent to SGD 18.2, SGD 19.3, and SGD 21.2 (the three in Durham, Strafford County) appears to be the most dominant through the period 1962-1998. Likewise as the rest of the watershed, a diminishing agricultural land use trend is observed in all SGD site wellhead areas except for SGD 21.2 where the land use categories remained unchanged in that period. This is particularly true for SGD 19.3, SGD 39.3, and SGD 73.1 where significant portions of land use have changed from agricultural to mostly residential and in a lesser degree to forest.

Table 10. Specific land use distribution for SGD study sites and ratios for identifying dominant land use category.

Site	Coverage Year	Residential	Transport.	Agriculture	Forested	Idle/other open	%Res	% Agricult.
							%forested	%forested
SGD 18.2	1962	0.0%	0.0%	79.1%	18.0%	0.0%	0.00	4.39
	1974	0.0%	0.0%	69.7%	18.3%	10.2%	0.00	3.81
	1998	0.0%	0.0%	63.4%	36.2%	0.4%	0.00	1.75
SGD 19.3	1962	0.0%	0.0%	74.5%	25.5%	0.0%	0.00	2.92
	1974	0.0%	0.0%	68.3%	25.1%	0.0%	0.00	2.72
	1998	20.2%	8.2%	34.8%	12.1%	18.1%	1.66	2.87
SGD 21.2	1962	6.1%	3.3%	90.6%	0.0%	0.0%	-	-
	1974	5.7%	3.3%	91.0%	0.0%	0.0%	-	-
	1998	5.7%	3.3%	91.0%	0.0%	0.0%	-	-
SGD 31.4	1962	0.0%	2.3%	67.9%	29.0%	0.0%	0.00	2.34
	1974	4.5%	2.9%	57.4%	31.3%	3.2%	0.14	1.83
	1998	17.1%	2.9%	48.6%	30.3%	0.4%	0.57	1.60
SGD 39.3	1962	10.9%	1.2%	51.3%	34.4%	1.9%	0.22	1.49
	1974	12.0%	1.4%	47.9%	35.7%	2.6%	0.21	1.34
	1998	40.4%	5.6%	1.4%	42.9%	9.2%	0.94	0.03
SGD 58.4	1962	6.8%	1.6%	25.7%	44.2%	19.9%	0.00	0.58
	1974	5.4%	2.7%	11.5%	52.1%	26.5%	0.00	0.05
	1998	0.0%	12.2%	8.3%	73.2%	4.5%	0.00	0.11
SGD 73.1	1962	6.9%	1.6%	39.4%	48.1%	4.1%	0.14	0.82
	1974	8.1%	1.6%	32.2%	56.3%	1.8%	0.14	0.57
	1998	48.5%	4.2%	5.7%	28.0%	13.4%	1.73	0.20

Residential and transportation land uses show their greatest increase during the period 1974-1998, redistributing the land use mosaics by diminishing the percentage of forested and agricultural lands. These observations are in agreement with what has been observed in the New Hampshire coastal region (NHEP, 2003). Figure 21 shows the evolution of the land use distribution for the study sites' wellheads and for the period of analysis using the mentioned factors. The fact of finding this effect in both large and small scale lead to the recognition that the lands immediately riparian to the Great Bay are an important zone during this period where land use distribution changes took place.

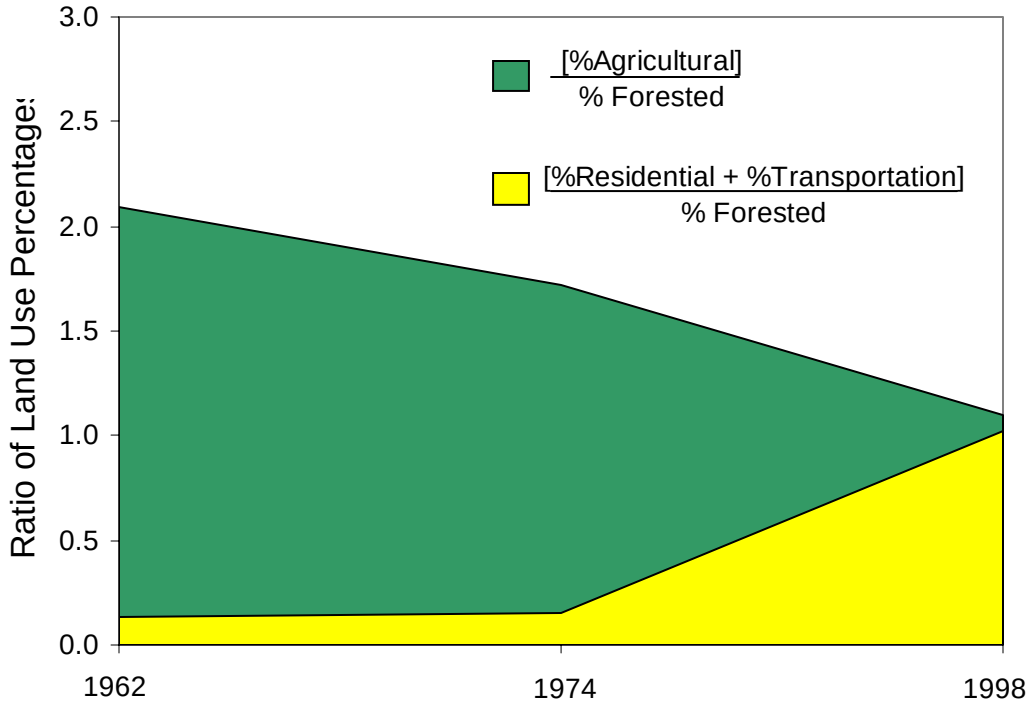

Figure 21. Distribution of land use mosaics within SGD site capture zones.

In Figure 22, the land use evolution of two of the targeted land use categories in the upgradient areas of SGD 73.1 (high residential development) and SGD 58.4 (undeveloped) is presented as an example. In the former, land use evolved by switching from agricultural to residential land use; and in the latter from agricultural and residential to forested land use. Nitrate concentrations measured at SGD 73.1 are 3.54, 1.71, and 2.08 mg/L taken at the discharge zone, from the upgradient SDW, and at the discharge zone reported by Roseen (2002). This site has the highest nitrate concentration reported among the SGD sites. Also it has the highest %Residential/%Forested factor (1.74) and %Residential land use among all SGD sites. The nitrate concentration measured at SGD 58.4 is 0.01 mg/L and at BK4N, its upgradient bedrock well, is 0.28 mg/L.

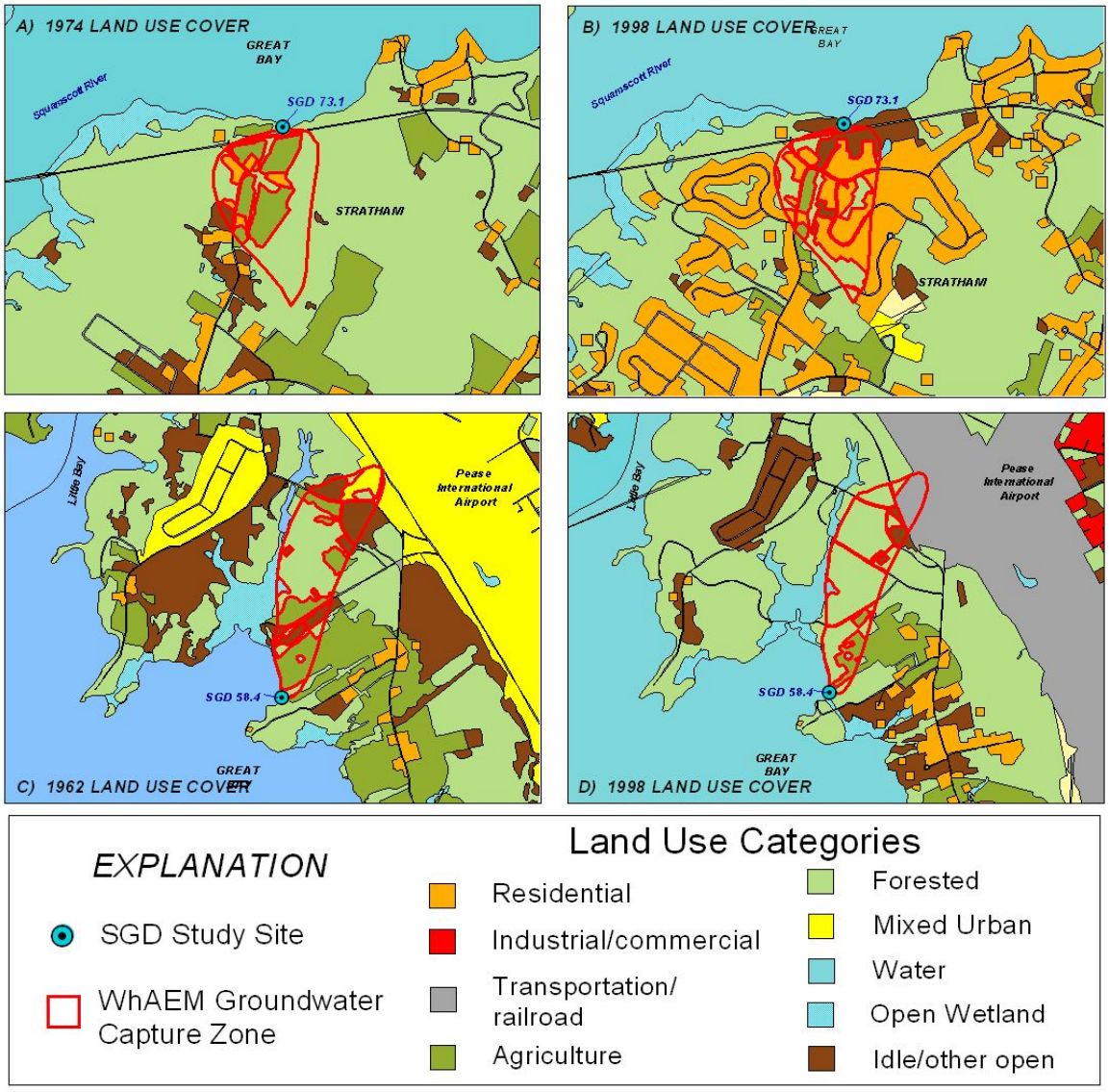

Figure 22. Evolution of the land use cover in the upgradient zone and within the capture zone for two SGD study sites: SGD 73.1 (A and B) and SGD 58.4 (C and D).

The Kruskal-Wallis analysis was used to test for water quality differences due to land use. The variables (groups of a given land use category) are composed by the nitrate concentrations from SGD sites, their associated bedrock wells, and upgradient SDW located within a wellhead area with an important percentage of the land use that defines the group. Forested land use water quality data was represented by all nitrate concentrations associated with SGD 58.4 and SGD 73.1. SGD 73.1 is included due to its high percentage of forested land in 1974 (56.3%), therefore the nitrate concentration of an SGD site, bedrock well, or SDW may appear in one or two groups. The land use groups considered for these analyses were: forested, agricultural, and residential land use and the number of nitrate concentrations for each group were: 4, 10, and 6, respectively. The Kruskal-Wallis test did not show significant differences ($\alpha = 0.05$) in nitrate

concentration by land use group. This is as a result of two factors; firstly, analyzing the nitrate concentration-land use category as a whole may be sometimes misleading given the need to create arbitrary thresholds to conform the groups. Secondly, the mixed urban land use category was not considered in the analysis due to its ambiguity and transitory condition in time since this category literally disappears from the land use mosaic after the dismantling of the Pease Military Base in Newington.

The rank sum test was used with one pair of groups in each run to test for significant differences. Each group is composed by all the nitrate concentrations associated to a given SGD watershed. Therefore, the SGD 58.4 nitrate concentrations conformed a group alone characterized as undeveloped land use that was compared to the rest of the groups/SGD watersheds. Unfortunately, with the collected information only two set of SGD watersheds can be compared: SGD 58.4-SGD 73.1 and SGD 58.4-SGD 19.3. This is because the rank sum test statistic (Wrs) needs at minimum a sample size combinatory of 3 (SGD 58.4), 4 (other SGD) of nitrate concentrations to be run. For these two groups the rank sum test showed significant difference in nitrate concentrations for the first group at a significance level of $\alpha = 0.036$ (SGD 58.4-SGD 73.1) and no significant differences ($\alpha = 0.086 > 0.05$) for the second group. The land use mosaic of SGD 73.1 differs from that of SGD 19.3 in that this latter was more dominated by agricultural use in 1974 than SGD 73.1 and that no residential use was present. The level of significance for each group is indicative of an existing stronger correlation between residential land use and nitrate bearing-groundwater than the same correlation with agricultural use. Even though the presence of forested land use in SGD 73.1 (accompanied by its buffering effect on nitrogen deposition) is considerable, still the relationship between anthropogenic nitrate in groundwater and residential land use remains important.

Accordingly, the % Residential land use is directly related to the nitrate concentration at the SGD sites. Kendall's Tau correlation statistic and Spearman's Rho statistic were both used to determine if the concentration of nitrate and other chemical elements were correlated with the percentage of residential and agricultural land use. Along with Kendall's Tau value is the p value, which is the possibility of finding the trend test result by chance when in fact there is no trend. Thereby, the smaller the p value, the stronger the evidence that the trend test result was not found by chance (Helsel and Hirsch, 1992; Bartos and Ogle, 2002). Both correlation statistics measured the monotonic (linear and non-linear) relation between these two variables. Both statistics showed a significant correlation between nitrate concentrations and % Residential land use: 0.67 (Tau's, $p = 0.043 < 0.05$) and 0.821 ($Rho > Rho_{critical}(\alpha=0.05, n=7) = 0.786$); and not significant with % Agricultural land use: 0.05 and 0.14, respectively. These statistics did not agree when correlating with other chemical constituents due to the influence of estuarine water in the chemistry of some SGD waters.

Nitrate Bearing-Groundwater and Groundwater Age

An inverse relation exists between nitrate concentration and groundwater apparent age (Figure 23). Kendall's Tau and Spearman's Rho correlation statistics were used to test whether there is a significant trend between these two variables. A significant trend was found with the set of data that included CFC-11-based apparent ages at $p = 0.021$

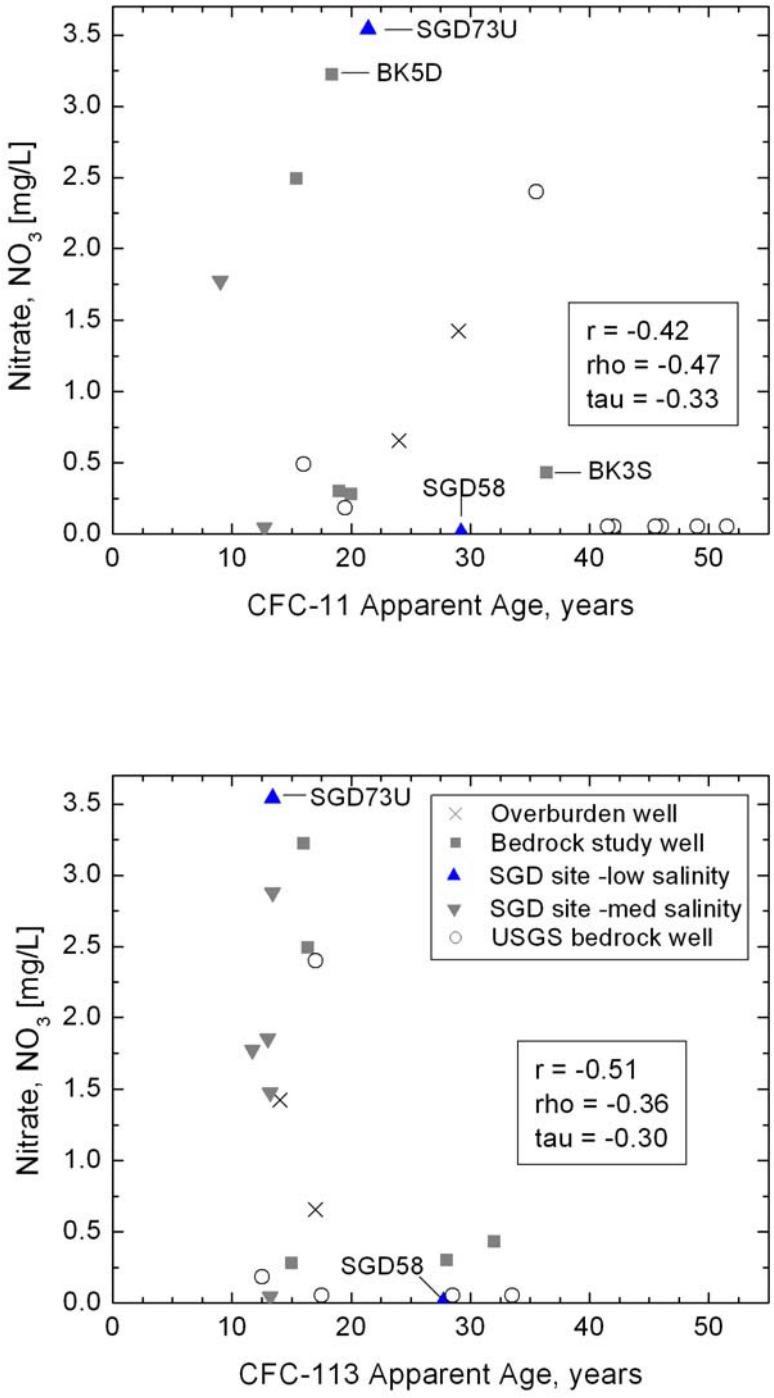

Figure 23. Relation of nitrate-bearing groundwater with piston flow CFC-based apparent groundwater ages. Spearman's Rho critical values are: 0.45 (α=0.05, n=20) and 0.475 (α=0.05, n=19) for the relation with CFC-11 and CFC-113, respectively.

(probability of error of not having found it by chance), which makes it significant (α=0.05, one sided) but at a weak level of negative correlation (-0.33). An even weaker and no significant correlation was detected between nitrate concentrations and CFC-113-based apparent ages (-0.30; p = 0.037, α=0.05, one-sided). Spearman's Tau statistic reported values in agreement with those of Kendall's Tau but greater in magnitude, which is expected since the range of values for this latter statistic varies from –0.75 to 0.75. Although it is not as a strong of a relationship, the results are interesting considering the small sample size (n = 20,19) use for its calculation and the results of other published studies (Katz et al., 1999).

The relation depicted in Figure 23 does not directly show (due to the lack of data in the overburden) where, in the aquifers, the major nitrate concentrations are distributed. However, the lowest concentrations tend to be in bedrock groundwater. Considering the fact that most of the groundwater at the SGD sites originated from the overburden, although still with some uncertainty, it is possible to say that recently recharged waters (last 10-25 years) are the most affected by nitrate contamination and that low to background nitrate concentrations are observed in deep (old) bedrock groundwater.

DISCUSSION

Three primary factors suggest that nitrate loading from submarine groundwater discharge will be increasing in the near future. First, most of the groundwater discharging to the Great Bay is from the overburden (~75%- 95%), as calculated based on major ion simple mixing models and also verified with the strontium, deuterium, and oxygen 18 isotopic composition of overburden and bedrock wells. Second, there has been a major increase of residential land use in the Great Bay area during the period of 1974-1998. The connection between residential land use and nitrate contaminated groundwater was shown to be statistically significant. Third, groundwater dating suggests residence times for submarine groundwater discharge are relatively short (~23 years). The younger waters are the most contaminated with nitrate and will eventually discharge to the Great Bay.

Results from this study indicate that current observations of nitrate concentrations at the SGD sites are the result of land use practices from the late 1970's to mid 1980's. However, groundwater discharge associated with the greatest nitrogen loading from the population growth observed during the 1990's is yet to come. Groundwater ages at the discharge zone sites in the study area averaged 23.2 years (±15.0 years). These relatively young groundwater ages indicate that changes in nitrate concentrations associated with land use affects will be seen in as few as 8 years and as many as 38 years.

Consistency in the nitrate concentrations were observed between this study and a previous related study (Roseen, 2002). It is indicative of the continuity of the nitrogen loading through the years. A seasonal or monthly sampling of these sites would have shown a greater variability. Data would need to be collected over a many year span to document these trends and for assessing the effectiveness of nutrient reduction strategies. Nitrogen loading, if given the conditions, can increase dramatically in short periods of time. Flipse and others (1984) found a total increase of 1.65 mg NO_3/L in a recently developed (residential) area during as short a period as 8 years. Long-term nitrate concentration data at the SGD sites constitute an important tool for detecting these trends and for future calculations of TMDLs.

This study demonstrated the difficulties faced when dealing with water quality data in coastal aquifers. Calcium (Ca^{2+}), Mg^{2+}, Cl^-, Na^+, and SO_4^{2-} were the most affected ions by sample contamination with estuarine waters, even with salinity values as low as 3.5 ppt. Examination of agricultural practices land use affects on groundwater were compromised due to seawater contamination. However, in general it was possible to identify water quality fingerprints for the various water compositions based on the groundwater chemistry in the study area. Sodium (Na^+) and Ca^{2+} enrichments in groundwater were characteristic in the area. These are the result of the salinization process of the groundwater attributed to the dissolution of Na-bearing minerals and/or cation exchange reactions of Ca^{2+} and Mg^{2+} ions for Na^+. A direct salinization with oceanic waters was also evidenced in groundwater along the coastal area of New Hampshire and Maine.

The use of CFCs in groundwater age determination was complex for the study area. A single sample seems to be affected by several factors altering the CFC concentration. CFC-12 was contaminated in 58% of the samples. Sorption processes can be a concern for CFC-113, but seems to not have been an issue. CFC-11 proved the ,sot successful tracer, and was verified in parts by the other CFC data. CFC-derived and lumped parameters-modeled groundwater ages in the study area averaged 25.2 years (± 15.0 years), with the oldest water at SGD 58.4 (27 years) and the youngest at SGD 39.3 (11 years). The CFC analysis provided the chronological evidence needed to relate the nitrate-contaminated groundwater observed at the SGD sites with the historical land use practices. Given the average groundwater age in the study area, the 1973 land use coverage was used for most of the SGD sites to evaluate this correlation.

Significant differences (Wrs, α=0.05) in nitrate between sites in developed (residential-dominated SGD 73.1) and undeveloped (forested-dominated SGD 58.4) watersheds were found for the study area. However, for a similar test, an agricultural-dominated (SGD 19.3) watershed showed no significant differences ($\alpha = 0.086 > 0.05$) in nitrate concentration with the control watershed. In addition, when correlating the percentage of residential and agricultural land use within a watershed with the observed nitrate concentrations, again, a significant positive correlation (Tau's: $p = 0.043 < 0.05$;Rho > 0.786) was related to residential land use. On the other hand, there was no correlation with increasing agricultural land use. The use of Boron isotopes enabled the identification of the septic-derived nitrate-contaminated groundwater fingerprint. Modeled estimates, based on Boron isotope concentrations, suggest mixing rates of ~5% of septic effluent and native groundwater, composed of overburden and bedrock groundwater. These analyses did not indicate any other significant nitrate sources. Statistical analyses shows that the residential land use, the prevalent land use, resulted in elevated groundwater nitrate concentrations around the Great Bay.

Spatially, the source of SGD-nitrate contamination is local, limited primarily to the overburden, and limited to ~1.5 miles away from the Great Bay. Temporally, this contamination was found to be negatively significantly correlated (Tau's, p=0.021) with CFC-11-derived apparent ages. Therefore, younger waters are bearing most of the nitrate contamination loading, and deep older waters are exhibiting values close to native nitrate concentrations.

SUMMARY

This study coupled residence time, water chemistry, isotope geochemistry, and GIS data and analysis to answer the question: Can we relate nitrate loading from groundwater to the Great Bay Estuary from the analysis of historical land use? The methodology that was used in this project was successful in answering this question. None of the individual components of the methodology would have provided enough evidence to test the hypothesis alone. The sensitivity of isotopes geochemistry to nitrate contamination, geochemical controls, and seawater intrusion, required the use of water chemistry fingerprints to understand parent waters and mixing ratios.

The results suggest that the anthropogenic source of nitrate loading observed currently in the submarine groundwater discharge is more dominated by the increased residential land use over the last 30 years rather than other land uses including the

agricultural activities. Valiela et al.(1997) observed that sewage effluents and agricultural activities are not the only nitrate loading sources present, but rather another major sources is the atmospheric loading occurring through wet and dry deposition. This non-point source component was not considered in the study, nor was its relationship with land cover (forested land) change over time.

RECOMMENDATIONS FOR FUTURE RESEARCH

To further detail the residence time there is the need to develop a model for a particular site at which several different tools for groundwater age assessments are made at different time spans. To define a residence time model that better describes the distribution of the travel time in a given aquifer system, at least three of these measurements are required. The development of a residence time model could be based on the FLOWPC program created by Maloszewski and Zuber (1996) or a similar program that incorporates the ability to fit lumped-parameter models to observations. The nitrogen loading model developed by Valiela and others (1997) for Waquoit Bay (Massachusetts) for rural and suburban watersheds underlain by unconsolidated sandy sediments, could be used as a basis for the type of targeted model needed for the Great Bay watershed .

Additionally, the monitoring of a few select groundwater discharge zones as part of a larger routine estuarine monitoring program would be useful to relate the parameters examined in this study with other indicators of environmental quality such as surface waters, biological indicators, among others. A suggested monitoring network for future work would include SGD 58.4, SGD 73.1, SGD 39.3, and SGD 19.3 sites. This selection is based on the ease of accessibility, and the low salinity content of the discharging groundwater. In addition, the watersheds include a variety of land uses from highly developed to undeveloped. A future monitoring network should put more emphasis on the overburden aquifer, which is the major source of the SGD sites. The focus should be on fewer sites in greater detail (three or four). Upgradient well installation would ideally use a Geoprobe or other similar mechanical means. The difficulty of installation of overburden wells prevented the widespread use of upgradient small diameter wells. Wells within the intertidal zone can be installed manually.

The use of water quality data, groundwater residence time, and an estimation of nitrogen loading from septic tank use and fertilizer application could be used as an indicator of future nitrogen loading from groundwater to coastal waters. Nitrate loading associated with the use of lawn and garden fertilizers is a significant source that needs to be explored in more detail because of its relationship with the increase of residential land use. There is limited information on historical and current usage of septic systems and on application of fertilizers. A better-defined nitrogen-N load per capita would need to be developed for this purpose. A homeowner survey on the use of fertilizer is needed to get application rate information. Boron isotopes analyses use are limited to Boron-based fertilizers. Alternative methods should be explored such as Nitrogen and Oxygen-18 isotopes.

SCIENTIFIC ACHIEVEMENT AND DISSEMINATION

The products of this research include a master thesis document, a poster presented in a national conference and an accepted poster for a conference being held in December, 2004.

The thesis entitled *Land Use Influence on the Characteristics of Groundwater Inputs to the Great Bay Estuary, New Hampshire*, was presented by Gabriel F. Bacca-Cortes in September of 2004 as part of a Master of Science Degree in Civil Engineering specializing in water resources, at the University of New Hampshire.

Presentations:

1. Bacca-Cortes, G., Roseen, R. M, and T.P. Ballestero, *Land Use Influence on the Characteristics of Groundwater Inputs to the Great Bay Estuary, New Hampshire* accepted for the American Geophysical Union Fall Meeting, 12/2004.

2. Bacca-Cortes, G., Roseen, R. M, and T.P. Ballestero, *Land Use Influence on the Characteristics of Groundwater Inputs to the Great Bay Estuary, New Hampshire* presented in 12/2003 at the National Groundwater Association Convention, Orlando, Fl.

LITERATURE CITED

1. Allen, D. M. (2004). Sources Of Ground Water Salinity On Islands Using ^{18}O, ^{2}H, and ^{34}S. Ground Water 42(1): 17-31.

2. Ayotte, J.P., M.G. Nielsen, G.R. Jr.,Robinson and R.B. Moore, (1999). Relation Of Arsenic, Iron, And Manganese In Ground Water To Aquifer Type, Bedrock Lithogeochemistry, And Land Use In The New England Coastal Basins: U.S. Geological Survey Water-Resources Investigations Report 99-4162, 61 p.

3. Baker, A. L., J. M. Eilers, R. B. Cook, P. R. Kaufmann and A. T. Herlihy (1991). Interregional Comparisons Of Surface Water Chemistry And Biogeochemical Processes. Chapter 17 in: Regional Case Studies: Acid Deposition and Aquatic Ecosystems, D. Charles, ed., Springer-Verlag. NY.

4. Baker, A. L. (1991). Appendix B: Regional Estimates Of Atmospheric Dry Deposition. Chapter 17 in: Regional Case Studies: Acid Deposition and Aquatic Ecosystems, D. Charles, ed., Springer-Verlag. NY.

5. Bassett, R.L., P.M. Buszka, G.R. Davidson and D.C. Diaz (1995). Identification Of Groundwater Solute Sources Using Boron Isotopic Composition. Environmental Science and Technology 29(12): 2915-2922.

6. Banks, W., R. Paylor and W. Hughes (1996). Using Thermal Infrared Imagery to Delineate Groundwater Discharge. Groundwater **34**: 434-444.

7. Banner, J.L. (2004). Radiogenic Isotopes: Systematics And Applications To Earth Surface Processes And Chemical Stratigraphy. Earth-Science Reviews, 65, 141 – 194.

8. Barringer, T., D. Dunn, W. Battaglin and E. Vowinkel (1990). Problems And Methods Involved In Relating Land Use To Ground-Water Quality. Water Resources Bulletin 26(1): 1-9.

9. Bartos, T.T. and K.M. Ogle (2002). Water Quality and Environmental Isotopic Analyses of Ground-Water Samples Collected from the Wasatch and Fort Union Formations in Areas of Coalbed Methane Development —Implications to Recharge and Ground-Water Flow, Eastern Powder River Basin, Wyoming. U.S. Geological Survey Water Resources Investigation Report 02:4045.

10. Bauer, S., C. Fulda and W. Shäfer (2001). A Multi-Tracer Study In A Shallow Aquifer Using A Shallow Aquifer Using Age Dating Tracers ^{3}H, ^{85}Kr, CFC-113

and SF_6 –Indication For Retarded transport of CFC-113. Journal of Hydrology 248:14-34.

11. Billings, M.P. (1956). Geology of New Hampshire, Pt. 2, Bedrock Geology : New Hampshire State Planning and Development Comission, Concord, New Hampshire, 203p., map.

12. Bu, X. and M.J. Warner (1995). Solubility Of Chlorofluorocarbon 113 In Water And Seawater. Deep-Sea Research 42(7):1151-1161.

13. Bullen, T.D., D.P. Krabbenhoft, C. Kendall (1996) Kinetic And Mineralogic Controls On The Evolution Of Groundwater Chemistry And $^{87}Sr/^{86}Sr$ In A Sandy Silicate Aquifer, Northern Wisconsin, USA, Geochimica et Cosmochimica Acta, 60: 1807-1821.

14. Bullen, T.D., Kendall, C. (1998). Tracing of weathering reactions and water flowpaths: a multi-isotope approach. In: Kendall, C., McDonnell, C.C. (Eds.), Isotope Tracers in Catchment Hydrology. Elsevier, Amsterdam, The Netherlands, pp. 610– 646.

15. Busenberg, E. and L.N. Plummer (1996). Concentrations Of Chlorofluorocarbons And Other Gases In Ground Water At Mirror Lake, New Hampshire. In Morganwalp, D. W. and Aronson, D.A., eds., U.S. Geological Survey Toxic Substances Hydrology Program. Proceedings Of The Technical Meeting, Colorado Springs, September 20-24, 1993: U.S. Geological Survey Water-Resources Investigations Report 94-4015: 151-158.

16. Busenberg, E. and L.N. Plummer (1992). Use Of Chlorofluorocarbons (CCl_3F and CCl_2F_2) As Hydrologic Tracers And Age-Dating Tools: The Alluvium And Terrace System Of Central Oklahoma: Water Resources Research 28: 2257-2283.

17. Busenberg, E. (2004). Electronic Mail Communication. April 13th.

18. Cain, D., D.R. Helsel and S.E. Ragone (1989). Preliminary Evaluations Of Regional Ground-Water Quality In Relation To Land Use. Ground Water 27:230-244.

19. Ciccioli P., W.T.Cooper, P.M. Hammer and J.M. Hayes (1980). Organic Solute-Mineral Surface Interactions: A New Method For The Determination Of Groundwater Velocities. Water Resource Research 16(1): 217-270.

20. Clark, I. and Fritz, P. (1997). Environmental Isotopes in Hydrogeology. Lewis Publishers, Boca Raton, 328 pp.

21. Cook P.G. and D.K. Solomon (1995). The Transport Of Atmospheric Trace Gases To The Water Table: Implications For Groundwater Dating With

Chlorofluorocarbons And Krypton-85. Water Resources Research 31(2): 263-270.

22. Coplen, T.B. (1994). Reporting Of Stable Hydrogen, Carbon, And Oxygen Isotopic Abundances. Pure and Applied Chemistry 66(2): 273-276.

23. Coplen, T.B. and C. Kendall (2000). Stable Hydrogen and Oxygen Isotope Ratios For Selected Sites Of The U.S. Geological Survey's NASQAN And Benchmarck Surface-Water Networks. U.S. Geological Survey Open File Report 00-160.

24. Davidson, G.R. and R.L. Bassett (1993). Application Of Boron Isotopes For Identifying Contaminants Such As Fly Ash Leachate In Groundwater. Environmental Science and Technology 27(1): 172-176.

25. Degnan, J.R., and Clark, S.F., Jr. (2002). Fracture-Correlated Lineaments At Great Bay, Southeastern New Hampshire: U.S. Geological Survey Open-File Report 02-13, 1 sheet, scale 1:24,000, 14 p.

26. Douglas, T.A., C.P. Chamberlain and J.D. Blum (2002). Land Use And Geologic Controls On The Major Elemental And Isotopic ($\delta^{15}N$ and $^{87}Sr/^{86}Sr$) Geochemistry Of The Connecticut River Watershed, USA. Chemical Geology 189:19-34.

27. Dunkle, S.A., L.N. Plummer, E. Busenberg, P.J. Phillips, J.M. Denver, P.A. Hamilton, R.L. Michel and T.B. Coplen (1993). Chlorofluorocarbons (CCl3F and CCl2F2) As Dating Tools And Hydrologic Tracers In Shallow Groundwater Of The Delmarva Peninsula, Atlantic Coastal Plain, United States. Water Resources Research 29(12): 3837-1708.

28. Elkins, J.W., T.M. Thompson, Swanson, J.H. Butler, B.D. Hall, S.O. Cummings, D.A. Fisher, and A.G. Raffo (1993). Decrease In The Growth Rates Of Atmospheric Chlorofluorocarbons 11 and 113. Nature 364: 780-783.

29. Eckhardt, D.A. and P.E. Stackelberg (1995). Relation Of Ground-Water Quality To Land Use On Long Island, New York. Ground Water 33(6): 1019-1033.

30. Ekwurzel, B., P. Schlosser, W.M. Smethie, L.N. Plummer, E. Busenberg, R.L. Michel, R. Weppernig and M. Stute (1994). Dating Of Shallow Groundwater: Comparison Of The Transient Tracers $^{3}H/^{3}He$, Chlorofluorocarbons And ^{85}Kr. Water Resources Research, 30(6):1693-1708.

31. Faure, G. and J.L. Powell (1972). Strontium Isotope Geology. Springer-Verlag Berlin-Heidelberg.

32. Fernandez, I.J. and R.A. Struchtemeyer (1985). Chemical Characteristics Of Soils Under Spruce-Fir Forests In Eastern Maine. Canadian Journal of Soil Science

33. Fisher, D.A. and P.M. Midgley (1993). Production And Release To The Atmosphere Of CFCs 113, 114 And 115. Atmospheric Environment 27A: 271-276.

34. Flanagan, S.M., M. G. Nielsen, K. W. Robinson and J. F. Coles (1999). Water-Quality Assessment Of The New England Coastal Basins In Maine, Massachusetts, New Hampshire, and Rhode Island: Environmental Settings And Implications For Water Quality And Aquatic Biota. U.S. Geological Survey Water-Resources Investigations Report 98-4249. 65 p.

35. Flipse, W.J., B.G. Katz, J.B. Lindner, and R. Markel (1984). Sources Of Nitrate In Ground Water In A Sewered Housing Development, Central Long Island, New York. Ground Water 22(4): 418-426.

36. Focazio, M.J., L.N. Plummer, J.K. Bohlke, E. Busenberg, L.J. Bachman, and D.S. Powars (1998) Preliminary Estimates Of Residence Times And Apparent Ages Of Ground Water In The Chesapeake Bay Watershed, And Water-Quality Data From A Survey Of Springs: U.S. Geological Survey Water-Resources Investigations Report 97-4225, 75 p.

37. Frankic, Anamarija, (1999) Technology And Information Needs Of The Coastal And Estuarine Management Community, CICEET, Durham, NH (available at: http://ciceet.unh.edu/).

38. Freeze R.A. and J.A. Cherry (1979). Groundwater. Prentice-Hall, Englewood Cliffs, 604 pp.

39. Frost, C.D. and R.N. Toner (2004) Strontium Isotopic Identification Of Water-Rock Interaction And Ground Water Mixing. Ground Water, 42, 418-432.

40. Goode, D.J., E. Busenberg, L.N. Plummer, A.M. Shapiro and D. A. Vroblesky (1999). CFC's in the Unsaturated Zone And In Shallow Ground Water at Mirror Lake, New Hampshire. In Morganwalp, D. W. and H.T. Buxton, eds., U.S. Geological Survey Toxic Substances Hydrology Program. Proceedings Of The Technical Meeting, Charleston, S.C., March 8–12, 1999. USGS Water-Resources Investigations Report 99-4018C: 809-820.

41. Haitjema, H.M. (1995). Analytic Element Modeling Of Groundwater Flow. Academic Press, San Diego, CA.

42. Haitjema, H.M.; V.A., Kelson, and K.H. Luther (2000). Analytic Element Modeling Of Ground-Water Flow And High Performance Computing. EPA Environmental Research Brief, EPA/600/S-00/001.

43. Helsel, D.R. and R.M. Hirsch (1992). Statistical Methods In Water Resources. Elsevier Science Publishers, The Netherlands.

44. Hem, J.D. (1985). Study And Interpretation Of The Chemical Characteristics Of Natural Water. U.S. Geological Survey Water-Supply Paper 2254. 272 p.

45. Herczeg, A.L., and W. M. Edmunds (2000). Inorganic Ions As Tracers. Chap ter 2 in: Environmental Tracers In Subsurface Hydrology, Edited by Peter Cook and Andrew Herczeg. Kluwer Academic Publishers; p.31-78.

46. Huntley, D. (1978). On The Detection Of Shallow Aquifers Using Thermal Infrared Imagery. Water Resources Research 14(6): 1075-1083.

47. Johnston, C.T., P.G. Cook, S.K. Frape, L.N. Plummer, E. Busenberg, and R.J. Blackport (1998). Ground Water Age And Nitrate Distribution Within A Glacial Aquifer Beneath A Thick Unsaturated Zone. Ground Water 36: 171-180.

48. Jones, S.H. (2000). A Technical Characterization Of Estuarine And Coastal New Hampshire. Published by New Hampshire Estuaries Project (NHEP).

49. Jones, S.H., R. Langan, L.K. Brannaka, T.P. Ballestero, and D. Marquis (1996). Assessment Of Septic System Design Criteria On Coastal Habitats And Water Quality. New Hampshire Office of State Planning, New Hampshire Coastal Program (Final Report).

50. Jones, S.H. (1998). The Fate Of Bacteria And Nutrients In New Hampshire Septic Systems: Analysis Of Septic System Effluent, Underlying Soils And Gravel. Final Report of the Septic System Roundtable, May 27, 199, Rochester, NH. NH Office of State Planning/Coastal Program, Concord, NH.12 pp.

51. Kahl, J.S., S.A. Norton, C.S. Cronan, I.J. Fernandez, T.A. Haines, and L.C. Bacon (1991). Chemical Relationships Of Surface Water Chemistry And Acidic Deposition In Maine. Chapter 7 in: Regional Case Studies: Acid Deposition and Aquatic Ecosystems, D. Charles, ed., Springer-Verlag. NY.

52. Katz, B. G., J. S. Catches, T. D. Bullen and R. L. Michel (1998). Changes In The Isotopic And Chemical Composition Of Ground Water Resulting From A Recharge Pulse From a Sinking Stream. Journal of Hydrology 211: 178-207. 59p.

53. Katz, B.G., H.B. Hornsby, J.F. Bohlke, and M.F. Mokray (1999). Sources and Chronology of Nitrate Contamination In Spring Waters, Suwannee River Basin, Florida. U.S. Geological Survey, Water Resources Investigation Report: 99-4252.

54. Katz, B.G., L.N. Plummer, E. Busenberg, K.M. Revesz, B.F. Jones and T.M. Lee (1995). Chemical Evolution Of Groundwater Near A Sinkhole Lake, Northern Florida: 2. Chemical Patterns, Mass Transfer Modeling, And Rates Of Mass Transfer Reactions. Water Resources Research 31(6):1565-1584.

55. Kraemer, S. (2004). Workshop On Ground-Water Modeling. Presentation on March 14.

56. Komor, S.C. (1997) Boron Contents And Isotopic Compositions Of Hog Manure, Selected Fertilizers and water in Minnesota. Journal of Environmental Quality 26: 1212-1222.

57. LeBlanc, D.R. (1984). Sewage Plume In A Sand And Gravel Aquifer, Cape Cod, Massachusetts. U.S. Geological Survey Water Supply Paper 2218, 28pp.

58. Leenhouts, J.M., R.L. Bassett and T. Maddock III (1998). Utilization Of Intrinsic Boron Isotopic As Co-Migrating Tracers For Identifying Potential Nitrate Contamination Sources. Ground Water 36(2): 240-250.

59. Lovley, D.R. and E.J. Phillips (1987). Competitive Mechanisms For Inhibition Of Sulfate Reduction And Methane Production In The Zone Of Ferric Iron Reduction Sediments. Applied and Environmental Microbiology 53: 2636-2641.

60. Lyons, W.B., S.W. Tyler, H.E. Gaudette, D.T. Long (1995). The Use Of Strontium Isotopes In Determining Groundwater Mixing And Brine Fingering In a Playa Spring Zone, Lake Tyrrell, Australia. Journal of Hydrology, 167, 225-239.

61. Lyons, J.B., W.A. Bothner, R.H. Moench and J.B. Jr. Thompson (1997). Bedrock Geologic Map Of New Hampshire:U.S. Geological Survey State Geologic Map, 2 sheets, scales 1: 250,000 and 1:500,000.

62. Mack, T.J., and Lawlor, S.M. (1992) Geohydrology And Water Quality Of Stratified-Drift Aquifers In The Bellamy, Cocheco, And Salmon Falls River Basins, southeastern New Hampshire: U.S . Geological SurveyWater-Resources Investigations Report 90-4161, 65 p.

63. Małoszewski, P. and A. Zuber (1996). Lumped Parameter Models For The Interpretation Of Environmental Tracer Data. Included in: Manual on Mathematical Models in Isotope Hydrology. IAEA-TECDOC- 910 with Supplement, IAEA, Vienna: 9–58.

64. Maloszewski, P. and A. Zuber (1982). Determining The Turnover Time Of Groundwater Systems With The Aid Of Environmental Tracers. I. Models And Their Applicability. Journal of Hydrology 57:207-231.

65. Marvinney, R.G., and W.B. Thompson (2000). A geologic history of Maine, *in* King, V.T. (editor), Mineralogy of Maine: Volume 2 – Mining history, gems, and geology: Maine Geological Survey, p. 1-8. (also at http://www.state.me.us/doc/nrimc/pubedinf/factsht/bedrock/megeol.htm)

66. McCarthy R.L., F.A. Bower and J.P. Jesson (1977). The Fluorocarbon-Ozone Theory –1. Production And Release - World Production And Release of CCl_3F and CCl_2F_2 (Fluorocarbons 11 and 12) through 1975. Atmospheric Environment 11: 491-497.

67. McDonald, A.M., W.G. Darling, D.F. Ball and H. Oster (2003). Identifying Trends In Groundwater Quality Using Residence Time Indicators: An Example From The Permian Aquifer Of Dumfries, Scotland. Hydrogeology Journal 11:504-517.

68. McNutt, R.H. (2000), Strontium Isotopes. Chapter 8 in Envirionmental Tracers in Subsurface Geology, ed. by P.G. Cook and A.L. Herczeg: 234-260.

69. Medalie, L. and R.B. Moore (1995). Ground-Water Resources In New Hampshire: Stratified-Drift Aquifers. U.S. Geological Survey Water-Resources Investigations Report 95-4100:39 p.

70. Moore, R.B., 1990, Geohydrology And Water Quality Of Stratified-Drift Aquifers In The Exeter, Lamprey, And Oyster River Basins, Southeastern New Hampshire: U.S. Geological Survey Water- Resources Investigations Report 88-4128, p. 60.

71. Morrissey, D.J. (1983). Hydrology Of The Little Androscoggin River Valley Aquifer, Oxford County, Maine. U.S. Geological Survey Water-Resources Investigations Report 83-4018: 79 p.

72. Morton, T.G., A.J. Gold, and W.M. Sullivan (1988). Influence of Overwatering and Fertilization on Nitrogen Losses From Home Lawns. Journal of Environmental Quality 17(1): 124-130.

73. Negrel, P., J. Casanova, J-F. Aranyossy (2001) Strontium Isotope Systematics Used To Decipher The Origin Of The Groundwaters Sampled From Granitoids: the Vienne Case (France). Chemical Geology, 177, 287-308.

74. NHEP (2003). Environmental Indicator Report: Land Use And Development. New Hampshire Estuaries Project, Portsmouth NH, p.p. 35

75. Novotny, R.F., 1969, The geology of the seacoast region New Hampshire: Concord, N.H., New Hampshire Department of Resources and Economic Development, 1 pl., scale 1:62,5000, 46 p.

76. Piper, A.M. (1944). A Graphic Procedure In The Geochemical Interpretation Of Water Analyses. Transac. Amer. Geophysical Union 25:914-923.

77. Plummer, L.N., S. Drenkard, P. Schlosser, B. Ekwurzel, R. Weppering, J. B. McConnell and R. L. Michel (1998). Flow Of River Water Into A Karstic Limeston Aquifer – 2. Dating The Young Fraction In Groundwater Mixtures In The Upper Floridan Aquifer Near Valdosta, Georgia. Applied Geochemistry 13: 1017-1043.

78. Plummer, L. N. and E. Busenberg (1999). Chlorofluorocarbons, in Environmental Tracers in Subsurface Hydrology, edited by P. Herczeg and A. Cook, pp. 441–478, Kluwer Acad., Norwell, Mass.

79. Portnoy, J.W., B.L. Nowicki, C.T. Roman, and D.W. Urish (1998). The Discharge Of Nitrate-Contaminated Groundwater From Developed Shoreline To Marsh-Fringed Estuary. Water Resources Research, 34, 3095-3104.

80. Pretti, V.A. and B.W. Stewart (2002) Solute Sources And Chemical Weathering In The Owens Lake watershed, Eastern California. Water Resources Research, 38, 2-1/2-18.

81. Robinson, K.W., S.M. Flanagan, J.D. Ayotte, K.W. Campo, A. Chalmers, J.F. Coles and T.F. Cuffney (2004). Water Quality in the New England Coastal Basins, Maine, New Hampshire, Massachusetts, and Rhode Island, 1999–2001. U.S. Geological Survey circular ; 1226, 48 p.

82. Rockingham Planning Commission (2000). Regional Open Space Plan. New Hampshire Department of Environmental Services and Rockingham Planning Commission.

83. Rosenau, J.C., Faulkner, G.L., Hendry, C.W. Jr., Hull, R.W. (1977). Springs of Florida, Florida Bureau of Geology, Bulletin, No. 31, 461 pp.

84. Roseen, R. (2002). Identifying Groundwater Discharge Utilizing Thermal Imagery and Conventional Groundwater Exploration Techniques for Estimating the Chemical Loading to a Meso-Scale Inland Estuary. University of New Hampshire, Durham, N.H., PhD. Dissertation, 188 p.

85. Roseen, R.M., J.R. Degnan, L.K. Brannaka, T.P. Ballestero, and T. J. Mack. (2003). Approximate Potentiometric Surface Of The Bedrock Aquifer At Great Bay, Southeastern New Hampshire, 2001. U.S. Geological Survey, Open-File Report :03-278.

86. Rowland, F.S. (1991). Stratospheric ozone in the 21st century – The chlorofluorocarbon problem: Environmental Science & Technology 25: 622-628.

87. Rozanski, K., Araguas-Araguas, L, Gonfiantini, R., 1993. Isotopic Pattern in Modern Global Precipitation. In: Climate change in Continental Isotopic Records, Geophysical Monograph 78. (Eds: Swart, P. K., Lohman, K. C., McKenzie, J. and Savin S.), American Geophysical Union, Washington, 1-36.

88. Scanlon, B. R., 1991, Evaluation Of Moisture Flux From Chloride Data In Desert Soils: Journal of Hydrology, v. 128, p. 137-156.

89. Scanlon, B. R., 2000, Uncertainties In Estimating Water Fluxes And Residence Times Using Environmental Tracers In An Arid Unsaturated Zone: Water Resources Research, v. 36, no. 2, pp. 395-409.

90. Schultz, T.R., J.H. Randall, L.G. Wilson, and S.N. Davis (1976). Tracing Sewage Effluent Recharge-Tucson, Arizona. Ground Water 14:463-470.

91. Stekl, P.J. and S. M. Flanagan (1992). Geohydrology And Water Quality Of Stratified-Drift Aquifers In The Lower Merrimack And Coastal River Basins: Southeastern New Hampshire. U.S. Geological Survey Water Resources Investigation Report 91-4025, 101 p.

92. Strack, D.L. (1989). Groundwater mechanics. Prentice-Hall, Inc., Englewood Cliffs, New Jersey.

93. Szabo, Z., D.E. Rice, L.N. Plummer, E. Busenberg, S. Drenkard and P. Schlosser (1996). Age Dating Of Shallow Groundwater With Chlorofluorocarbons, Tritium/Helium 3, and Flow Path Analysis, Southern New Jersey Coastal Plain. Water Resources Research 32(4): 1023-1038.

94. Thompson, G. M., and J. M. Hayes (1979). Trichlorfluoromethane In Groundwater: A Possible Tracer And Indicator Of Groundwater Age, Water Resource Research 15:546–554.

95. Trojan, M.D., J.S. Maloney, J.M. Stockinger, E.P. Eid, and M.J. Lahtinen (2002). Effects of Land Use on Ground Water Quality in the Anoka Sand Plain Aquifer of Minnesota. Ground Water 41(4): 482-492

96. U.S. Census Bureau, 2000 (2002). Census Of Population And Housing, Summary Population and Housing Characteristics, PHC-1-31, New Hampshire Washington, DC, pp. 195.

97. U.S. Environmental Protection Agency, (2000) Current Drinking Water Standards—National Primary And Secondary Drinking Water Regulations: Office of Ground Water and Drinking Water, accessed December 27, 2000, at URL: http//www.epa.gov/safewater/standards.htm

98. Valiela, I., and J.L. Bowen (2002). Nitrogen Sources To Watersheds And Estuaries: Role Of Land Cover Mosaics And Losses Within Watersheds. Environmental Pollution 118:239-248.

99. Valiela, I., G. Collins, J. Kremer, K. Lajtha, M. Geist, B. Seely, J. Brawley, and H. Sham (1997). Nitrogen Loading From Coastal Watersheds to Receiving Estuaries: New Method and Application. Ecological Applications 7(2): 358 -380.

100. Vengosh, A., A. R. Chivas, and M. T. McCulloch (1989). Direct Determination Of Boron And Chlorine Isotopes In Geological Materials By Negative Thermal-Ionization Mass Spectrometry. Chemical Geology 79: 333-343.

101. Vengosh, A., A. R Chivas, M.T. McCulloch, A. Starinsky, Y. Kolodny (1991). Geochim. Cosmochim. Acta 55: 2591-2607.

102. Vengosh A. and Spivack A.J. (1999). Boron Isotopes In Groundwater, Environmental Isotopes in Subsurface Hydrology, Kluwer Academic Publishers, chap 16.1: 479-485

103. Vengosh A. (1994). Boron Isotope Application For Tracing Sources Of Contamination In Groundwater. Environmental Science and Technology 28: 1968-1974.

104. Vengosh, A., A.J. Spivack, Y. Artzi, A. Ayalon (1999). Geochemical And Boron, Strontium and Oxygen Isotopic Constraints On The Origin Of The Salinity In Groundwater From The Mediterranean Coast Of Israel. Water Resources Research, 35, 1877-1894.